6-10-2015

Strain Promoted Click Chemistry of 8-Azidopurine and 5-Azidopyrimidine Nucleosides and Nucleotides with Cyclooctynes and Applications to Living Cell Imaging

Jessica Zayas
Florida International University, jzaya003@fiu.edu

DOI: 10.25148/etd.FIDC000125

FLORIDA INTERNATIONAL UNIVERSITY

Miami, Florida

STRAIN PROMOTED CLICK CHEMISTRY OF 8-AZIDOPURINE AND 5-AZIDOPYRIMIDINE NUCLEOSIDES AND NUCLEOTIDES WITH CYCLOOCTYNES AND APPLICATIONS TO LIVING CELL IMAGING

A dissertation submitted in partial fulfillment of

the requirements for the degree of

DOCTOR OF PHILOSOPHY

in

CHEMISTRY

by

Jessica Zayas

2015

To: Dean Michael R. Heithaus
College of Arts and Sciences

This dissertation, written by Jessica Zayas, and entitled Strain Promoted Click Chemistry of 8-Azidopurine and 5-Azidopyrimidine Nucleosides and Nucleotides with Cyclooctynes and Applications to Living Cell Imaging, having been approved in respect to style and intellectual content, is referred to you for judgment.

We have read this dissertation and recommend that it be approved.

_____
Jeffrey Joens

_____
Joong-ho Moon

_____
Yuan Liu

_____
Prem P. Chapagain

_____
Stanislaw F. Wnuk, Major Professor

Date of Defense: June 10, 2015

The dissertation of Jessica Zayas is approved.

_____
Dean Michael R. Heithaus
College of Arts and Sciences

_____
Dean Lakshmi N. Reddi
University Graduate School

Florida International University, 2015

DEDICATION

To my God, family, future husband and Ph.D. mentor for without all your prayers, love and guidance this dissertation would not have been completed.

ACKNOWLEDGMENTS

First, I would like to that my mentor Dr. Stanislaw Wnuk for providing me guidance, wisdom and intellectual freedom throughout these past 8 years. Words cannot express how much I value all the wisdom and love you have given me these past 8 years. You have become my second father and will always have a special place in my heart.

I would also like to thank my committee members: Dr. Joong-ho Moon, Dr. Jeff Joens, Dr. Yuan Liu and Dr. Prem Chapagain for providing support and insight throughout my doctoral studies. I would also like to extend my gratitude to the Department of Chemistry and Biochemistry at Florida International University; you all have welcomed me with open arms and allowed me to make this lab and department my home for the past 8 years. Next, I would like to thank the MBRS RISE program and staff for providing me with a research fellowship and supporting me throughout this journey.

I would like to thank my collaborators whom without this work and dissertation would not have been possible: Dr. Quentin Felty and Dr. Jayanta Das from FIU's Department of Environmental and Occupational Health for doing all the fluorescent microscopy, cell culture and determining the cytotoxicity of my nucleoside analogues, Dr. Jaroslava Miksovska and future Dr. Walter Gonzalez from FIU's Department of Chemistry for doing the photophysical and lifetime characterization of my click adducts, Dr. Akira Chiba and Dr. Nima Sharifai from the Department of Biology at the University of Miami for defining the *in vivo* lifetime of our compounds using FLIM, and Dr. Kirkwood Land and Dr. Lisa Wrischnik from the Department of Biology at the University of the Pacific for testing many of our compounds for parasitic activity.

I would also like to thank Dr. Adam Sobczak, Dr. Pablo Sacasa, Dr. Jean-Philippe Pitteloud and Dr. Thao Dang for patiently training and helping me throughout my research career in the Wnuk laboratory including. To my current lab-mates, Dr. Yong Liang, Dr. Ramanjaneyulu Rayala, and the future Dr. Mukesh Mudgal for their synthetic contributions and most importantly for allowing me to make the lab my second home, you have not only become some of my dearest friends but also a part of my family. Marie Annoual, my student and friend, thank you for all your contributions to our project ("our baby") and to my Ph.D, this work would have not been completed without your help and support. A special thank you to my friend, the future Dr. Cesar Gonzalez, for always providing a listening ear and a helpful hand whenever I needed it, you were always eager to help even if it was for something that you thought it was ridiculous.

Lastly, I would like to thank my wonderful parents for their unending support, unconditional love, encouragement and prayers throughout my life. My sister, for loving me and always cheering me up when I was stressed out and for (unknowingly at times) saying just the right words I needed to hear. To my grandparents, aunt, uncle and cousins for their continuous prayers and support. To my godparents and cousins, thank you for sharing a special bond with me and for being a constant source of love and encouragement. You have helped shape me into the person I am today. To my 2nd family, the Pulido family, thank you for opening your home and hearts to me so many years ago.

Most importantly, I would like to thank my Jesse. Not many people are lucky enough to have their future husband as a colleague throughout their studies and much less as their partner from such an early age. Without your constant love, support and

encouragement, many things would not have been possible. I look forward to not only becoming the chemist, Dr. Jessica Zayas but also your wife, Mrs. Jessica Pulido.

ABSTRACT OF THE DISSERTATION

STRAIN PROMOTED CLICK CHEMISTRY OF 8-AZIDOPURINE AND 5-AZIDOPYRIMIDINE NUCLEOSIDES AND NUCLEOTIDES WITH CYCLOOCTYNES AND APPLICATIONS TO LIVING CELL IMAGING

by

Jessica Zayas

Florida International University, 2015

Miami, Florida

Professor Stanislaw F. Wnuk, Major Professor

The strain promoted azide alkyne cycloaddition (SPAAC) of azido nucleobase modified nucleosides and nucleotides with cyclooctynes to give fluorescent triazoles has been relatively unexplored. Thus, SPAAC between azido-nucleobases and various cyclooctynes in aqueous solution at ambient temperature resulted in the efficient formation (3 min - 2 h) of triazole products with inherent fluorescent properties. The 2- and 8-azidoadenine nucleosides reacted with fused cyclopropyl cyclooctyne, dibenzylcyclooctyne or monofluorocyclooctyne to produce click products functionalized with hydroxyl, amino, *N*-hydroxysuccinimide, or biotin moieties. The previously unexplored 5-azidouridine and labile 5-azido-2'-deoxyuridine were similarly converted to the analogous triazole products in quantitative yields in less than 5 minutes. The 8-azido-ATP quantitatively afforded the triazole product with fused cyclopropyl cyclooctyne (3 h). Addition of a triazole ring at the 2 or 8 position of adenine or 5-position of uracil induces fluorescent properties which were used for direct imaging with fluorescent microscopy in MCF-7 cancer cells without the need for traditional fluorogenic reporters.

Fluorescent lifetime imaging microscopy of the click adducts in live cells were used to determine the lifetime of each fluorophore in the cellular nuclei demonstrating the potential utility of the synthesized triazole adducts for dynamic measuring and tracking of events inside single living cancer cells.

The SPAAC methodology developed has also been applied to study the cellular targets in protozoal parasite, *Trichomonas vaginalis* and bacteria, *Pseudomonas aeruginosa*. The 9-(2-deoxy-2-fluoro-β,D-arabino-furanosyl)adenine (*arabino*-F-Ado) was modified with an azido moiety at the C8 position for use in click chemistry. Tagging and subcellular localization studies using azido modified *arabino*-F-Ado could provide insight into the mechanism of action of *arabino*-F-Ado.

An activated analogue of S-adenosyl-L-methionine (SAM) with an EnYn group on the sulfur instead of a methyl group was prepared to study the transfer of the methyl group from SAM. I found that the EnYn group was transferred from SAM to a guanosine on tRNA by methytransferase Trm1. Thus, AdoEnYn is a competitive inhibitor of SAM and can be incorporated into tRNA in place of SAM.

TABLE OF CONTENTS

LIST OF TABLES

TABLE PAGE

LIST OF FIGURES

FIGURE PAGE

LIST OF SCHEMES

SCHEME PAGE

LIST OF ABBREVIATIONS

α-KG	α-ketoglutarate
A_3AR	selective Gi-coupled A3 adenosine receptor
Abs	absorbance
ACN	acetonitrile
AcOH	acetic acid
AdoHcy	S-adenosyl-L-homocysteine
ADHY	AdoHcy hydrolase
Ar	aromatic (NMR)
β	beta
BCN	bicyclo[6.1.0]nonyne
Bn	benzyl
Boc	*tert*-buyloxycarbonyl
br	broad (NMR)
t-Bu	*tert*-butyl
calcd	calculated (HRMS)
cAMP	3′,5′-Cyclic adenosine monophosphate
º C	degrees Celsius
conc.	concentrated
CuAAC	Copper-catalyzed Azide-Alkyne Cycloaddition
CTD	C-terminal domain
δ	delta
d	doublet (NMR)

DAST	diethylaminosulfur trifluoride
DBH	1,3-Dibromo-5,5-dimethylhydantoin
DCM	dichloromethane
DFPA	2,2-Difluoropentanedioic Acid
DIBO	dibenzylcyclooctyne
DIC	*N,N*′-Diisopropylcarbodiimide
DMEM	Dulbecco's modified eagle's medium
DMF	*N,N*-dimethylformamide
DMSO	dimethylsulfoxide
DMTr	dimethoxytrityl
dNTP	deoxynucleotide triphosphate
DTT	Dithiothreitol
ε	epsilon
ED_{50}	effective dose
EdC	5-ethynyl-2′-deoxycytidine
ESI	electrospray ionization
Et	ethyl
λ	gamma
g	gram(s)
GalNAc	*N*-acetylgalactosamine
GI	gastrointestinal
h	hour(s)
HdCK	human deoxycytidine kinase

Hz	hertz
HPLC	high performance liquid chromatography
HRMS	high resolution mass spectroscopy
HGXPRT	hypoxanthine-guanine-xanthine phosphoribosyltransferase
HOBt	Hydroxybenzotriazole
IC_{50}	half maximal inhibitory concentration
J	coupling constant in Hz (NMR)
K_d	enzyme dissociation constant
L	liter(s)
LAH	lithium aluminum hydride
LDA	lithium diisopropylamide
m	milli; multiplet (NMR)
μ	micro
M	moles per liter
MALDI-TOF	matrix-assisted laser desorption/ionization-time of flight
MeOH	methanol
min	minute(s)
MK	myokinase
mM	milimolar
mol	mole(s)
MS	mass spectrometry
MTases	methyltransferases
MTT	3-(4,5-dimethylthiazol-2-yl)-2,5-diphenyltetrazolium bromide

m/z	mass to charge ratio (MS)
NA	nucleoside analogue(s)
NaN_3	sodium azide
NH_3	ammonia
NHS	*N*-hydroxysuccinimide
NIT	Nitazoxinide
NMR	nuclear magnetic resonance
nM	nano Molar
NTD	N-terminal domain
NTP	nucleoside triphosphate
OCT	symmetrically fused cyclopropyl cyclooctyne
ODNs	oligodeoxynucleotides
ONs	oligonucleotides
p	para
PAMPA	Parallel artificial membrane permeability assay
PBS	phosphate buffered saline
PEP	phosphoenolpyruvate
PET	Positron Emission Tomography
PK	pyruvate kinase
PTFE	polytetrafluoroethylene
pyr	pyridine
%	percentage
q	quartet (NMR)

quin	quintet (NMR)
rt	room temperature
s	second(s); singlet (NMR)
S.A.	specific activity
SAH	*S*-adenosyl-*L*-homosysteine
SAM	*S*-adenosyl-*L*-methionine
siRNA	small interfering RNAs
S_N2	nucleophilic substitution
$SnCl_4$	Tin(IV) chloride
SNP	single nucleotide polymorphism
SPAAC	strain promoted azide alkyne cycloaddition
SPOS	solid-phase oligonucleotide synthesis
RCM	ring closure metathesis
RP	reverse phase (HPLC)
t	triplet (NMR)
TBAF	tetra-n-butylammonium fluoride
TBDMS	tertbutyldimethylsilyl
tBuOH	*tert*-butylalcohol
TEA	triethylamine
TFA	trifluoroacetic acid
THF	tetrahydrofuran
TIPS	triisopropylsilyl ether
TIZ	tizoxanide

TLC	thin layer chromatography
Tol	toluene
t_R	retention time (HPLC)
Trm1	tRNA(m^2_2G)dimethyltransferase
TrmD	tRNA(m^1G37)methyltransferase
UMP-CMP	cytidylate kinase
UV	ultraviolet
VIS	visible
VZV	varicella zoster virus
vs	versus
ZFP	zinc finger proteins

1. Introduction

1.1 Nucleosides for Medicinal Applications

Nucleosides and nucleotides make up the basic building blocks of DNA and RNA. They are involved in many important cellular process including cell signaling, enzyme regulation and metabolism.[1] As such, nucleoside and nucleotide derivatives have been developed to mimic their parent compounds and thus are able to exploit cellular metabolism by being incorporated into DNA and RNA.[2] Nucleoside and nucleotide analogues enter cells using nucleoside transporters;[3-4] once inside they interact with and inhibit important enzymes including polymerases, kinases and ribonucleotide reductase.[1] After incorporation and phosphorylation, the nucleoside analogues are typically able to inhibit cellular division, viral replication and act as chain terminators causing cellular apoptosis and potential therapeutic benefits.[5]

1.1.1 FDA Approved Nucleoside Based Anticancer and Antiviral Agents

The 6-mercaptopurine and acyclovir, two important antiviral agents, were first developed by Elion and Hitchings.[6-7] The first antiviral nucleoside analogue approved by the FDA was edoxudine in 1969, but it is no longer used in the clinic. Since then work by De Clerq and Holy has allowed the development and eventual FDA approval of several landmark nucleoside based drugs.[8-9] Currently, there are over 25 FDA approved nucleoside and nucleotide analogues that are used as antiviral or anticancer agents and several more in the clinical trial stage, Table 1.[2] Despite the widespread availability of anticancer and antiviral nucleoside analogues, the development of derivatives with

improved properties is imperative in order to overcome metabolic resistance,[10] poor oral bioavailability,[11] long term toxicity[12] and variability from patient to patient.[1]

Drug	Parent Category	Year
5-aza-2'-deoxycytidine (Decitabine)	2′-Deoxycytidine	2006
O^6-methylarabinofuranosyl guanine (Nelarabine)	Guanosine	2005
5-aza-cytidine (Azacitidine)	2′-Deoxyadenosine	2004
2'-fluoro-2'-deoxyarabinofuranosyl-2-chloroadenine (Clofarabine)	Cytidine	2004
N^4-pentyloxycarbonyl-5'-deoxy-5-fluorocytidine (Capecitabine)	Cytidine	1998
2,2-difluoro-2'-deoxycytidine (Gemcitabine)	2′-Deoxycytidine	1996
2-chloro-2'-deoxyadenosine (Cladribine)	2′-Deoxyadenosine	1992
2'-deoxycoformycin (Pentostatin)	Adenosine	1991
Arabinofuranosyl-2-fluoroadenine (Fludarabine)	Purine analogue	1991
5-fluoro-2'-deoxyuridine (Floxuridine)	2′-Deoxyuridine	1970
Arabinofuranosylcytosine (Cytarabine)	Cytidine	1969
6-thioguanine (Lanvis)	Guanine	1966
5-fluorouracil (Adrucil)	Uracil	1962
6-mercaptopurine (Purinethol)	Purine	1953

Table 1. FDA Approved Anticancer nucleoside analogues

Cytarabine, 1-β-D-arabinofuranosylcytosine, was approved in 1969 by the FDA for the treatment of white blood cell cancers. It contributes to the cure of acute myeloid leukemia and non-Hodgkin lymphoma[13] in about 30% of cancer patients. Cytarabine also possesses potent antiviral activity and has been long used to treat herpes infections;[14] however, it causes severe side effects including bone marrow suppression and is toxic at higher dosages.[10, 15]

Several adenosine analogues display potent antiviral and anticancer activities including 8-chloro and 8-aminoadenosine[16-17] which decrease the intracellular concentration of ATP, cause a decrease in RNA production and ultimately cell death.[18] The 8-chloroadenosine triphosphate also inhibits the polymerization of actin[19] and the activity of topoisomerase II.[20] It is currently being tested for activity against breast

cancer[21-22] and is in a Phase I clinical trial for the treatment of chronic lymphocytic leukemia.[23-24]

1.2 Click Chemistry

"Click Chemistry" is a term first introduced by K. Barry Sharpless in 1998 and fully described in 2001 to describe reactions that generate substances by joining small building blocks together with heteroatom links (C-X-C). In his landmark review "Click Chemistry: Diverse Chemical Function from a Few Good Reactions,"[25] Sharpless described a set of criteria that a reaction must meet to be considered a click reaction. Thus, a desirable click reaction should be high yielding, wide in scope, be stereospecific and create only inoffensive by-products that can be removed without chromatography. Simple reaction conditions, readily available starting materials and the use of a solvent that is benign or easily removed are other characteristics attributed to the click reaction. Several transformations have been identified to fit the concept of click chemistry, the most common examples being the cycloaddition of unsaturated species such as 1,3-dipolar cycloaddition reactions and the Diels-Alder reactions.[25] Nucleophilic substitution chemistry, specifically ring opening reactions of epoxides and other strained heterocyclic electrophiles, "non-aldol" type carbonyl chemistry and, oxidative addition to carbon-carbon multiple bonds such as epoxidation and dihydroxylation are also considered to fit the concept of the ideal click reaction.

1.2.1 Early Examples of Click Chemistry

1.2.1.1 Huisgen Work

The earliest 1,3-dipolar cycloadditions were described in the late 19th and early 20th centuries; however, the bulk of the mechanistic investigation and synthetic

application was established by Rolf Huisgen in the 1960s. Thus, the 1,3-dipolar cycloaddition is the reaction of a dipolarophile and a 1,3-dipole to give a 5 membered heterocyclic ring reaction and is commonly referred to as the Huisgen cycloaddition.[26] Typically dipolarophiles are alkenes, alkynes and molecules that possess functional groups with heteroatoms such as carbonyls and nitriles. More recently, the Huisgen cycloaddition is often used to describe the 1,3-dipolar cycloaddition between an organic azide[27-28] and an alkyne to generate 1,2,3-triazole, Scheme 1. The commonly employed Huisgen cycloaddition is slow and requires heating at upwards of 100 °C, often produceing mixtures of two regioisomers when an asymmetric alkyne is used.

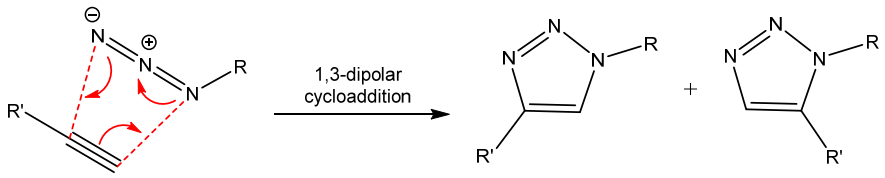

Scheme 1. Husigen 1,3-dipolar cycloaddition

1.2.1.2 Sharpless Work

In 2002 Morton Meldal,[29] at the Carlsberg Laboratory in Denmark, and K. Barry Sharpless,[30] at the Scripps Research Institute in California, independently developed a copper(I)-catalyzed Huisgen cycloaddition which they entitled the Copper-catalyzed Azide-Alkyne Cycloaddition (CuAAC), Scheme 2. The addition of the copper catalyst allowed the Huisgen reaction to proceed under mild and physiological conditions including room temperature. The CuAAC specifically allowed for the synthesis of the 1,4-disubstituted regioisomers specifically.[30]

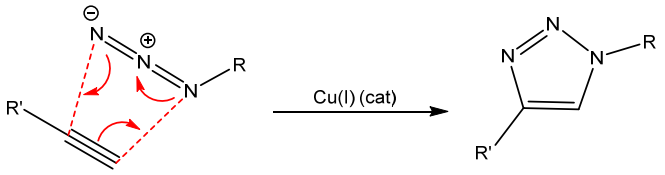

Scheme 2. Copper catalyzed azide alkyne cycloaddition

Recently, click chemistry has found many applications in the broad areas of materials science,[31] drug discovery,[32] bioconjugation,[33] proteomic profiling and potential identification of cellular targets.[34] However, the cytotoxicity of copper is a major drawback of CuAAC and a limiting factor in the *in vivo* application of the copper catalyzed click reaction. The presence of copper and/or reducing agents such as sodium ascorbate have also been reported to cause DNA degradation[35-37] or aggregation of biomolecules.[38]

1.2.1.3 Bertozzi Work

The strain promoted 1,3-dipolar [3+2] cycloaddition of azides and cyclooctynes (SPAAC) was later developed by Bertozzi and coworkers,[39-44] as a modified Huisgen and Sharpless cycloaddition, Scheme 3. The SPAAC reactions occur readily under physiological conditions and in the absence of supplementary reagents such as copper and microwave heating. Furthermore, the SPAAC reaction is a bioorthogonal reaction because it can occur inside a living system without interfering with naturally occurring processes.[39] The azide component of the reaction is bioorthogonal because it is small (similar size to a methyl group), metabolically stable, and does not naturally exist in cells. Although the alkyne is not quite as small as the azide, it is sill bioorthogonal enough for *in vivo* studies. The SPAAC reaction has been used for the selective modification of compounds or living cells[40] including those in live zebrafish[12] and mice.[45]

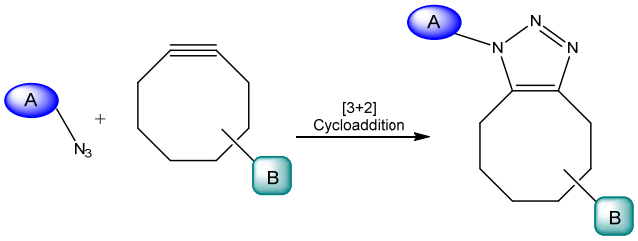

Scheme 3. Strain promoted 1,3-dipolar [3+2] cycloaddition

The classic Sharpless copper-catalyzed click reaction is fast and effective for bioconjugation but unsuitable for live cells as a result of the toxicity of the copper ions required for the reaction. The need for copper catalysis was bypassed by strain promoted click reaction by exploiting the strain experienced by the alkyne (~18 kcal/mol) and 160° bond angle in the eight-membered ring deviating from the typical alkyne bond angle of 180°, Figure 1.[44]

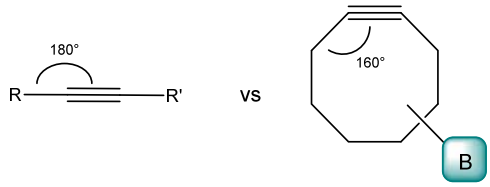

Figure 1. Bond angle comparison in liner alkyne vs cyclooctyne

The first cyclooctyne developed by the Bertozzi group, designated **OCT**, reacted with azides at room temperature but lacked water solubility,[39] Figure 2. The aryl-less octyne, **ALO**, had improved water solubility but was still sluggish when reacting with azide partners. The monofluorinated cyclooctyne, **MOFO**, and difluorinated cyclooctyne, **DIFO**, were created to increase reaction rate though electronic modulation by the addition of an electron-withdrawing fluorine. The dibenzylcyclooctyne, **DIBO**, was developed by fusing two aryl rings onto a simple cyclooctyne, resulting in high ring strain and a decrease in distortion energy.[44] The biarylazacyclooctynone, known as **BARAC,** is an analogue of **DIBO** with an amide bond in the ring which adds an sp^2

center and increases reaction rate by ring distortion. Adjustments on the structure of **BARAC** yielded **DIBAC** by adding distal ring strain which reduced the steric bulk around the alkyne and further increased reactivity of the alkyne. The dimethoxyazacyclooctyne, **DIMAC**, was developed in response to **DIFO** being extremely reactive in labeling live cells but performing poorly in animal models. The two methoxy groups α and β to the alkyne increased **DIMAC**'s water solubility, polarity and its pharmokinetics.[46]

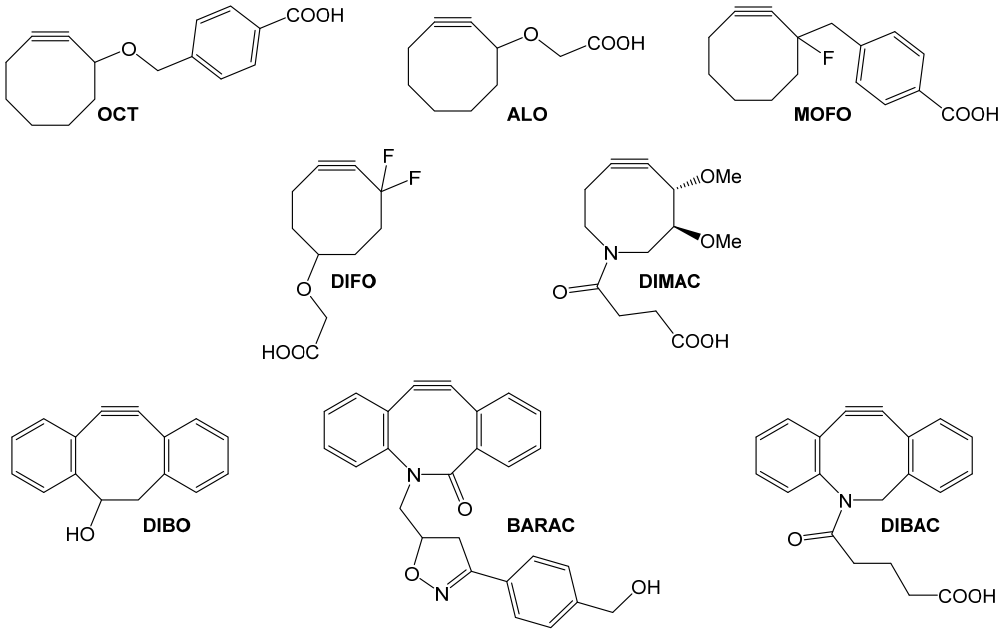

Figure 2. Representative Cyclooctynes[39-50]

The most popular application of the SPAAC reaction is in imaging of live cells or animals using an azide tagged biomolecule and cyclooctyne with an imaging agent.[48] Copper-free click chemistry is also being explored for the synthesis of Positron Emission Tomography (PET) imaging agents. A challenge for the click-PET probes is rapid synthesis of the cyclooctyne to minimize the isotopic decay of the radionuclides (^{18}F or ^{64}Cu).[51-53]

1.2.2 Click Chemistry with Nucleosides and Nucleotides

Click chemistry was developed to provide a simple method for joining organic building blocks and has been applied extensively for introduction of substituents onto nucleosides, nucleotides, nucleic acids and DNA. Nucleosides and oligonucleotides with alkyne modified heterocyclic bases have been conjugated with azide modified fluorescent dyes, sugars and peptides for imaging and drug discovery.[33, 54-56]

1.2.2.1 Azide Modified Sugars

The discovery of therapeutically applicable azido sugar modified nucleosides such as Zidovudine, AZT, Figure 3, provided the foundation for the discovery and application of other azido modified sugar derivatives of nucleosides.

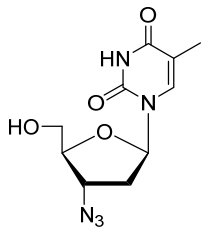

AZT, Zidovudine

Figure 3. Example of an azido sugar modified nucleosides, Zidovudine (AZT)

1.2.2.1.1 Copper Catalyzed Click Chemistry

The Cu(I) catalyzed click reaction has been utilized towards the functionalization of sugar moieties on nucleosides. In 2005, Zhou *et al.*[57] reported the synthesis of various analogues of the antiviral AZT with hydroxyl **1**, amino **2** and carboxylic **3**-**5** modifications, Figure 4; however these compounds, were found to be inactive against several viruses including HIV, herpes simplex, and cowpox. Inactivity of 3'-azido modified AZT can at least be party attributed to a failure to be phosphorylated by cellular or viral kinases. Later, AZT was also conjugated with a series of propargyl β-D-

glycosides via a copper catalyzed click reaction to give 1,2,3-triazole linked oligosaccharides **6-9**,[58] providing a new avenue for attaching carbohydrate residues to pharmaceutical compounds, Figure 4.

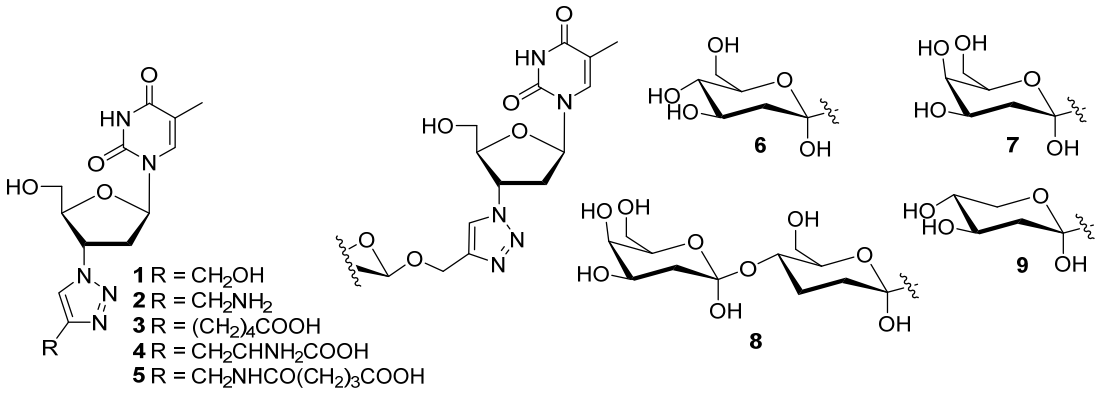

Figure 4. 3'-Triazolo modified thymidine analogues[57-58]

The 5'-triazolo modified thymidine analogues **11-14** were synthesized by Byun *et al.* from 5'-azide **10** using Sharpless "style" click chemistry, Scheme 4.[59] *In vitro* growth inhibition studies of the analogues on *B. anthrasis* Sterne revealed that only compound **12**, with a *para*-fluoro substituent on the phenyl ring, was active (IC_{50} of 113 μM).

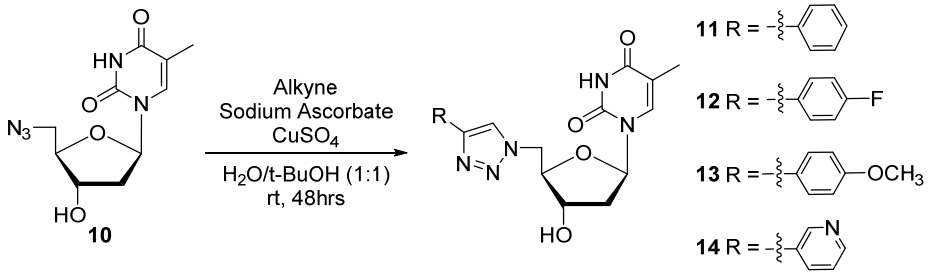

Scheme 4. 5'-Triazolo Modified Thymidine[59]

Double headed nucleosides are nucleosides that contain two nucleobases. They have been used as building blocks of unnatural nucleic acids.[60-65] Dimer **16** was an attempt by Danel *et al.*[65] to synthesize an asymmetric, double headed nucleoside drug via CuAAC reaction, Scheme 5. Thus, **AZT** was conjugated with the thymine analogue **15**,[66] a known potent inhibitor of HIV-1, to afford triazole **16**. The di-thymine analogue **16**

demonstrated activity against wild type HIV-1 and mutant strains. However, derivative 16 showed low activity against the drug resistant Y181C mutated stain; therefore, it is unlikely that the nucleoside portion of **16** functions as a reverse transcriptase inhibitor.[65]

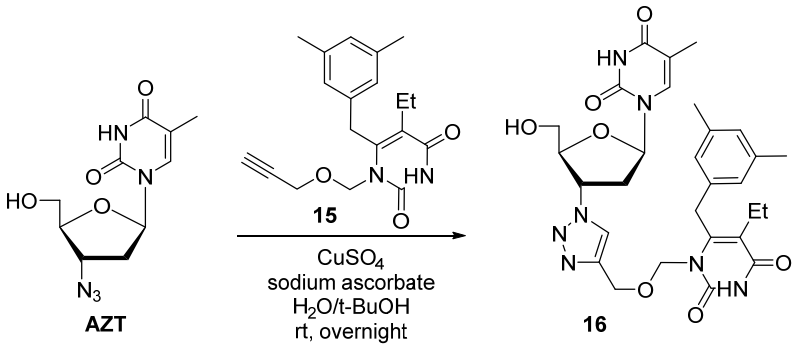

Scheme 5. Synthesis of double headed thymidine[65]

Recently, locked nucleic acids (LNAs) have received attention because of their promising therapeutic antisense properties.[67-69] Enderlin and Nielsen[70] used CuAAC with microwave heating to synthesize the double-headed nucleoside **18** with a triazole linking an additional thymine to the 6'-position of the LNA-nucleoside monomer, Scheme 6. When the phosphoramidite of triazole **18** was incorporated into an oligonucleotide **19** a large increase in thermal stability was seen and the bulky substituent was well accommodated in the minor groove;[71] thus, double headed nucleosides can be an important tool in the construction of artificial oligonucleotides.

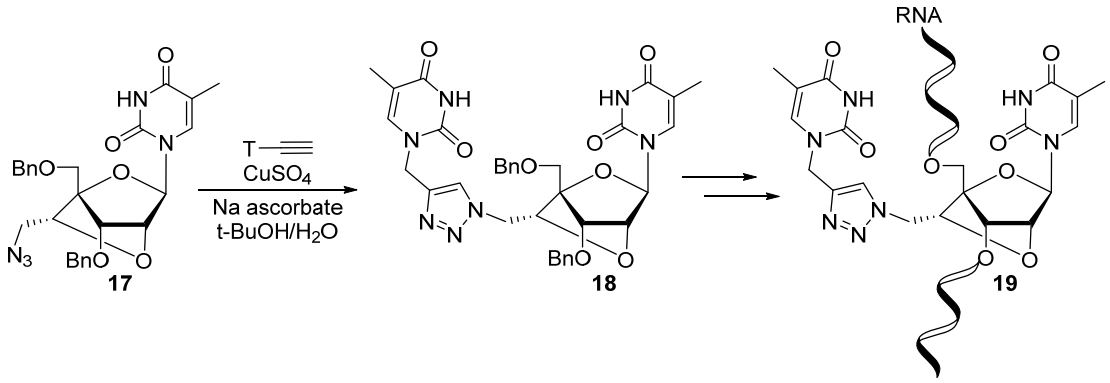

Scheme 6. Synthesis of locked thymdine via CuAAC[70]

Cytidine and adenosine analogues with 5'-triazole moieties were prepared by conversion of a 5'-phosphate ester intermediate followed by an azide substitution reaction and click reaction in the presence of copper sulfate and sodium ascorbate. Resulting compounds **20**-**26**, Figure 5, were evaluated against α-2,3-sialyl-transferase. Interestingly, cytidine analogue **23** with the phenyl substituent was the most active compound with an IC_{50} of 37.5 μM, suggesting that a hydrophobic functionality and a cytosine ring are necessary for optimal binding and inhibition.[72] Novel acyltriazole adenosine **27** was synthesized via a click cycloaddition between protected 5'-azido-5'-deoxyadenosine and a carboxyalkyne. It was examined as an inhibitor of *Mycobacterium tuberculosis* but showed no inhibition of growth up to 100 μM. Molecular modeling of **27** showed the hydrogen bonds involving the phosphate of the natural substrate are lost when the triazole replaces the phosphate. Furthermore, the planar geometry of the triazole was a poor fit for the binding site, requiring out of plane bending of the ring substituents.[73]

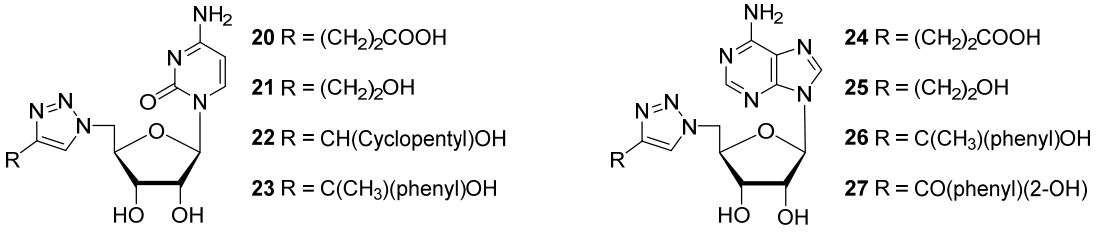

Figure 5. 5'-Triazolo modified cytidine and adenosine analogues[72-73]

The Grøtli group employed a copper(I)-catalyzed [3+2] cycloaddition reaction between 2'-azido-2'-deoxyadenosine and various alkynes using catalytic amounts of sodium ascorbate and copper sulfate overnight at ambient temperature to give analogues **28**-**36**, Figure 6.[74] These compounds are considered non-hydrolyzable isoteres of 2'-aminoacyladenoisne that are a crucial component in the tRNA synthetases enzymatic cascade and currently are of use in x-ray crystallographic studies for the elucidation of

the editing mechanism of various tRNA synthetases.[75]

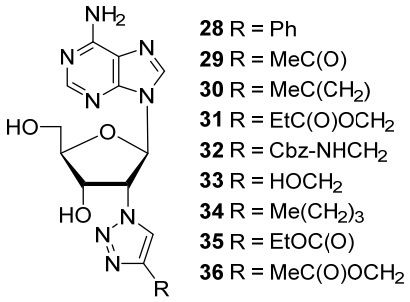

Figure 6. 2'-Triazolo Modified Adenosine Analogues[74]

Kosiova *et al.*[76] prepared novel coumarin-nucleoside conjugates via a Cu(I) catalyzed click reaction of an alkyne modified coumarin and a 3'- or 5'- azido modified thymidine, Figure 7. The resulting triazoles **37** and **38** exhibited promising fluorescent properties. The fluorescent intensity of the newly synthesized conjugates depended on the position of the of the coumarin modification. The approach for using coumarin as a fluorescence reporter is also currently being used for the preparation of fluorescent bioconjugates including fluorescent carbohydrates.[77]

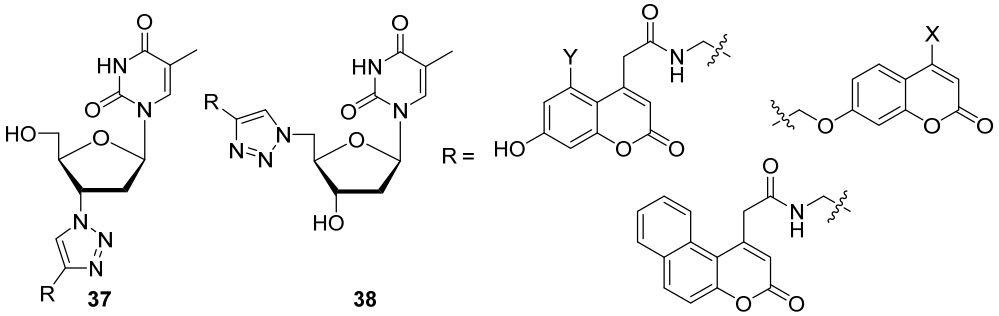

Figure 7. Thymidine-coumarin conjugates[76]

Novel oligonucleotides **40** and **41** containing triazole residues with nucleobase tethers were synthesized via CuAAC of *N*-9 propargylpurines or *N*-1 propargylpyrimidines with the tolouyl protected 1-azido-2'-deoxyribofuranose **39**, Scheme 7. Melting experiments of the resulting oligodeoxynucleotides (ODN's)

demonstrated that triazole nucleosides destabilize DNA duplexes. The destabilization is the result of the inability of tethered nucleosides to form base pairs with opposite bases because of the structural variations caused by the auxiliary triazole ring.[78]

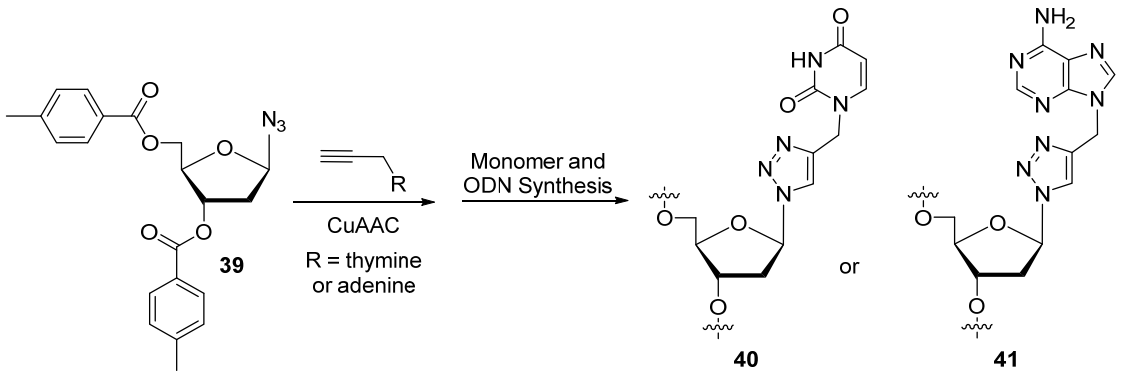

Scheme 7. Synthesis of DNA containing triazole-bridged nucleobases[78]

1.2.2.1.2 Strain Promoted Click Chemistry

The strain promoted click reaction (SPAAC) has been much less extensively studied on azido modified sugars. A SPAAC reaction has been reported at the 2'-azide position of all four possible bases (A, C, G, U) which were incorporated at the 3' terminus on a strand of RNA **42**, Scheme 8. The ligase mediated site specific incorporation of a single modified nucleotide of choice (A, C, G, U) containing an azide made this method unique. Furthermore, the azide **42** was reacted with a fluorophore cycloalkyne to give site specific fluorescent labeling of the *de novo* synthesized RNA **43**.[79]

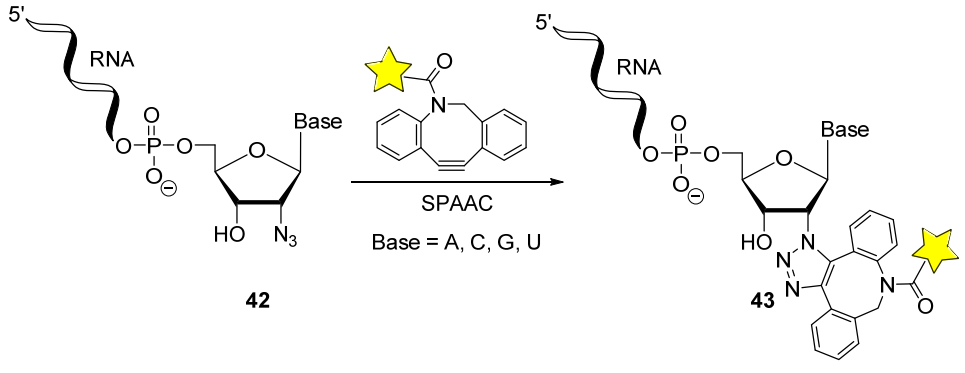

Scheme 8. Site specific SPAAC on the 3' terminus of RNA[79]

1.2.2.2 Alkyne Modified Sugars

As previously described modification of the sugar moiety is usually preferred to modification on the base because it has, in general, a less negative impact on the resultant oligonucleotide and can sometimes improve the oligonucleotide's thermodynamics.

1.2.2.2.1 Copper Catalyzed Click Chemistry

The appendage or substitution of an azide is one of the most preferred modifications on a sugar; therefore, the alkyne modification on the sugar is more difficult to accomplish and has thus been explored less often. Attachment of a propargyl group at the 2'-hydroxyl group of the ribose sugar on a stand of DNA does not affect duplex stability making the 2'-position ideal for label attachment. This tagging strategy has been employed by Berndl *et al.*[80] for the post-modification of oligonucleotides, Figure 8. The 2'-propargyl modified uridine was conjugated via a copper catalyzed click reaction to blue phenoxazinium azide yielding blue fluorescent product **44** or red coumarin azide yielding triazole **45**. Interestingly, the 2'-dye modified uridines **44** and **45** still base pair with adenine and do not exhibit reduced thermal stability compared with unmodified duplexes. A Stokes shift of ~100 nm was also observed, validating this approach as a convenient fluorescent label for nucleic acids in assays or cell biology.

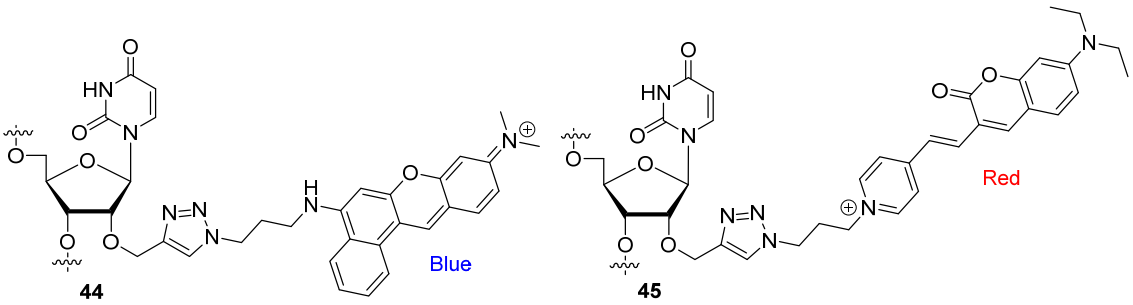

Figure 8. Fluorescent dye labeling of uridine in ODNs using the CuAAC reaction[80]

Solid phase synthesis (SPOS) using phosphoramidites is the preferred method for

the synthesis of oligonucleotides.[81] Triazole analogues modified with either 5'-linoleyl **47** or *N*-Acetylgalactosamine (GalNAc) **48** moieties, were prepared by Yamada *et al.*[82] via a CuAAC reaction in which the Cu(I) catalyst was made *in situ* from $[Cu(CH_3CN)_4]PF_6$ and elemental copper, Scheme 9. These analogues were later phosphorylated and incorporated into oligonucleotides, yielding small interfering RNA (siRNA) analogues which effectively silenced expression of the luciferase gene in HeLa cells.[82]

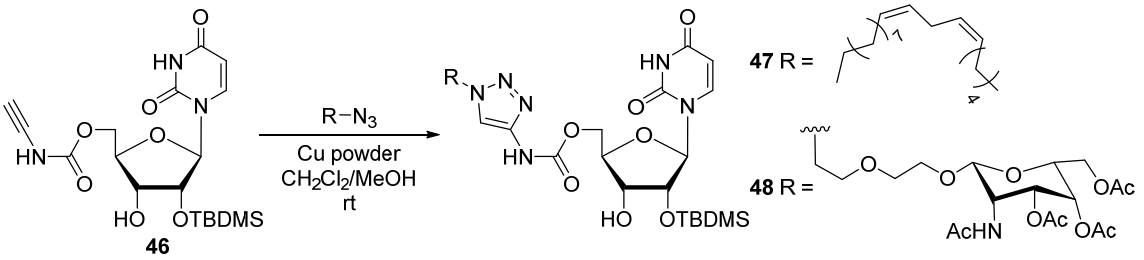

Scheme 9. Synthesis of 5'-linoleyl and N-acetylgalactosaminyl uridine click monomers[82]

Kawagoe *et al.*[83] prepared thymidine **49** bearing a propargylic group at the C6' via a selective bromination followed by a substitution. The alkyne **49** was then reacted with 6-azido-6-deoxycellulose **50** in the presence of $CuBr_2$ to give the click adduct **51**, Scheme 10. Interestingly, **51** was observed to form nanocomposites and function as "wrapping papers" to disperse single-walled carbon nanotubes in water.

Scheme 10. Synthesis of 2'-deoxythymidine modules onto cellulose main chain[83]

Incorporation of a triazole ring into ODNs has been used to confer enhanced resistance to chemical and enzymatic degradation.[84-85] Therefore, because of their

potential antitumor and antiviral properties, functionalized ODN's have recently received much attention. Varizhuk *et al.*[86] synthesized a dinucleoside building block **54** with internucleotide linkage using click chemistry, Scheme 11. A two-phase solvent system (CH_2Cl_2/H_2O) was used to increase the click reaction rate as the starting materials alkyne **52** and azido **53** had poor solubility in the typical click reaction solvents.[86] Melting temperature studies revealed that these short triazole linkages distort the double helix and cause destabilization of the duplex.

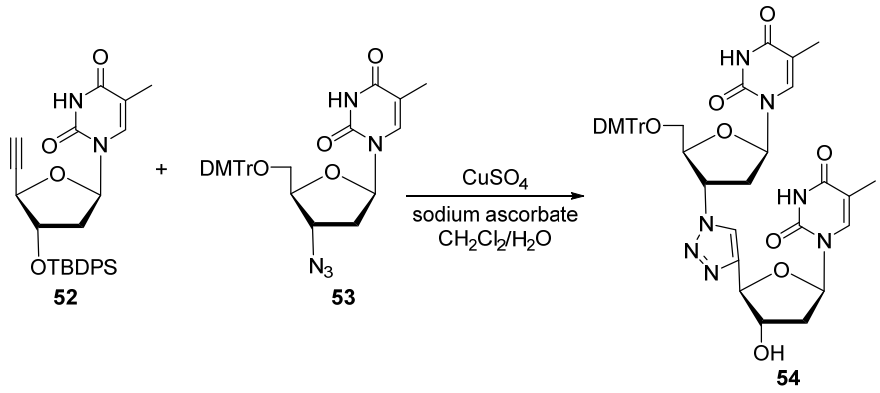

Scheme 11. Fragment of modified ODN with triazole linkage[86]

The RNA oligonucleotides containing triazole linkages between uridine and adenosine nucleosides have been reported.[87-90] Mutisya *et al.*[87] prepared the key triazole intermediate **57** using a click reaction between 2'-*O*-alkynylated uridine **55** and *N*-benzoyl protected azido adenosine derivative **56**, Scheme 12. As shown by UV melting and circular dichroism (CD) of the modified oligonucleotide once incorporated into RNA, **57** strongly destabilized the RNA duplex. Nuclear magnetic resonance (NMR) studies also conducted suggested that in spite of the relative flexibility around the modified linkage, all base pairs were formed.

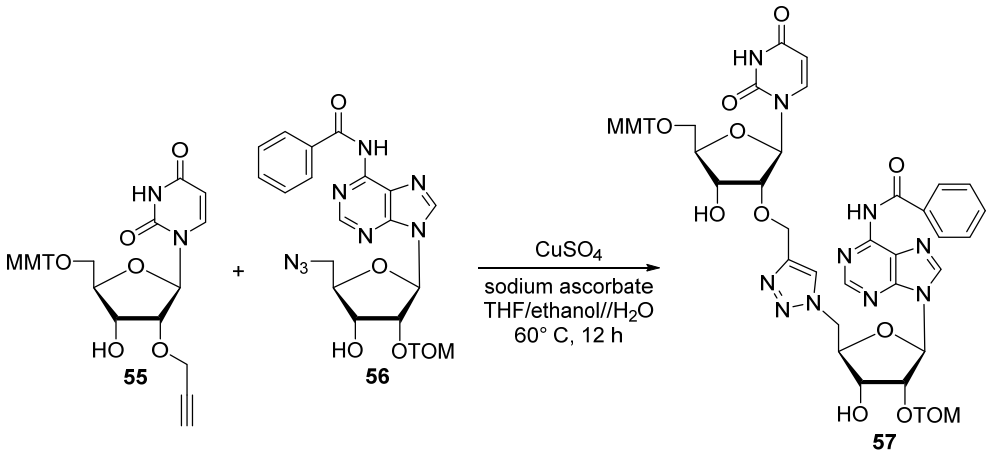

Scheme 12. Fragment of modified ONs with a six-bond triazole linkage[87]

The Pujari group conducted some interesting studies involving antiparallel strands of DNA ligated using a "bis-click" protocol, where in 2'-*O*-propargylated ribonucleosides were reacted in a click reaction with a bis-azide in the presence of a copper catalyst yielding 3'-5'-oligonucleotide **58**, Figure 9.[90] The modification displayed only a minor effect on duplex stability and allowed the DNA duplex to remain intact. The "bis-click" protocol was similarly utilized with 3'-*O*-propargylated ribonucleosides resulting in an unusual 2' and 5' phosphodiester linkage and increased destabilization.[89] This new methodology is unique in that it can be introduced at any position (terminal or internal) in the oligonucleotide and theoretically be applicable to any nucleoside substrate bearing a propargylic group on the sugar moiety. Recently, Pujari and Seela introduced internal sugar cross-links into oligonucleotides with parallel chain orientation.[90] They found that the cross-links stabilize anti-parallel and parallel duplexes significantly. Furthermore, the increase in T_m is similar in both cases, indicating that he cross-links are well accommodated leading to strong stabilization, which is unexpected as the anti-parallel and parallel strands of DNA have different geometries.

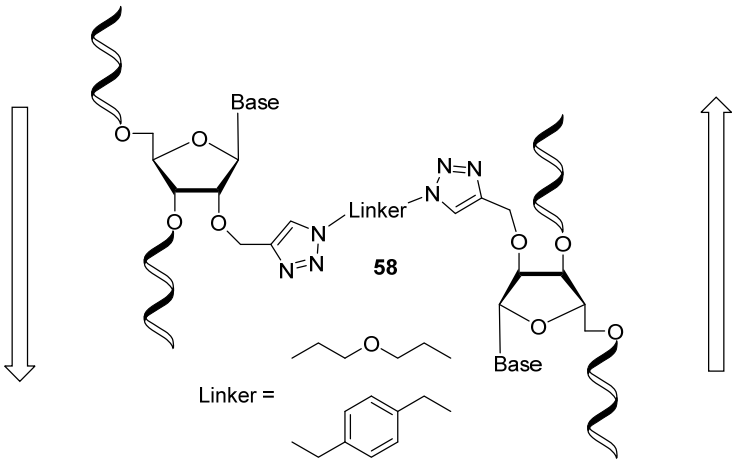

Figure 9. Sugar cross linked DNA[90]

Recently, the synthetic advantage of microwave assisted click chemistry has also been applied to solid phase bound oligonucleotides.[82] A variety of solid supported alkyne oligonucleotide scaffolds (e.g., **59**) were shown to conjugate to virtually any azido-functionalized ligand.[82] The microwave click reaction was versatile in that it readily occurred at a desired site within the oligonucleotide sequence and at any selected position on the ribosugar (2', 3' or 5' positions) to yield 5'-triazole **60**, Scheme 13. The siRNA conjugate **60** was evaluated for *in vitro* RNAi activity using a HeLa cell line transformed with the firefly and renilla luciferase gene and demonstrated the capacity to effectively silence the expression of the luciferase gene. Although, this approach was demonstrated on uridine derivatives, it is applicable to other propargylated compounds.[91-93]

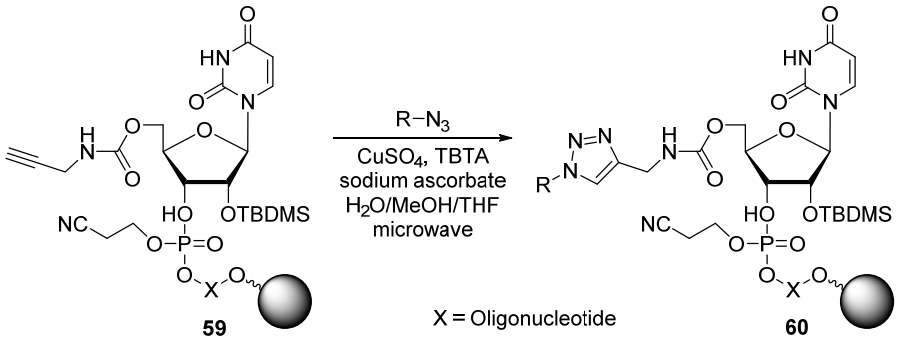

Scheme 13. Click reaction of an azide with alkyne-oligonucleotide scaffold[82]

El-Sagheer and Brown utilized a copper catalyzed click reaction of 3'-azide **61** and 5'-propargylamido **62** to prepare DNA strand **63**, with unnatural triazole linkage, as a PCR template.[94] Amplification of template **63** proceeded efficiently with a variety of polymerases to give amplicon **64**, Scheme 14. Sequencing of the DNA amplicon revealed the presence of a single thymidine at the ligation site, making this the first example of highly efficient nonenzymatic DNA strand ligation combined with reproducible amplification. The ability of thermostable polymerases to read through such an unnatural backbone opens up intriguing possibilities in biology and nanotechnology.

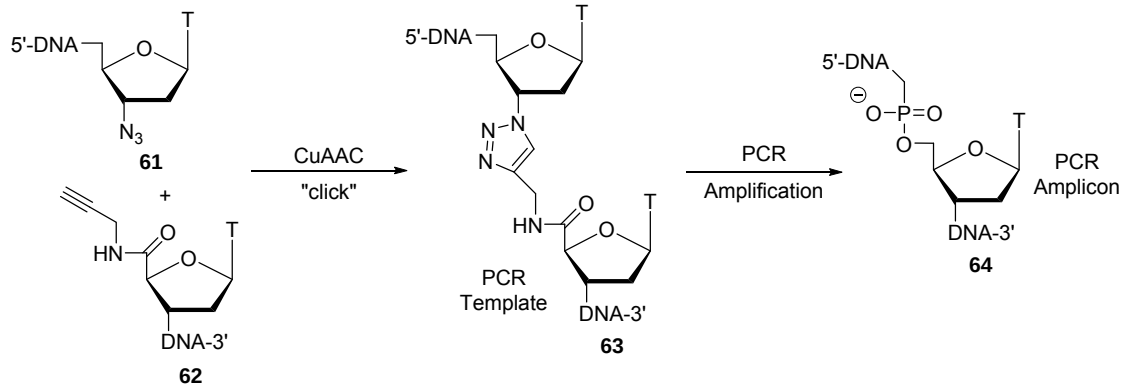

Scheme 14. Click Ligation of Alkyne and Azide Oligonucleotides Produces a PCR Template[94]

1.2.2.2.2 Strain Promoted Click Chemistry

Copper free click chemistry is a mild and fast method for the selective conjugation and modification of ONs. The site-specific introduction of the requisite large (and typically hydrophobic) cyclooctynes has proved challenging. Jawalekar *et al.* reported a method for incorporating of bicyclo[6.1.0]nonyne (BCN) into synthetic ODNs using standard solid phase phosphoramidite chemistry, Scheme 15.[95] Thus, 2'-amino modified ODN **65** was coupled with azidohexanoic acid or a BCN derivative and later cleaved from solid support to give either azide derivative **66** or BCN-derivative **67**,

respectively. Overnight stirring of azide **66** and cyclooctyne **67** gave the corresponding triazole linked oligo **68**; confirmed by HPLC and MALDI-TOF. This cross-linking approach was unique in that it demonstrated a straightforward and high-yielding conjugation of ODNs at any adenosine in the ribose backbone of RNA.

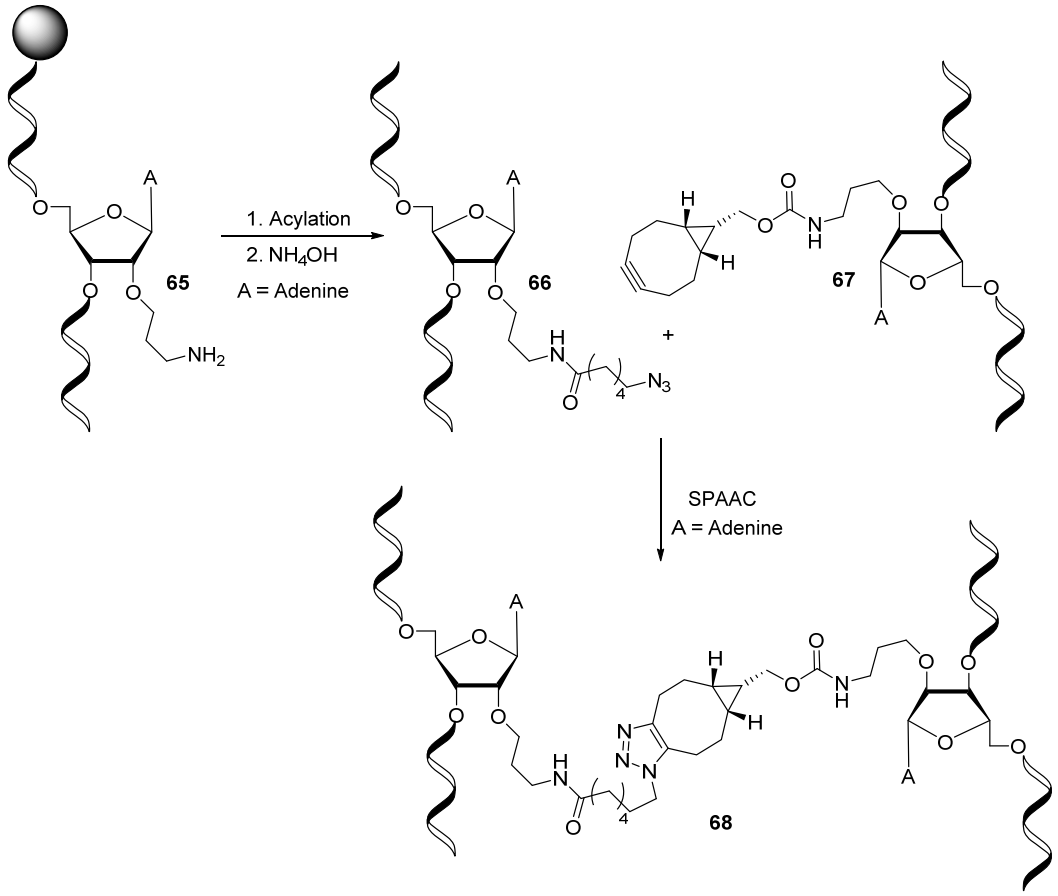

Scheme 15. RNA dimerization via SPAAC[95]

1.2.2.3 Azide Modified Bases

Azide modified sugars such as AZT have also been studied in click chemistry, with typical reaction conditions including the addition of Cu(I) and microwave assisted heating.[96-99] However, the application of the nucleosides bearing an azido group in heterocyclic bases in the click chemistry with alkyne partners has received much less attention thus far. A limiting factor in the development of base modified azido

nucleosides and oligonucleotides is their lack of compatibility with the solid-phase synthesis of DNA fragments which required trivalent phosphorous-based precursors.

1.2.2.3.1 Copper Catalyzed Click Chemistry

Owing to their relatively high stability, aryl azides have found many biological and industrial uses.[100] However, aryl azides have also been found to be relatively unreactive in click reactions and usually require extensive heating for a reaction to occur.[101-103] The Hudson group demonstrated the unreactivity of 8-azidoadenosine **69** with terminal alkyne bearing cyclen Eu^{3+} complex **70** even after prolonged reaction times (120 h), addition of a large excess of $CuSO_4 \cdot 5H_2O$ and sodium ascorbate and refluxing in DMF, Scheme 16.[101]

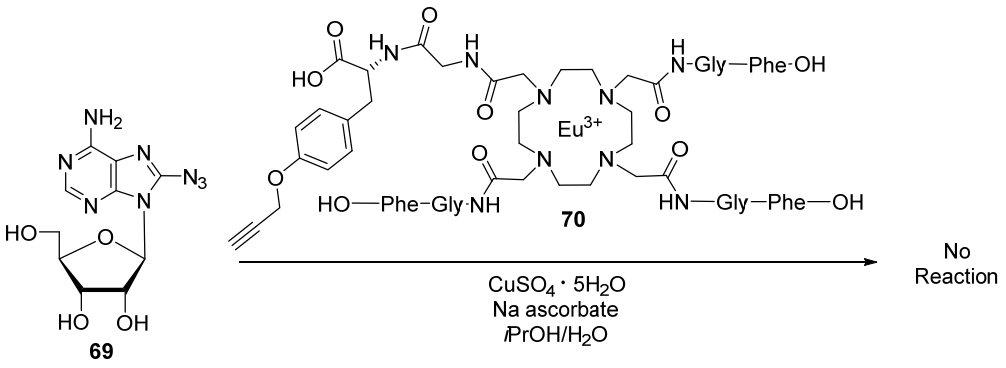

Scheme 16. Click Reaction between azido modified adenosine and cyclen Eu^{3+} complex[101]

Gunji and Vasella demonstrated the "inconsistent" reactivity of base modified nucleosides in CuAAC reactions. Reaction of protected 8-azidoadenosine **71** with (trimethylsilyl)acetylene at 80 °C for 20 h afforded triazole product **72** in modest yields; however, azide **71** was unreactive when reacted with phenyl acetylene and did not yield triazole **73**, Scheme 17.[103]

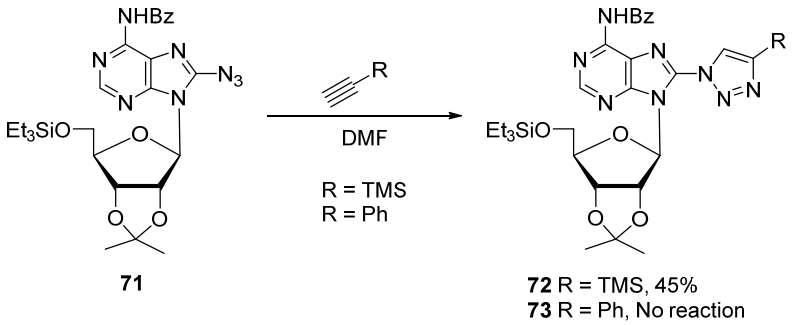

Scheme 17. Synthesis of protected 8-triazole adenosines[103]

Similar to the results previously mentioned by Gunji,[103] Schaeffer[104] prepared the protected 2-azidoadenosine **74** that was only moderately reactive in copper catalyzed click reactions and which also required excess of alkyne and a prolonged reaction times, Scheme 18.[105] The click analogues **75** – **81** constitute a novel class of highly potent and selective Gi-coupled A_3 adenosine receptor (A_3AR) partial agonists and antagonists with "potential" to be used as pharmacological agents.

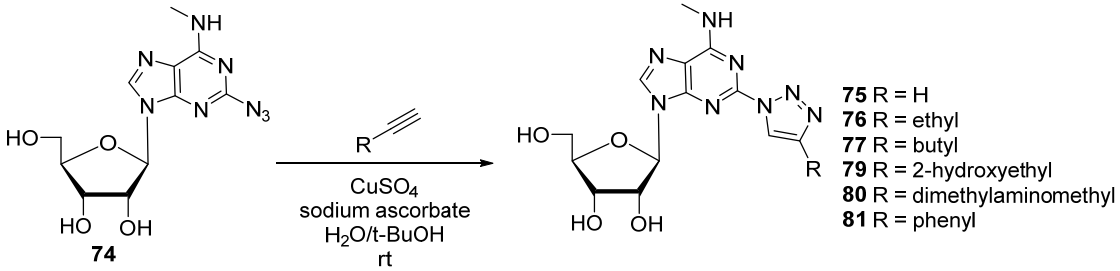

Scheme 18. Synthesis of 2-Triazole-1-yl Analogues of N6-Methyladenosine[105]

A library of 2-triazole substituted analogues of 5′-*O*-[*N*-(Salicyl)sulfamoyl]adenosine (e.g., **83** and **84**) were synthesized by Gupte via a Cu(I)-catalyzed click reaction of azide **82** with a panel of 30 alkynes, Scheme 19.[106] The 30 alkynes were selected systematically to explore the van der Waal and electrostatic interactions provided by the subsequent 1,4-substitued triazoles, Scheme 17. Evaluation of these analogues for effects on the aryl acid adenylating enzyme (AAAE) known as MbtA and activity against whole-cell M. *tuberculosis* under iron-deficient and iron-

replete conditions, demonstrated remarkably, all compounds having potent AAAE inhibition. Furthermore, on the basis of potency, selectivity, lack of cytotoxicity and decreased hydrophobicity, phenyltriazole **84** proved to be the best candidate of the analogues tested and merits further clinical evaluation against M. *tuberculosis.*

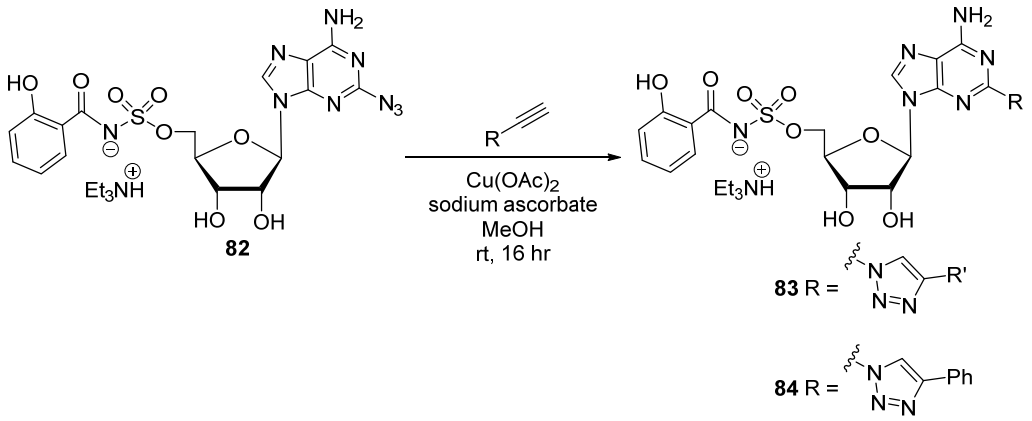

Scheme 19. Synthesis of 2 triazole analogues of 5′-O-[N-(Salicyl)sulfamoyl]adenosine[106]

Lakshman prepared C2-triazolylinosine derivatives using CuAAC, Scheme 20, and the compounds were evaluated for antiviral activity against a broad spectrum of DNA and RNA viruses. None of the OTBDMS protected analogues proved to be active against most of the tested viral strains at sub-cytotoxic concentrations. It is worthy to note that moderate inhibitory activities were observed for the phenyltriazole **86** and butyltriazole **87** against vesicular stomatitis virus and cytomegalovirus, respectively.[107]

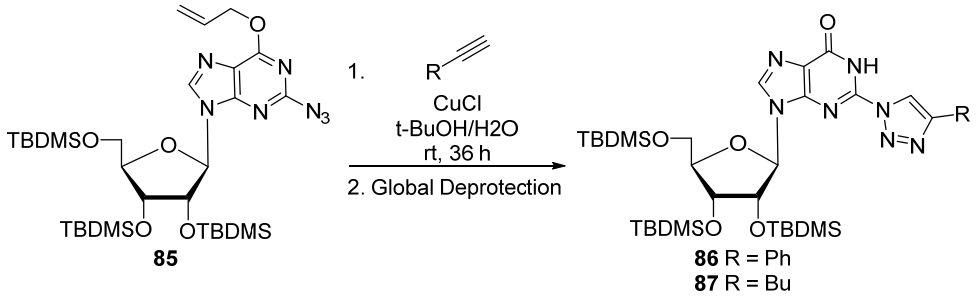

Scheme 20. Synthesis of C-2 Triazolinosine Derivatives[107]

Azido modified pyrimidine nucleosides have also been shown to undergo the

copper catalyzed click reaction.[108-110] Several studies have used the CuAAC with a 5-triazole modified uridine derivative as the attachment point for labeling of ODNs through 5-ethnyluridine.[111-112] Recently, the *in situ* generated 5-azidouracil moiety **88** has also been used.[108] The 5-phenyltriazole modified uridine **89** was prepared by Kumar using a CuAAC between **88** and commercially available phenyl acetylene, Scheme 21.[109] The addition of monomer **89** to DNA proved to significantly destabilize the DNA:RNA duplex, however stacking interactions in the major groove compensated for the destabilization when two to four monomers were incorporated consecutively, Figure 10. Similarly, oligonucleotides that contain a 5-iodo-2'-deoxyuridine in the sequence can be applied for a postsynthetic click modification with ethynyl-modified nile red as a fluorescent label by in situ formation of the intermediate azide forming **89**.[108]

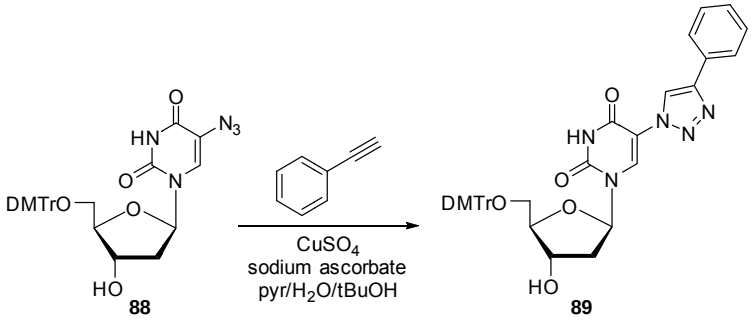

Scheme 21. Synthesis of 5-Phenyltriazole 2'-deoxyuridine[109]

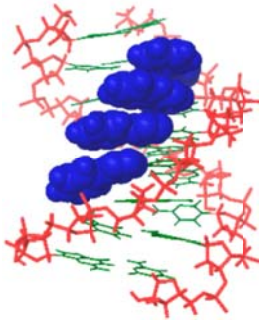

Figure 10. π Stacking interactions[109]

In a study by Neef *et al.*[110] the 5-azido-2'-deoxyuridine **90** and 5-(azidomethyl)-2'-deoxyuridine **91** were synthesized to evaluate the potential metabolic incorporation and detection of azide groups in cellular DNA. The 5-azido-2'-deoxyuridine **90** was found to exhibit a 4 h half-life in water,[113] as a result of its instability it gives little to no detectable labeling of cellular DNA. In contrast, the benzylic azide **91** is stable in solution at 37 °C and, upon addition of fluorescent alkyne derivatives and ensuing CuAAC reaction, gives

robust labeling of cellular DNA forming triazole **92**, Scheme 22.[110]

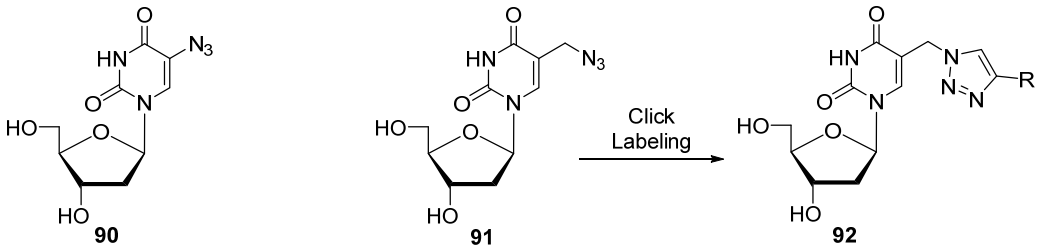

Scheme 22. Click metabolic labeling of DNA[110]

Jin *et al.*[114-115] saw a potential application for the CuAAC reaction by conjugating various carbohydrates with bicyclic furo[2,3-*d*]pyrimidine thymidine analogues active against varicella-zoster virus (VZV), Scheme 23.[116] The concept was varying the carbohydrate moiety would offer improved solubility and molecular recognition of their active parent drugs. Thus, the azido analogue **90** was reacted with various propargylic carbohydrate derivatives in the presence of $CuSO_4$ and sodium ascorbate to give corresponding triazole sugars derivative of type **94**. The biological testing of the aforementioned deprotected substrates of type **94** has yet to be reported.[117]

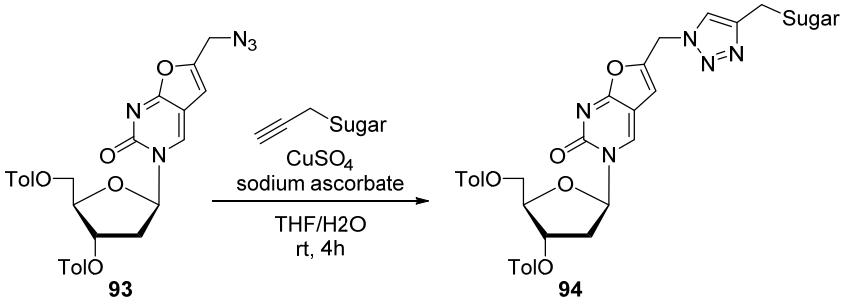

Scheme 23. Synthesis of Bicyclic Pyrimidine Nucleosides[116]

1.2.2.3.2 Strain Promoted Click Chemistry

One of the most important secondary messengers in the human body is 3′,5′-Cyclic adenosine monophosphate (cAMP);[118-120] however, its direct detection has always been troublesome.[121-123] The previously developed detection sensors depend on protein

expression to measure cAMP which is unavoidably insensitive and do not directly detect cAMP.[121-123] The 8-Azidoadenosine 3′,5′-cyclic monophosphate (8-azido cAMP) **95**, a direct analogue of the naturally occurring cAMP, was directly detected in living cells by applying SPAAC.[124] By incorporating a DIFO[41-42, 45] probe via a click reaction, it was possible to directly detect the fluorescent cAMP derivative **96** in living cells without the usual fixing and washing steps, Scheme 24. This approach may allow be a detection method for specific intracellular sites of cAMP derivatives and enable the real time measurement of cAMP fluctuations.[124]

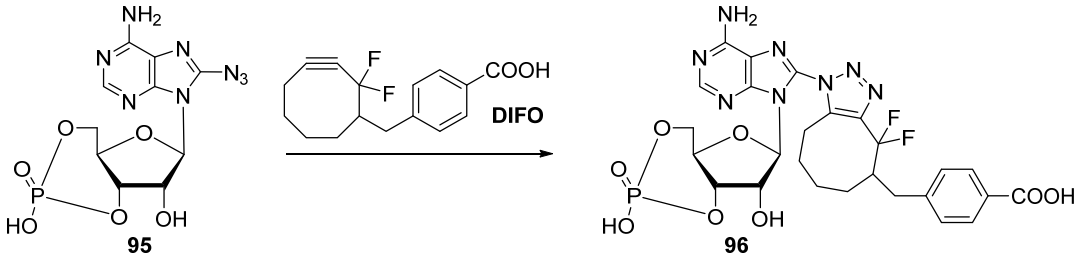

Scheme 24. Strain promoted click chemistry of 8-azido-cAMP[124]

As previously discussed, 5-(azidomethyl)-2'-deoxyuridine **91** was synthesized by the Luedtke group in an effort to overcome the instability observed with 5-azidouridine **90** and to evaluate the potential metabolic incorporation and detection of azide groups in cellular DNA.[110] To evaluate the reactivity of azide **91** in SPAAC, a fluorescent alkyne derivative was added and strain promoted click reaction ensued with significant labeling of cellular DNA forming triazole **97** and bright fluorescence, Scheme 25.[110] Covalent attachment of a bulky substituent to DNA, resulted in a loss of cellular respiration; measured 4h after SPAAC labeling. This tagging method, is useful for the detection of azide-modified DNA near the end of live-cell experiment, especially in cases where fixation and/or copper salts lead to degradation of the specimen.[36]

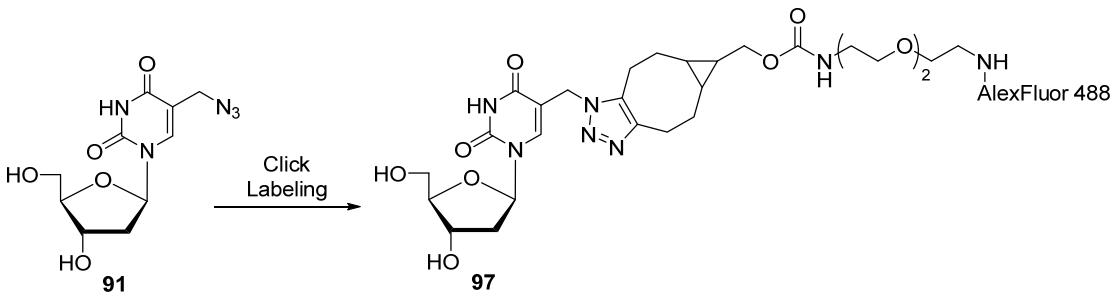

Scheme 25. SPAAC of 5-azidomethyl-2'-deoxyuridine[110]

1.2.2.4 Alkyne Modified Bases

The introduction of an alkyne onto nucleoside bases can easily be accomplished using a palladium catalyzed Sonogashira reaction.[125] Thereby, the synthesis and use of alkyne modified nucleosides is popular with click reactions.

1.2.2.4.1 Copper Catalyzed Click Chemistry

A series of 8-triazole modified adenosine derivatives was prepared by Dyrager *et al.*[126] from 8-acetylene modified adenosine **98** using a Sonogashira coupling and CuAAC, Scheme 26. The modified nucleosides **99** - **107** showed high absorptivities attributed to a single electronic transition; the isopentyl derivative **102** was also noted as having high fluorescence quantum yields.[126] Further studies of the pentyl analogue **103** showed that DNA duplexes are only slightly destabilized by steric clashes of the substituent triazole ring and pentyl chain with the phosphate backbone and sugar moieties. Steric clash would account for a considerable energy cost if the base is to be accommodated in the duplex in its anti-conformation to cause minimal structural perturbations to normal B-DNA.[127] Interestingly, it was found that **103** forms equally stable base pairs not only with thymidine but also normal adenine residues.[127] The excellent photophysical properties of the target compounds **99** - **107** along with an intact hydrogen-bonding pattern make these analogues promising fluorescent probes of nucleic acids.

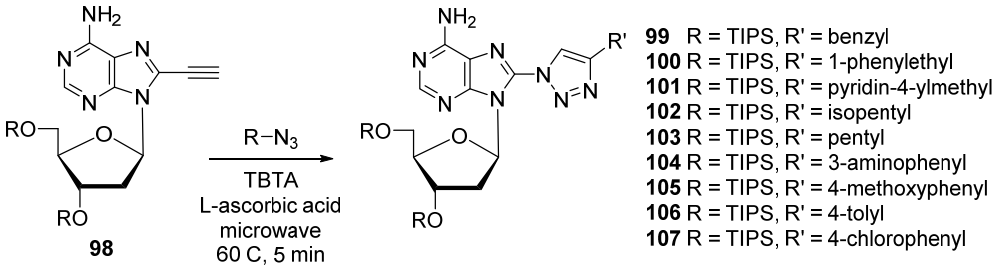

Scheme 26. Synthesis of Fluorescent 8-Triazoyl Adenosine Derivative[126]

Using the same method previously described by Dyrager[126] and Dierckx,[127] O'Mahony and coworkers[128] employed a Huisgen intramolecular [3+2]-cycloaddition between a 2'-modified azide and a disubstituted alkyne **108** by microwave heating at 150 °C for 15 min to afford several novel adenosine containing cyclonucleosides (e.g., **109)**, with fluorescence in the visible range, Scheme 27. Triazole modified adenosine **109** is expected to act as a biological probe because of its inherent fluorescent properties; thereby, circumventing the need for any additional and typically bulky fluorescent labels.[129]

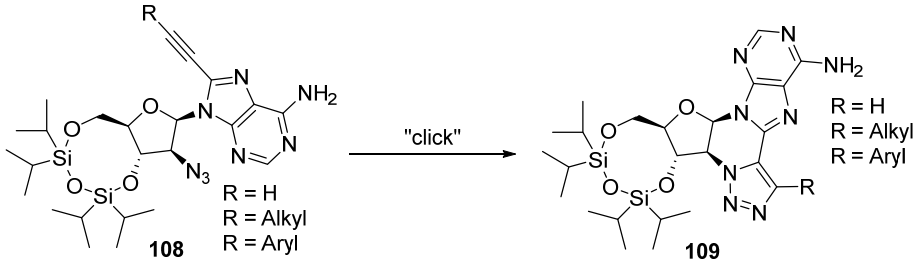

Scheme 27. Cyclonucleosides synthesized using click chemistry[128]

Cosyn *et al.*[105] prepared a series of 1,2,3-triazol-4-yl adenosine analogues **111** – **113** employing copper catalyzed click chemistry on C-2 acetylene adenosine, Scheme 28. Binding affinities of the adenosine triazole derivatives **111** – **113** were measured in CHO (Chinese hamster ovary) cells at the human A_1, A_{2A}, and A_3AR (G-protein-coupled adenosine) receptors. It was found that analogues **111 - 113** constitute a new class of highly potent and selective A_3AR antagonists, partial agonists and agonists.

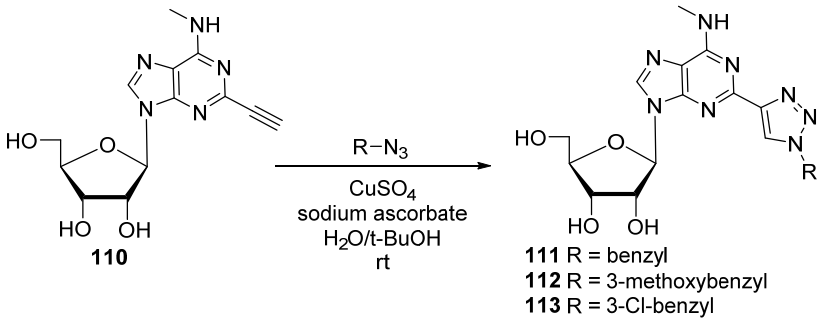

Scheme 28. Synthesis of 2-Triazole-4-yl Analogues of N6-Methyladenosine[105]

The Nielsen group synthesized 5-modifed 2'-deoxyuridine nucleosides using copper catalyzed click chemistry[109, 130] and later incorporated into oligonucleotides using a solid phase oligonucleotide synthesis to give analogues **114** and **115**, Figure 11.[78, 98] The meta-aminomethyl substituent on the phenyl ring of **115** was found to thermally stabilize a 9-mer DNA:RNA duplex, presumably through the partial neutralization of the negatively charged phosphate backbone. Additionally, a high thermal stability was observed in ODN **115** as a consequence of the stacking interactions of the aminomethyl moiety in the major groove.

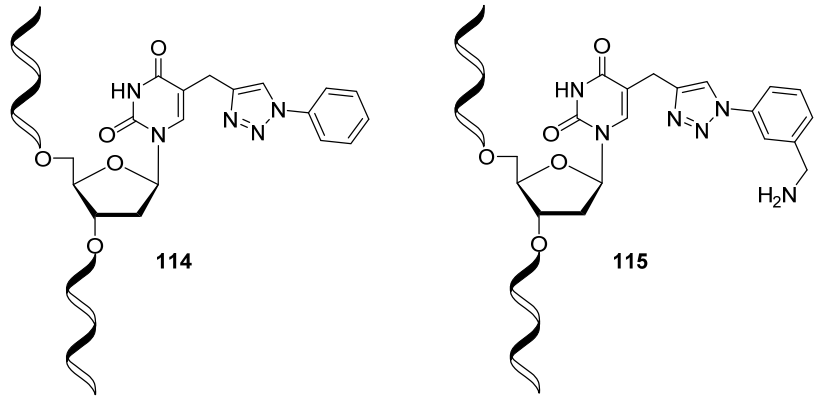

Figure 11. Structure of 5-fuctionalized 2'-deoxyuridine oligonucleotides[78,98]

Gierlich *et al.*[112] developed a CuAAC protocol for the multiple postsynthetic labeling of alkyne modified DNA. They prepared a series of alkyne modified ODNs of type **117** from 5-ethynyluridine **116** and investigated the click reaction using various

azide labels, Scheme 29. Complete conversion to the click product **118** was seen for ODNs that had up to six consecutive 5-acetylene uridine residues. This method is also applicable to long DNA strands obtained by PCR and is currently being investigated for the detection of single nucleotide polymorphism in the human p53 suppressor gene[131] and for the synthesis of backbone branched DNA.[132-134] In another study by Jao and Salic,[135] 5-ethylnyluridine labeled cellular RNA **110** was detected quickly and with high sensitivity using CuAAC with a fluorescent azide partner. Using fluorescent microscopy imaging, it was found that transcription rates vary greatly among the different tissue samples and cells within organs.[135]

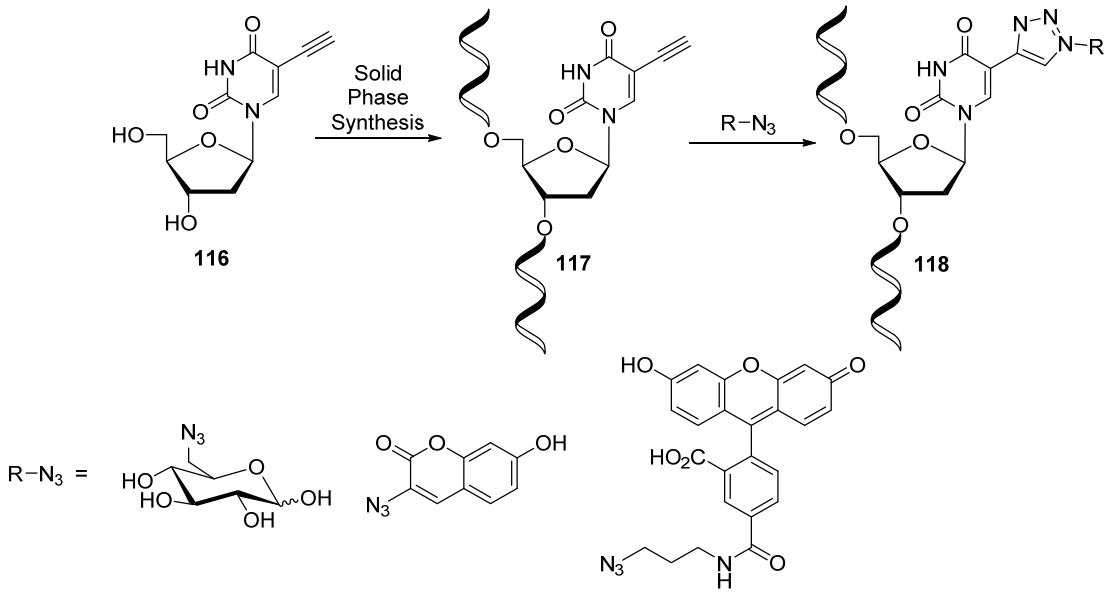

Scheme 29. Postsynthetic Functionalization of Alkyne Modified DNA[112]

The Fujimoto group incorporated the 5-ethynylvinyl-2'-deoxyuridine phosphoramidite into an ODN using standard solid phase synthesis which gave the alkyne modified ODN **119**. Fujimoto *et al.*[136] carried out a CuAAC on alkyne **119** using several different azides which gave photoreactive triazole **120**, Scheme 30. The triazole modified ODNs of type **120** were subjected to photoligation with ODNs containing 3'-

cytosine bases; efficiency of ODN ligation was confirmed by HPLC analysis. The 5-ethynylvinyl-2'-deoxyuridine photosensitive ODN probe was also useful for the construction of a single nucleotide polymorphism (SNP) probe.[136-139]

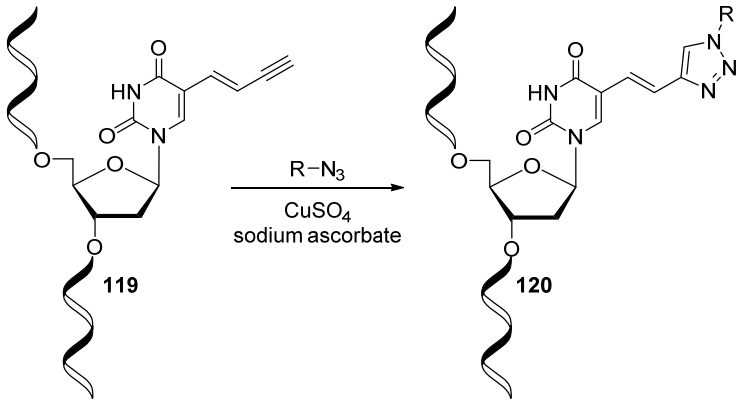

Scheme 30. DNA Photoligation via CuAAC[136]

The Seela group has used CuAAC to introduce two fluorescent labels into a single thymidine monomer, Scheme 31.[134] The 5-tripropargylamine-2'-deoxyuridine **121** via a Sonogashira coupling, then converted it to a phosphoramidite monomer and incorporated it into an ODN. The resulting tripropargyl modified nucleoside **121** was clicked to non-fluorescent 3-azido-7-hydroxycoumarin to give ditriazole derivative **122**. The bis-labeled ODN **122** was less fluorescent than ODNs labeled with a single coumarin triazole because of self-quenching between the fluorophores. However, the tripropargyl analogue **121** was found to slightly stabilize DNA duplexes because of the "clickable" moieties protruding into the major groove of duplex DNA which do not disturb the base stacking.

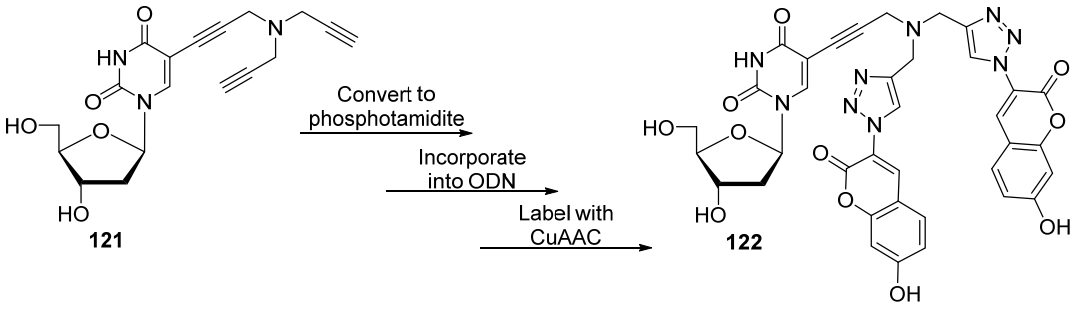

Scheme 31. Synthesis of DNA with branched internal side chains[134]

DNA is an ideal material for the preparation of nano- and microscale assemblies which can be used in nanoelectric devices. Burley *et al.*[111] found that DNA strands of interest can be selectively metallized via the incorporation of 5-acetylene containing nucleotide triphosphates. Thus, the Burley group used a click reaction of acetylene derivative **123** with an azide bearing a terminal aldehyde moiety, as a chemical reporter, to give the click adduct **124**, Scheme 32. Further treatment of the aldehyde-labeled DNA **124** with the Tollens reagent, $[Ag(NH_3)_2]^+$, results in the selective metallization of modified strands of DNA. Experiments to determine whether metallized DNA strands constructed using the aforementioned method conduct electricity are currently underway.[111, 140-141]

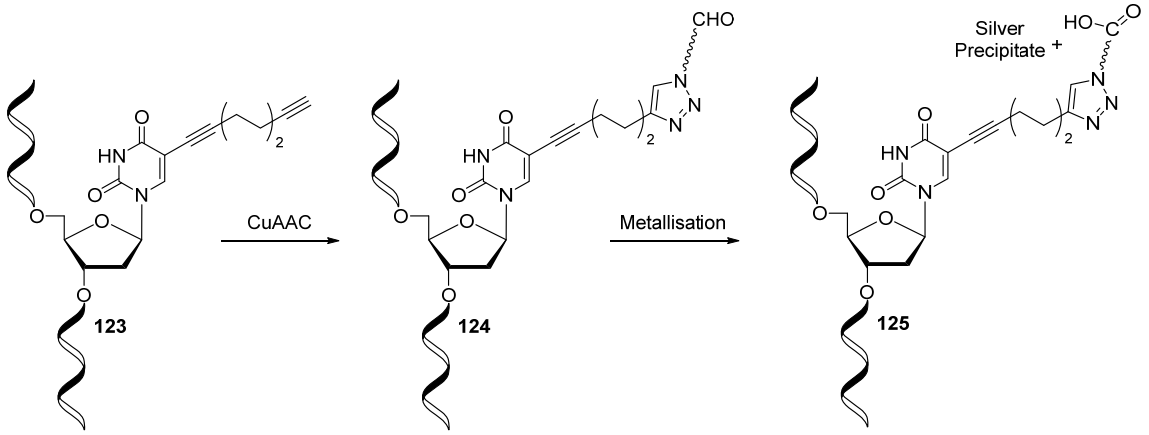

Scheme 32. Directed DNA metallization via CuAAC[111]

The Zhang group developed the novel 5-ethynyl-2′-deoxycytidine[142] (EdC) method for the detection of DNA synthesis *in vitro* and *in vivo* with a comparable sensitivity level to the commonly emplyed and highly cytotoxic[143] 5-ethynyl-2′-deoxyuridine.[144-145] The EdC that was added to culture medium of adenocarcinomic human alveolar basal epithelial cells (A549) were incorporated by cellular polymerases into newly synthesized DNA to give alkynylated DNA strands **126**. These modified DNA strands were then subjected to CuAAC in the presence of a Cy3-azide and $CuSO_4$ which afforded fluorescent the derivative **127** and was visualized with fluorescent microscopy, Scheme 33. Incorporation of EdC can be used for the long term detection and visualization of DNA synthesis because of its non-cytotoxic nature.

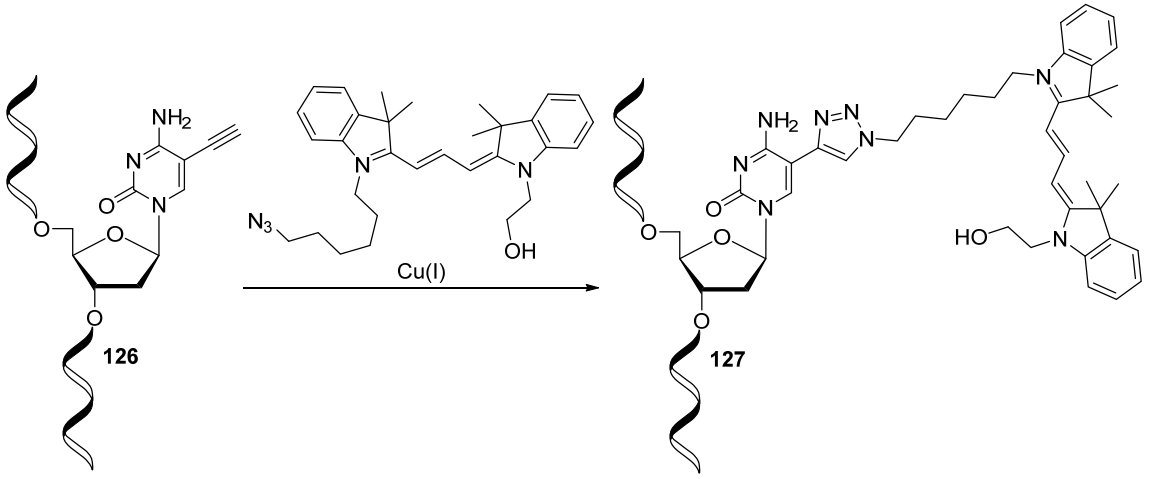

Scheme 33. DNA labeling with fluorescent azide[142]

1.2.2.4.2 Strain Promoted Click Chemistry

Ren *et al.*[146] labeled the 5-amino group of key intermediate 2'-dUTP **128** with either BCN or DIBO to give **129** or **131**, respectively, which were then incorporated into DNA by linear extension using two different templates and a variety of DNA polymerases, Scheme 34. Labeling of the modified extension products (**129** or **131**) with

Cy3-hexylazide via the SPAAC reaction gave either ODN, **130** or **132**, both of which demonstrated the efficient labeling of these cyclooctyne modified ODNs, Scheme 34. The acceptance of the cyclooctyne modified triphosphates (**129** and **131**) as substrates for DNA polymerase substrates in PCR is encouraging for future *in vitro* and *in vivo* biological and medicinal applications.

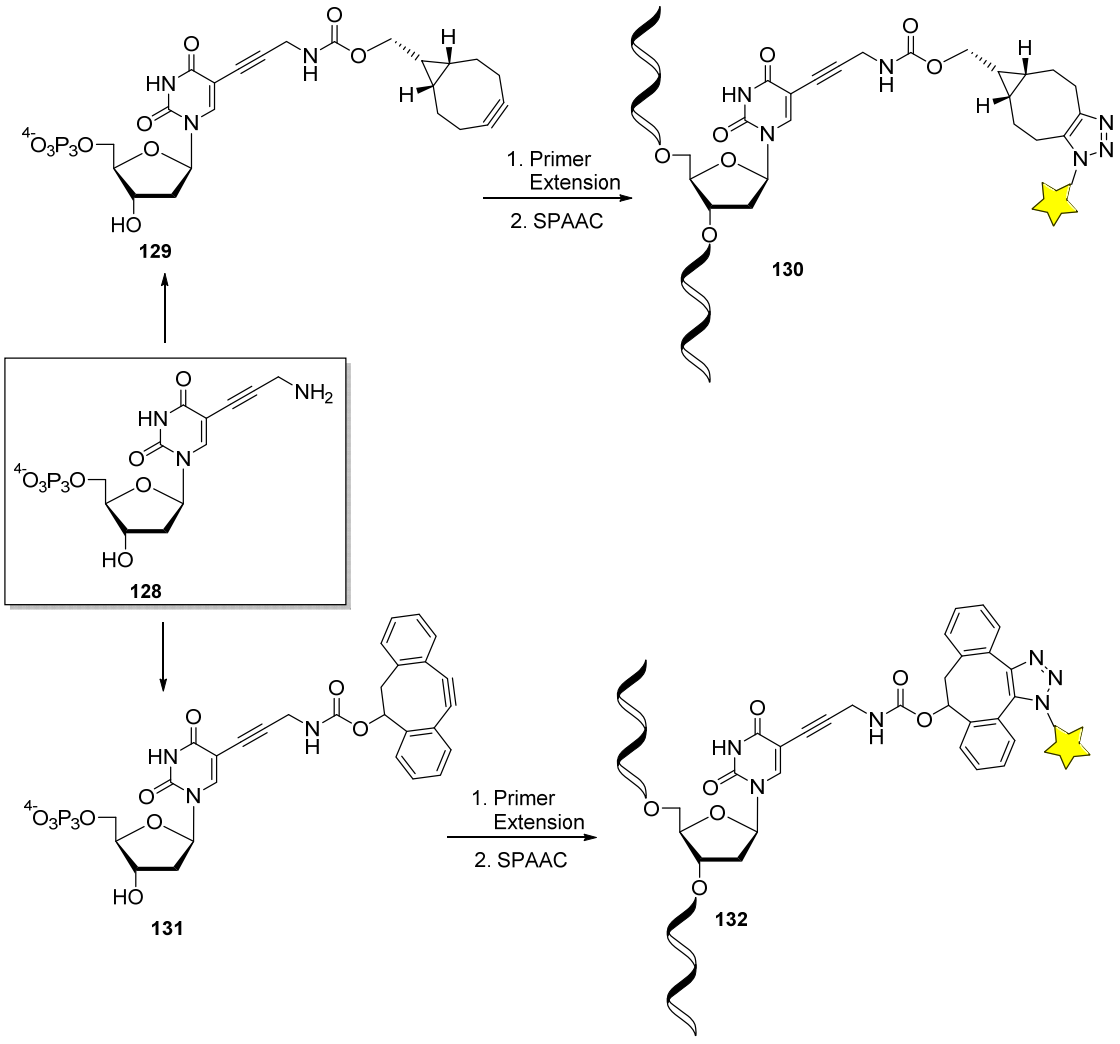

Scheme 34. Labeling of amino-propargyl-dUTP with BCN and DIBO[146]

Rotaxane is a multicomponent molecule consisting of a dumbbell shaped molecule which is threaded through a macrocycle. Recently, the rotaxane architecture has been extended to nucleic acids for DNA nanotechnology,[147-152] topological labels[153-156]

and the stabilization of triplex formation.[157-159] Onizuka *et al.*[160] designed a novel method for templated pseudorotaxane formation that targets nucleic acids using a pair of reactive ODNs, Scheme 35. Thus, the two components Onizuka envisioned were ODN **133** with DBCO in the internal position and a phosphorothioate group at the 3' end and ODN **134** which contains an azide moiety at the internal position and a chloroacetyl group at the 5' end. When reacted together an S_N2 type chemical ligation was observed between the phosphorothioate group (3' end) and chloroacetyl group (5' end). The SPAAC reaction also proceeded between the internal DBCO and azide groups when the two ODNs hybridized with a DNA at the proper position to give pseudorotaxane **135**. Once formed, pseudorotaxane disassociates from its complimentary DNA strand to give ODN **136** which is able to reversibly slip off of the DNA template to give free circular ODN **137**. This new methodology for the formation of a pseudorotaxane with any single stranded nucleic acid using only a pair of ODNs, a SPAAC and a substitution reaction paves the way for a variety of applications including new DNA nanotechnologies and antisense ODNs.[160]

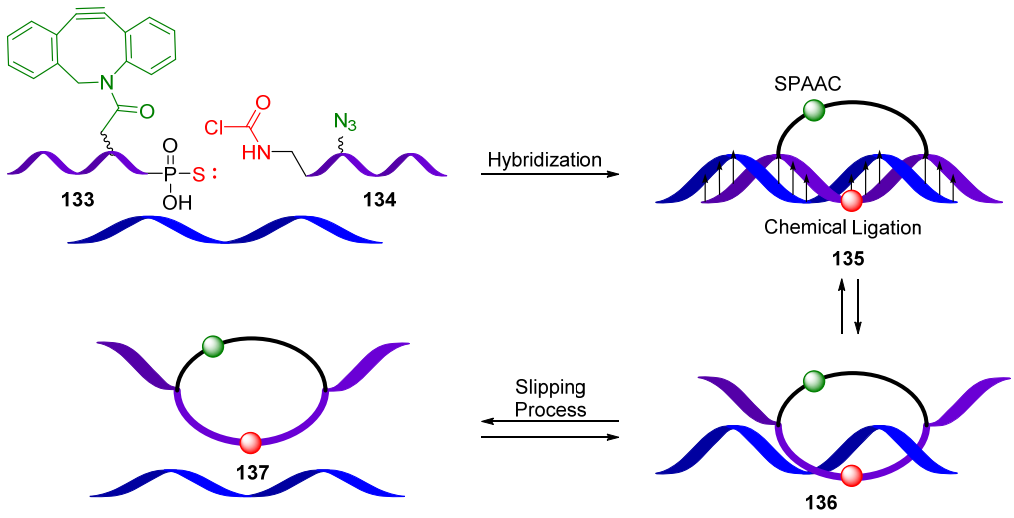

Scheme 35. Schematic representation of pseudorotaxane formation via SPAAC[160]

1.2.2.5 Miscellaneous Strain Promoted Click Chemistry

Several groups including Bertozzi and coworkers,[39-40] Boons[161] and van Delft[95, 162-163] have worked towards the development of a catalyst free click reaction (SPAAC). The SPAAC reaction has been applied to the selective modification of compounds or living cells[40] including live zebrafish[12] and mice.[45] However, one area that remains less explored is the bioconjugation of DNA through the phosphate backbone.

The Taton group described the solid-phase synthesis and characterization of 5'-DIBO modified oligonucleotides **139**, prepared using a new DIBO phosphoramidite **138**, Scheme 36.[164] As expected, the DIBO modified ODN **139** reacted quantitatively with organic azides to give click adducts **140** and **141**. Cyclooctyne modified ODN **139** was also used as a PCR primer for the amplification of a 500 base-pair sequence from bacteriophage λ DNA.[164] Incubation of the crude PCR mixture with fluorescent dye, Texas Red azide, and further agarose gel electrophoresis of the PCR product demonstrated that the amplification with primer **139** had been successful and that the DIBO group remained reactive as indicated by the Texas Red labeled product **140**. A similar labeling method is currently being used by van Delft for the conjugation of RNA to a phosphoramidite modified DIBO.[165]

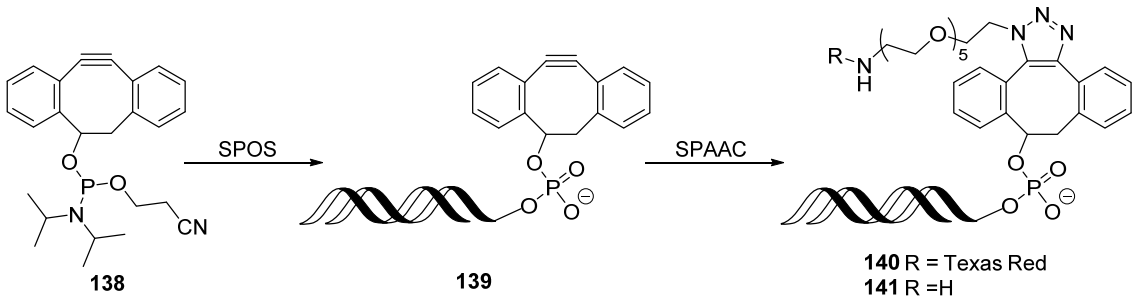

Scheme 36. SPAAC for terminal labeling of DNA[164]

Kim and colleagues developed a method for labeling zinc finger proteins (ZFP)

using SPAAC, Scheme 37.[166] An azide modified ZFP **143** was reacted with DIBO conjugated dye **142** resulting in fluorescently labeled ZFP **144**, Scheme 37. Typically the DNA binding activity of ZFPs labeled by copper catalyzed click chemistry is completely eliminated.[167] However, when ZFPs were labeled using SPAAC to give **145**, the DNA binding activity was retained under native conditions. The labeling strategy using DBCO and an azide modified protein can also be applied for the labeling of other metalloproteins containing copper or iron cofactors.[168]

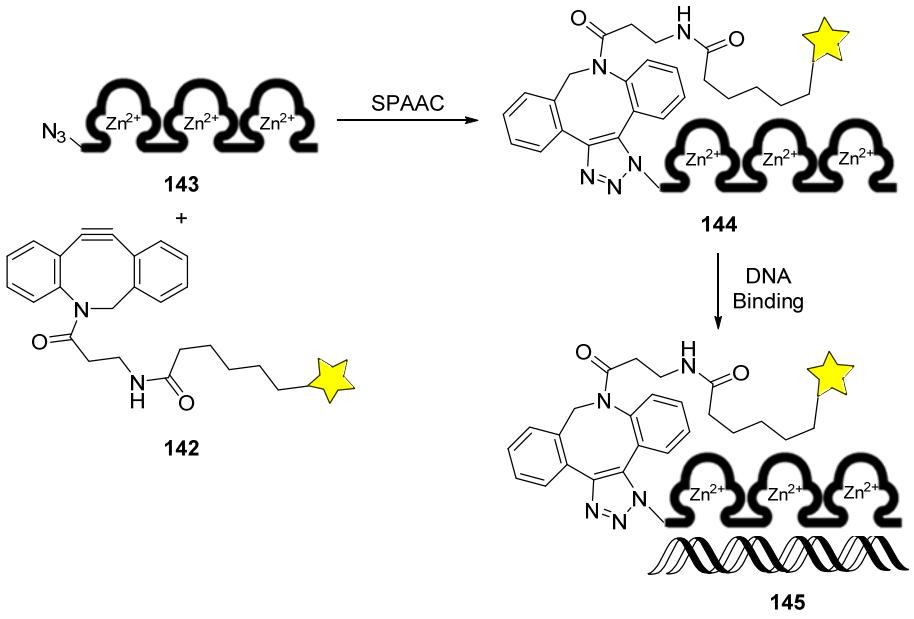

Scheme 37. SPAAC for the conjugation of DBCO-dyes to Zinc finger proteins[166]

Small interfering RNAs have been shown to be powerful tools for silencing expression of specific genes and have the potential to become a class of powerful therapeutics;[169] however, their efficient distribution and intracellular delivery *in vivo* remains challenging.[170] Jayaprakash *et al.*[171] designed a conjugation strategy between RNA ONs and several ligands that should improve cellular delivery of siRNAs. Thus, DIBO modified ON **146** was reacted in a SPAAC reaction with several azides to

quantitatively give click adducts of type **147**, Scheme 38. This procedure served as a foundation for the development of new methods for the functionalization of RNA by click chemistry. Variations of this RNA tagging methodology were recently reported by the Heaney group for solid phase post-synthetic RNA conjugation[172] and by the Rentmeister group for the bioorthogonal site-specific labeling of the 5'-cap structure of eukaryotic mRNAs.[173]

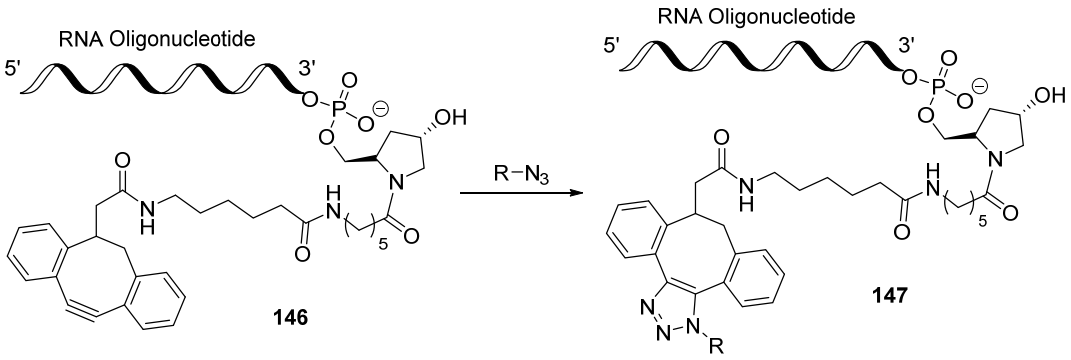

Scheme 38. RNA conjugation by SPAAC[171]

The El-Sagheer group designed a SPAAC reaction for the ligation of templated DNA, Scheme 39.[174] The controlled ligation of templated DNA occurs only in the presence of a complimentary DNA template, ensuring that only the desired DNA duplex is formed; the presence of a single base pair mismatch was shown in being sufficient to inhibit this reaction from occurring. Thus, triazole **149** was formed as soon as the two new DNA strands of **148** became correctly templated with the existing DNA primer. Interestingly, the addition of Cu(I) completely inhibited this SPAAC reaction, probably as a result of the complexation of the cyclooctyne with the copper ions. The labeling protocol has possible applications in biology, genomics[175] and nanotechnology;[176-177] and is currently being used to build topological polymers[178] and very long oligonucleotides.[179]

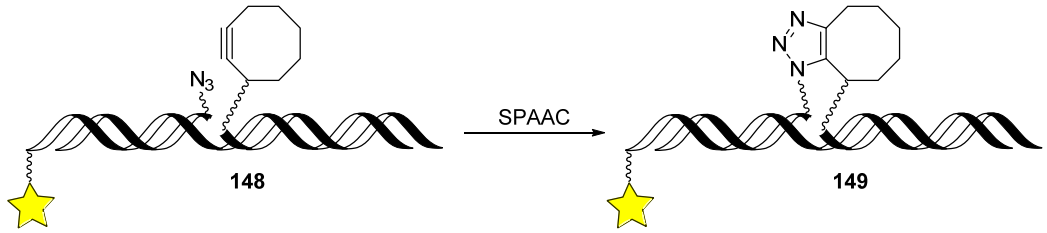

Scheme 39. SPAAC DNA ligation between azide and cyclooctyne labeled ODNs[174]

1.3 Synthesis and Biological Applications of Fluorescent Nucleosides

Naturally occurring nucleic acid components are usually non-fluorescent; therefore, fluorescence has typically been conferred on nucleosides by several methods including extending π conjugation of the heterocyclic base[180-181] or by conjugation with known fluorophores.[182-183] When carefully implemented, fluorescent nucleosides have been used to determine fundamental biochemical transformations and have become instrumental in modern nucleic acids biophysics.[184-186]

1.3.1 Naturally Occurring Fluorescent Base Analogues

Naturally occurring modified nucleosides **150** – **153** are all slightly fluorescent and have been used by Bokacheva and coworkers[187-189] as reporter probes for tRNA, Figure 12. The use of analogues **150** - **152** in observing the structure and dynamics of tRNA has not been widespread because of their weak emissive properties.[190-191] The Wyosine derivative **153**, in contrast, emits strongly and has been used to study the tertiary structure of tRNA.[192]

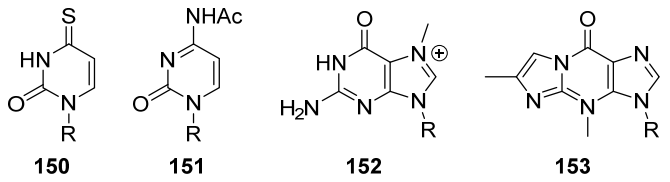

Figure 12. Naturally occurring fluorescent nucleosides. R = ribose

1.3.2 Synthetic Modifications to the Base

Synthetic modifications to the purine and pyrimidine bases have been widely used to confer fluorescent properties to nucleosides and oligonucleotides.

1.3.2.1 Base Replacements

Purine and pyrimidine bases have been replaced with hydrocarbon and heterocyclic rings resulting in modified nucleosides with fluorescent properties Figure 13. Fluorescent analogues **154** and **155** were synthesized by Strassler *et al.,* through a Grignard reaction of a brominated fluorescent molecule and Hoffer's chlorosugar.[193] These compounds were used as probes to study the complexation of nucleic acids with proteins and because of their fluorescent color tunability can potentially be used as biomedical diagnostic tools; they, however, do not form canonical base pairs.[194-196]

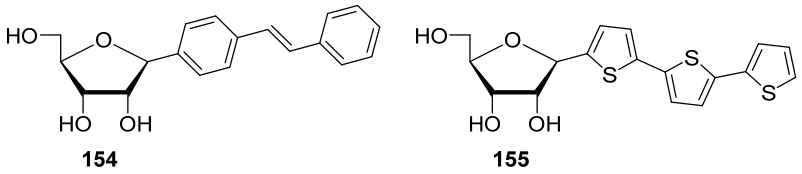

154 **155**

Figure 13. Nucleosides with fluorescent base replacements

1.3.2.2 Isomorphic Base Analogues

Isomorphic nucleobases are heterocycles that bear a resemblance to natural nucleoside bases with respect to their overall size, hydrogen bonding capacity and ability to form Watson-Crick base pairs, Figure 14.[181, 197] The 2-aminopurine **156**, is possibly the most widely recognized fluorescent nucleoside, is an emissive isosteric adenosine analogue[198] and has been used extensively in biochemical studies and assay development.[199-200] Variations of **156**, including modified 7-deaza and 8-aza-7-deaza analogues have been studied by Seela and coworkers as click chemistry substrates.[201]

Isomorphic pyrimidine analogues 5-methylpyrimidin-2-one **157** and pyrrolo-C **158** have been used to probe the RecA DNA complexes in *E. coli*[202] and T7 RNA polymerases, respectively.

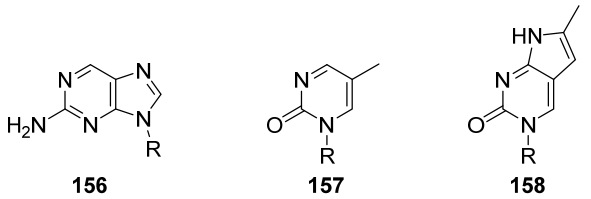

Figure 14. Isomorphic purine and pyrimidine bases

1.3.2.3 Pteridines

Pteridines are fluorescent heterocycles that are comprised of two fused six membered rings instead of the natural configuration of a five membered ring fused to a six membered ring, Figure 15.[203-204] All four pteridines analogues, mainly the guanosine analogue **159** and adenosine analogue **160**, retained their overall absorption and emission characteristics when incorporated into ODNs; however, significant sequence dependent quenching was observed. Incorporating of these nucleoside analogues also typically resulted in destabilizing effects similar to a single base pair mismatch.[205]

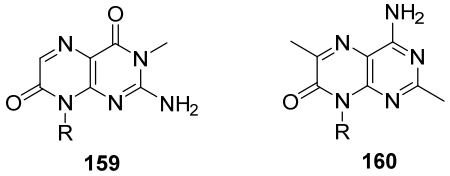

Figure 15. Examples of guanosine and adenosine pteridine analogues

1.3.2.4 Extended Nucleobases

Extending the conjugation of the natural bases by condensing an etheno bridge over the H-bonding face of the purines and pyrimidines has resulted in modified

nucleosides with favorable fluorescence properties,[197] one of the first examples being 1,N^6-ethnoadenine **161**, Figure 16.[206-207] Another approach used by Leonard[208] and Kool[209] involves the introduction of an aromatic ring between the native pyrimidine and imidazole rings (e.g., **162**). These benzo analogues deviate from the natural base's scaffold and thus cannot form Watson-Crick base pairs or be accommodated within a traditional Watson-Crick duplex.[210] The addition of an additional aromatic ring at the periphery of the nucleobase (e.g., **163**) represents another approach utilized by Godde and coworkers to monitor the binding of the HIV-1 Tat protein or of antisense oligonucleotides to the TAR RNA Stem-Loop.[211]

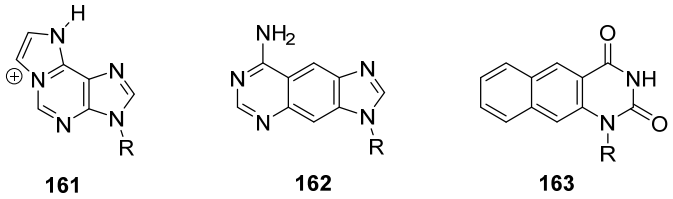

161 **162** **163**

Figure 16. Fluorescent extended nucleobases

1.3.2.5 Conjugation to Fluorescent Molecules

Linking nucleosides to fluorescent chromophores using a palladium mediated cross coupling reaction has been shown to give nucleoside analogues with high emissive properties, Figure 17.[197] Several examples of fluorescent nucleoside conjugates are uridine conjugated to a pyrene[212-213] **164**, phenanthroline[214] **165**, and anthracene[215] **166** which were used to study RNA-small molecule binding,[216] to distinguish between perfect and mismatched complementary oligonucleotides[214] and for genetic analysis to detect point mutations and SNPs,[215] respectively. The hybridization properties of the native nucleosides are maintained because the fluorescent chromophores protrude into the major

groove of the double helix and can be used to detect the presence of abasic DNA sites.[217]

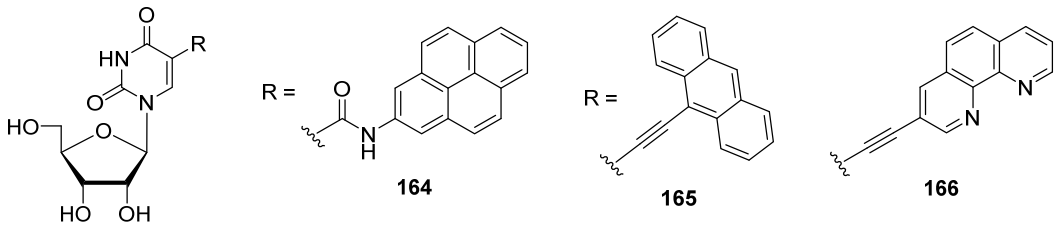

Figure 17. Examples of uridine conjugated to a fluorophore

1.4 Current Status on Drug Discovery Against Protozoal Parasite *Trichomonas vaginalis* and *Tritrichomonas foetus*

1.4.1 *Trichomonas vaginalis* General Introduction

Trichomonas vaginalis is a flagellated protozoan that causes the sexually transmitted disease trichomoniasis in humans. The most common symptoms in women are a frothy malodorous green discharge and edema.[218] *Colpitis macularis*, also known as strawberry cervix, is a clinical sign of this disease, found during microscopic analysis of the tissue.[219-220] The disease is not restricted to the vagina, and may also infect the urinary tract.[221] Women who are infected during pregnancy are pre-disposed to premature rupture of placental membranes, early labor and low-birth infants.[222] Furthermore, Trichomoniasis may also be associated with high-risk strains of human papillomavirus and cervical cancer in women.[219] Trichomoniasis in men is largely asymptomatic, and these men are considered to be asymptomatic carriers of *T. vaginalis*; when men do manifest symptoms, they typically include urethral discharge and dysuria.[219]

The standard treatment for trichomoniasis is 250 mg of metronidazole **167**, given orally, three times a day for 7 days or a single 2 g dose, Figure 18. Metronidazole is administered as a pro-drug that enters the cell through diffusion and is activated in the

hydrogenosomes of *T. vaginalis*.[223-224] Addition of a single electron to the nitro group of metronidzole leads to activation and a nitroso free radical is formed. Cellular response is rapid with cell division and motility ceasing within 1 hour and cell death within 8 h.[225] However, approximately 2.5-5% of all diagnosed cases of this disease are resistant at some level.[226] Resistant infections are treated with larger doses of drug than the typical prescribed 2 g, and for a longer period of time,[227] which is not ideal because patients are at risk for harsher side effects.

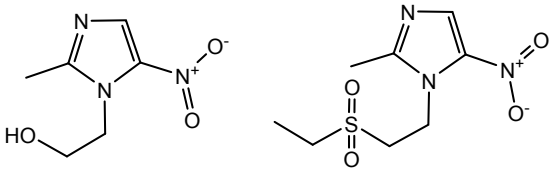

Metronidazole: **167** Tinidazole: **168**

Figure 18. Standard treatment for trichomoniasis

Clearly, new anti-protozoan agents are needed to treat resistant strains of *T. vaginalis*. Although many other nitroimidazoles have been tested against *T. vaginalis*, only metronidazole and tinidazole **168** are available in North America. Unfortunately, all nitroimidazoles have similar modes of activity,[228] so resistance to metronidazole often includes resistance to the other nitroimidazoles.[229]

1.4.2 Drug Discovery Against *Trichomonas vaginalis*

Several studies have focused on the identification of new drugs against *T. vaginalis* and their targets; however, there are really no detailed and systematic studies on potential targets for new drug development. Many different strains of *T. vaginalis* exist and are used for biological and drug discovery studies. When screening potential inhibitors against the parasite, the effects of the inhibitors on various strains need to be

taken into account. Different strains of the same organism behave differently under the same pressures. A study of a small compound library of 3,4-dichloroaniline amides against two well-known strains of *T. vaginalis* (T1 and G3) illustrates this point.[230] These twenty-one compounds, when screened for inhibitory activity, displayed different results with the compounds at the same concentration and performed under the same conditions. In this study, the most effective compound against both strains of the library was amide analogue **169** which possesses a tri-fluoromethyl group in the *meta* position, Figure 19; however, it's inhibitory effect is not as great at that shown by metronidazole.

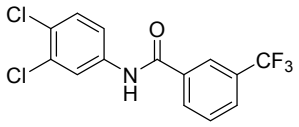

169

Figure 19. 3,4-Dichloroaniline amide as antiparasitic agents

S-Adenosyl-*L*-homocysteine hydrolase is an enzyme that regulates *S*-adenosyl-*L*-methionine-dependent methylation reactions. This enzyme catalyzes the reversible hydrolysis reaction of S-adenosyl-L-homocysteine (AdoHcy) into adenosine and homocysteine. In protozoan parasites, this enzyme exists and functions in a similar fashion to other known AdoHcy hydrolases (ADHY). Trypanosomes in particular possess a unique, highly-methylated 5' cap on mRNA. In trypanosome protozoa, the pathways of methionine/AdoMet/decarboxylated AdoMet/AdoHcy and polyamine metabolism are closely related. These metabolic pathways have both been successfully targeted in the design of trypanocides.[231] A small library of 5'-modified adenosine derivatives, including 5'-deoxy-5'-(iodomethylene)-adenosine (e.g., **170** and **171**), 6-*N*-cyclopropyl **172** and 5'-oxime **173** analogues were screened and some of these molecules blocked growth of *T.*

vaginalis up to 95%, Figure 20.[232] Although IC_{50} determination of the these compounds did not reveal values better than those for metronidazole, the results were highly suggestive of a critical biological role for ADHY hydrolase in this protozoan parasite.

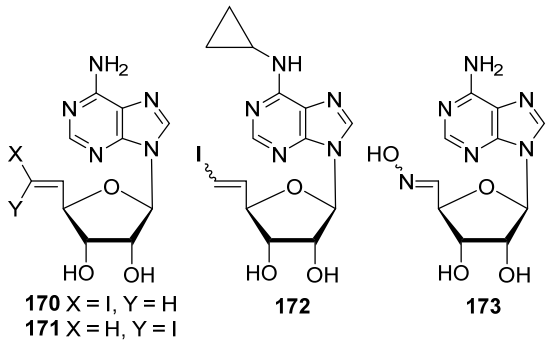

Figure 20. 5'-Modified adenosine analogues and related 6-N-cyclopropyl derivatives.

Nitazoxinide (NIT) **174**, a thiazolide, is a broad spectrum anti-protozoal pro-drug, Figure 21. Following oral administration, it is hydrolyzed to its active metabolite, tizoxanide **175**.[233] Benzologues, **176** and **177**, of each of these drugs were prepared by Navarrete-Vázquez and tested for potency against *T. vaginalis*.[234] Acetyl protected benzologue **159** showed nanomolar activity with an IC_{50} of 68 nM; however, it was significantly less potent than its parent drug NIT, metronidazole and TIZ. Analogue **177** was also less potent than metronidazole, NIT and TIZ. A structure activity assay showed that the insertion of a benzene ring between the nitro and thiazole generated a new anti-protozoal scaffold which can be further explored for cytotoxicity in other parasites.

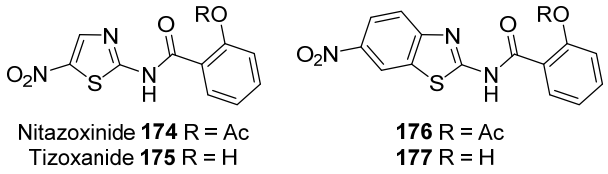

Figure 21. Nitazoxinide and Tizoxanide and their benzologues

A series of novel benzimidazole-pentamidine hybrids were also prepared by the Navarrete-Vázquez group and tested against *T. vaginalis*, Figure 22.[235] An *in vivo* assay showed the 5–methoxy analogue **179** to be two times as active as the commonly used metronidazole and 23 times more potent than its parent drug pentamidine. The methyl analogue **180** and nitro **182** with a methoxy group at 2nd position in the benzene were 4 and 5 times more potent than pentamidine, respectively. Lastly, unsubstituted analogue **178**, methyl analogue **180** and trifluoromethano analogue **181** exhibited the same activity than pentamidine. The results obtained by the authors are promising since several of the compounds tested showed activity greater than or comparable with the current used anti-protozoal drugs.

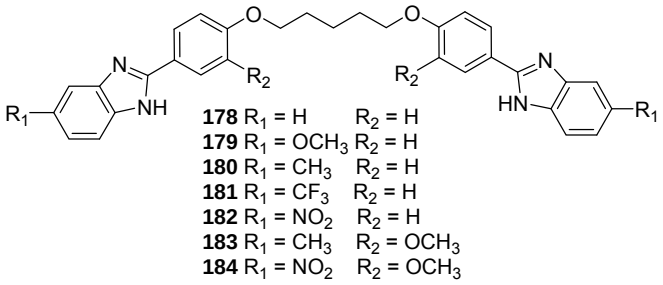

Figure 22. Benzimidazole-pentamidine hybids

Adams *et al.*[236] prepared a small library of aryl-functionalized and ferrocenyl monothiosemicarbazone compounds via a general Schiff-base condensation reaction, Figure 23. The thiosemicarbazone ligands act as bidentate chelating ligands that coordinate ruthenium(II) via the nitrogen of the imine group and the sulfur of the thione group. The ruthenium(II)-arene thiosemicarbazone complexes were evaluated for anti-protozoal activity in the G3 strain of *T. vaginalis*. They determined that in order to have correct charge distribution and therefore parasitic inhibition, an electron withdrawing

group must be present. Thus, the most active compounds **185** and **186** contained a chloro-aryl thiosemicarbazone moiety and exhibited IC_{50} values less than 10 μM.

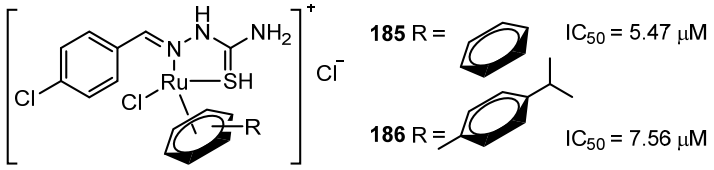

Figure 23. Aryl and Ferrocenyl-derived thiosemicarbazone ruthenium(II)-arene complexes.

1.4.3 *Tritrichomonas foetus* General Introduction

Tritrichomonas foetus, the feline and bovine counterpart of *Trichomonas vaginalis*, is a protozoal parasite that infects the bovine reproductive tract and causes infertility and occasional spontaneous abortions in cattle. It also affects the feline intestinal tract causing diarrhea. Currently there is no FDA approved treatment for animals infected with *T. foetus*. Therefore, the identification of potential molecules that could serve as the basis for new drug discovery against this important veterinary pathogen is warranted.[237-239]

1.4.4 Drug Discovery Against *Tritrichomonas foetus*

Currently there is no FDA approved treatment for animals infected with *T. foetus*; however, there are several notable studies include the effects of vinyl sulfone inhibitors,[240] D-allose and D-psicose,[241] benzimidazoles,[242] hypoxanthine-guanine-xanthine phosphoribosyltransferases,[243] and ronidazole[244] on *T. foetus* infections.

Aronov *et al*. targeted the purine salvage enzyme hypoxanthine-guanine-xanthine phosphoribosyltransferase (HGXPRT) from the protozoan parasite *Tritrichomonas foetus* in their studies, Figure 24.[243] A virtual library of substituted 4-phthalimidocarboxanilides

of type **187** was constructed using methods of structure-based drug design, and was implemented synthetically on solid support. Phenyl analogue **187** was used in combinatorial chemistry to produce a second more focused library of low micromolar inhibitors of HGXPRT. Bromo-phenyl analogue **188** was found to inhibit the growth of *T. foetus* in a concentration dependent manner with an ED_{50} of 2.8 μM. Interestingly, this inhibitory effect can be reversed by the addition of exogenous hypoxanthine demonstrating that parasitic protozoa lack the ability to synthesize purine nucleotides de novo, and rely on enzymes to salvage purine bases from the host.

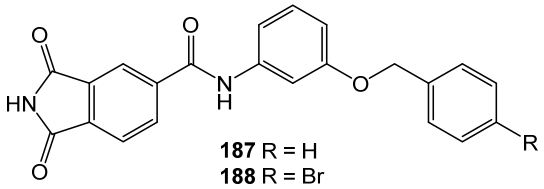

Figure 24. Inhibitors of *Tritrichomonas foetus*

The trichomonicidal activity of benzimidazole analogues were evaluated by Carvalho and Gadelha against *T. foetus*, Figure 25.[242] They found that mebendazole **190** presented the highest inhibitory activity with of IC_{50} 2.3 mM, when compared with albendazole **191** (IC_{50} 9.4 mM) and thiabendazole **189** (IC_{50} 142.6 mM). They also found that the inhibitory effects of the tested benzimidazole analogues **189** – **191** were irreversible. Furthermore, the treated cells demonstrated increased cellular volume, internalization of flagella, nuclear perturbations, multiplication of organelles and cytoplasmic vacuolization. Thus, demonstrating that mebendazole is a viable pathway for the therapy of bovine trichomoniasis.[242]

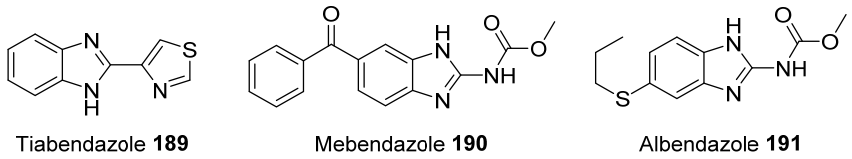

Tiabendazole **189** Mebendazole **190** Albendazole **191**

Figure 25. Benzimidazole analogues evaluated against *T. Foetus*

Kather and coworkers evaluated the *in vitro* susceptibility of feline *T. Foetus* isolates against several known antimicrobial agents, Figure 26.[245] They found that omeprazole **194** showed no effect at concentrations less than 80 μg/mL; however, ronidazole **192** and furazolidone **193** both showed activity similar to that displayed by metronidazole. Interestingly, **192** demonstrated a faster rate in the reduction of trophozite survival than metronidazole.

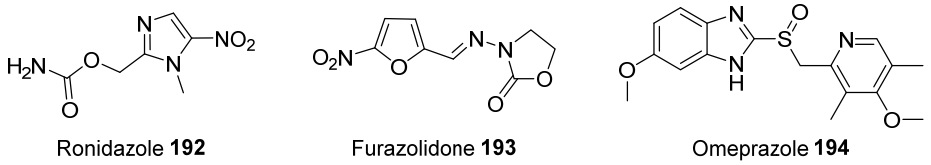

Ronidazole **192** Furazolidone **193** Omeprazole **194**

Figure 26. Imidazole analogues evaluated against *T. foetus*

The Arai group investigated the inhibitory effects of D-allose **195** and D-psicose **196** on *T. foetus*, Figure 27.[241] When either of these sugars were cultured in a medium including a dose of ED_{50} metronidazole, the parasite density was significantly less than in a medium of metronidazole alone. Although, it is known that the mechanisms of the two sugars used in this study are not the same, the authors hypothesize that they may interfere with the electron transport chain and thus reinforce the action of metronidazole. The dosage of metronidazole given could, therefore, be lowered and thus the development of drug resistance of protozoal parasites could be circumvented.

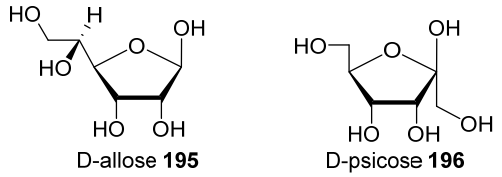

Figure 27. D-allose and D-psicose tested against *T. foetus*

Nisha and coworkers described the Cu(I)Cl mediated synthesis of N-propargylated-isatin-7-chloroquinoline conjugates (e.g., **197-199**).[246] The prepared bis-conjugates were tested for their *in vitro* activity against *T. foetus*, Figure 28. Preliminary analysis revealed that the addition of the electron withdrawing chlorine atom (e.g., **198**, IC_{50} 11.3 μM) enhanced the activity profile over the addition of an electron donating methyl group (e.g., **199**, IC_{50} 24.5 μM) or unsubstituted parent scaffold **197** (IC_{50} 22.2 μM). Studies with human cell lines showed that these analogues are devoid of virtually all cytotoxic activity and thus are an excellent starting point for the synthesis of new pharmacological scaffolds against *T. foetus*.

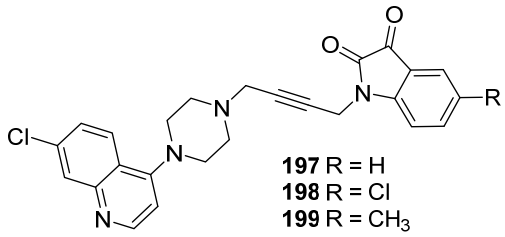

Figure 28. N-propargylated-isatin-7-chloroquinoline conjugates tested against *T. foetus*

2 Research Objectives

The first objective of this dissertation was to develop and study *in vitro* and *in vivo* the novel click chemistry of azido modified purine and pyrimidine bases with cyclooctynes, Figure 29. These analogues were intended to be used (1) to explore the strain promoted click chemistry (SPAAC) of azido nucleosides at the monomer level, (2) to investigate the properties of click adducts for the fluorescent imaging of live cells and (3) to explore the sparsely known strain promoted click chemistry on azido modified DNA or RNA.

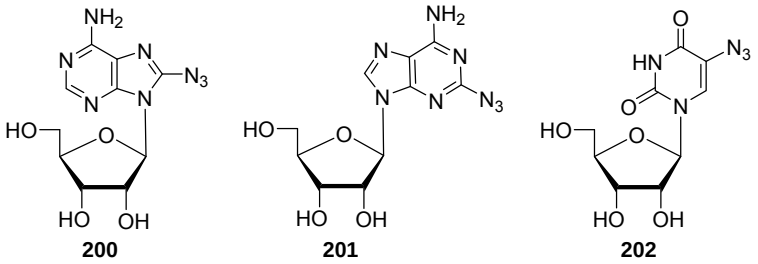

Figure 29. Azido modified nucleosides for SPAAC

Unsubstituted nucleosides are typically weakly fluorescent and therefore not suitable for fluorescent tagging in living systems. However, direct conjugation of a triazole ring with a nucleobase at the C2, C5 and C8 position results in nucleoside derivatives with fluorescent properties. Relatively few studies examples have explored the exploitation of the inherent fluorescent properties of modified purine nucleosides as fluorescent reporters. Furthermore, visualization of living cells using pyrimidine based click adduct nucleosides without the use of fluorescent reporters has yet to be described.

Thus, the proposed synthetic approach targets the most underdeveloped synthetic click precursors in nucleosides; azide modified nucleobases. The underdeveloped strain promoted azide-alkyne cycloaddition (SPAAC) in nucleosides will be explored to obtain

fluorescent triazole adducts. The proposed click substrates are designed having the azido group on the heterocyclic base which are suitable for eventual conjugation with cyclooctynes designed by Bertozzi, Boons, or van Delft.

The click reaction between non-fluorescent azido nucleosides (e.g., **200**-**202**) and a cyclooctyne directly should yield a triazole product (e.g., **203**-**205**) with fluorescent properties without the need for additional modification to achieve visualization. I hence endeavored to investigate the fluorescent properties of click adducts in live cancer cells using fluorescent microscopy. Fluorescence lifetime imaging microscopy (FLIM) will also be used to characterize the *in vivo* lifetime of several of the synthesized triazole adducts in living cancer cells. The formation and presence of the desired triazole analogues will also be determined in living cancer cells by comparing the observed *in vivo* and *in vitro* lifetime values.

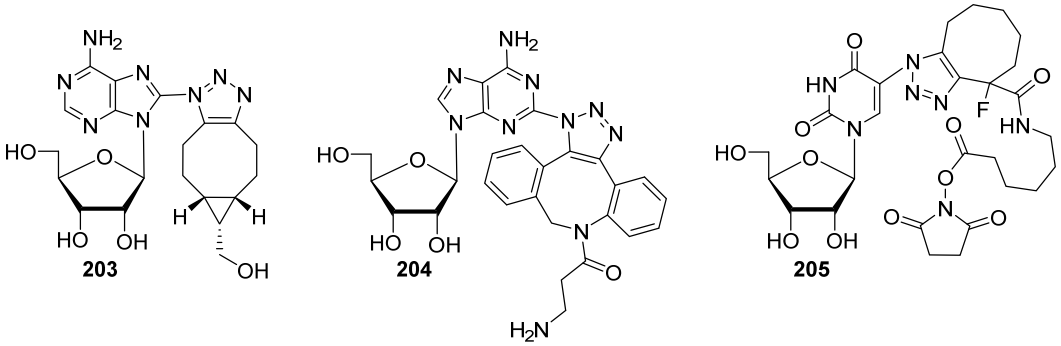

Figure 30. Fluorescent click adducts for live cell imaging

Methods for the synthesis of azido-nucleobase modified 5'-triphosphates and the possibility of performing click chemistry on such modified nucleotides at the polynucleotide level will also be explored. The desired triphosphates could be incorporated into RNA and DNA chemically or enzymatically with the aid of polymerases. Azido modified nucleosides are typically incompatible with solid phase

synthetic methods because of the known reduction reaction between the azide moiety and the P(III) present in the requisite phosphoramidite reagent. When the azido modified DNA or RNA is coupled through a click reaction with a cyclooctyne, a fluorescent oligonucleotide will be formed. The fluorescence can be utilized for direct visualization of native DNA or RNA in live cells without the need for the traditional fluorescent dyes.

The second objective of my dissertation explores the application of the click chemistry methodology established in the first objective of my dissertation to study the cellular targets in parasites and bacteria. Thus, initially the anti-protozoal properties of a library of purine and pyrimidine nucleosides with base and sugar modifications would be evaluated against protozoan parasites *Trichomonas vaginalis* and *Tritrichomonas foetus*. Following characterization of cytostatic profiles, promising analogs will be modified with an azide group on its nucleobase. The resulting adducts of a click reaction between the azido modified substrate and cyclooctyne can be used for investigation. Their inherent fluorescent properties could be exploited to study their mechanism and cellular targets in parasite containing cells via fluorescent microscopy or biotin and streptavidin tagging.[247]

The third objective of this dissertation was to study the transfer of the protruding methyl group present from S-adenosyl-L-methionine (SAM), when SAM is in the tRNA(m1G37)methyltransferase (TrmD) binding pocket. I endeavored to synthesize constrained and activated S-adenosyl-L-methionine (SAM) analogues which mimic the naturally occurring bent conformation of SAM in the TrmD binding pocket. The bicyclic nucleoside derivatives having 9, 10, or 11 membered rings bridging from the C5' thioether to either the 3' or 2' OH groups could be undertaken using several methods including lactonization, lactamization or metathesis methods. These cyclic analogues

could be potential inhibitors of tRNA and can be utilized as probes to study the transfer of the methyl group. To probe the mechanism of action of the TrmD enzyme an analogue with an EnYn group on the sulfur instead of a methyl can be prepared. The EnYn analogue can be used in reactions with methyltansferases, enzymatic tagging and click chemistry for eventual introduction of a fluorophore.

3 Results and Discussion

3.1 Design, synthesis and click chemistry of C2 and C8 azido modified purine and C5 azido modified pyrimidine analogues.

Typically purine nucleosides can be conveniently modified at the C2, C6 and C8 positions and pyrimidine nucleosides at C5 or C6 positions because these modifications remain in the major groove and do not affect the formation of the DNA duplex.[248] Even bulky groups introduced in these positions are typically well tolerated, making them one of the best sites for derivatization. Sugar modifications on nucleosides normally change the characteristics of the parent compound making them not ideal of tagging. Furthermore, tagging at the 3' and 5' hydroxyl groups impedes phosphorylation by native kinases possible changing the mechanism of action of the parent drug. Thus, the initial targets of my dissertation were the synthesis of C2 and C8 position azido modified purines and C5 modified pyrimidine nucleosides and nucleotides which are suitable for further modification via the SPAAC. Introduction of a triazole ring to either the purine or pyrimidine rings results in nucleosides with fluorescent properties that can be used for fluorescent microscopy.

3.1.1 SPAAC of 8-Azidoadenine Nucleosides and Nucleotide

3.1.1.1 Preparation of Substrates

The 8-azidoadenine nucleoside analogues **200-203** have been traditionally prepared using the methodology as reported by Holmes.[249] I found, however, that bromination of adenosine **206** with 1.75 equivalents of 1,3-dibromo-5,5-dimethylhydantoin (DBH) in DMF[250] gave the corresponding 8-bromo derivative **210**

in 45% yield after column chromatography. Further treatment of bromo analogue **210** with sodium azide in DMF at 65 °C for 12 h gave 8-azido derivative **200** in good yields, Scheme 40. Tracking the progress of this azidation can be troublesome because the R_f of the bromo and azido analogues are similar; therefore, the progress of the reaction must be tracked by integrating disappearance of H2 of **210** at 8.10 ppm and appearance of H2 at 8.09 ppm for product **200** in the ^{1}H NMR spectra. The arabino analogue **214**, fluoro-arabino analogue **215** (see section 3.4.3 for detailed discussion) and deoxy analogue **216** were all prepared in a similar manner.

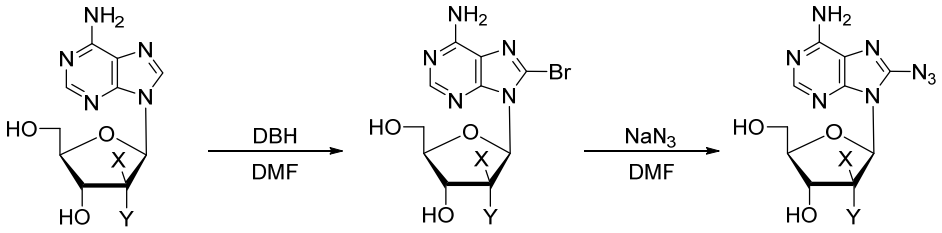

206 X = H, Y = OH
207 X = OH, Y = H
208 X =F, Y = H
209 X = H, Y = H

210 X = H, Y = OH
211 X = OH, Y = H
212 X =F, Y = H
213 X = H, Y = H

200 X = H, Y = OH
214 X = OH, Y = H
215 X =F, Y = H
216 X = H, Y = H

Scheme 40. Synthesis of 8-Azidoadenine Nucleosides

3.1.1.2 SPAAC Reaction

The reaction between the equivalent amounts of 8-azidoadenosine[249] **200** and symmetrically fused cyclopropyl cyclooctyne[162] **217** occurred efficiently in an aqueous solution of acetonitrile (ACN) at ambient temperature (3 h) to produce a triazole **203** in 96% yield after silica gel chromatography, Scheme 41. I was also able to purify the reaction by direct injection into the HPLC; thus, the entire reaction mixture was injected into a into a Phenomenex Gemini semi-preparative RP-C18 column (5μ, 25 cm X 1 cm) via 2 mL loop and eluted with isocratic mobile phase mixture 17% CH_3CN in H_2O at a flow rate = 2 mL/min to give **203** (94%) as a white solid t_R = 4.5 – 8.2 min. The reaction

also occurred efficiently in MeOH, EtOH and Opti-MEM cell culture media, once again showing that the click reaction can proceed efficiently in any aqueous or organic media as long as both substrates demonstrate suitable solubility in the reaction solvent.

The reaction between 8-azido-9-(β-D-arabinofuranosyl)adenine **214** or 8-azido-2'-deoxy-2'-fluoro-9-(β-D-arabinofuranosyl)adenine **215** and **217** (OCT) also proceeded smoothly (3 h, rt) in ACN/H_2O (3:1) to give the corresponding triazole products **219** and **221**, quantitatively. Both of these reactions were easily monitored by TLC since the product formed a more polar spot with a distinctive blue fluorescent color. Analogous treatment of 8-azido-2'-deoxyadenosine **216** with **217** gave the click product **222** (97%), the crude reaction mixture was passed through a 0.2 μm PTFE syringe filter, and then similarly injected into a semipreparative HPLC column (Phenomenex Gemini RP-C18 column; 5 μ, 25 cm × 1 cm) via a 2 mL loop. The HPLC column was eluted with an isocratic mobile phase mixture of 17% CH_3CN/H_2O at a flow rate of 2.0 mL/min to give **22** (77%) as a mixture of inseparable regioisomers (t_R = 13.0 – 16.2 min). The reaction of azide **201** with biotin modified OCT **235** afforded adduct **238** (100%, 57% purified yield). The HPLC purification and ^1H NMR of this compound was quite complex because of the large biotin modification; however, biotin tagging using click chemistry is important because the biotin-avidin interaction is commonly used by biochemists to detect and/or purify proteins and DNA. A summary of the click reaction conditions between the 8-azidoadenine nucleosides and cyclooctynes can be seen in Table 2.

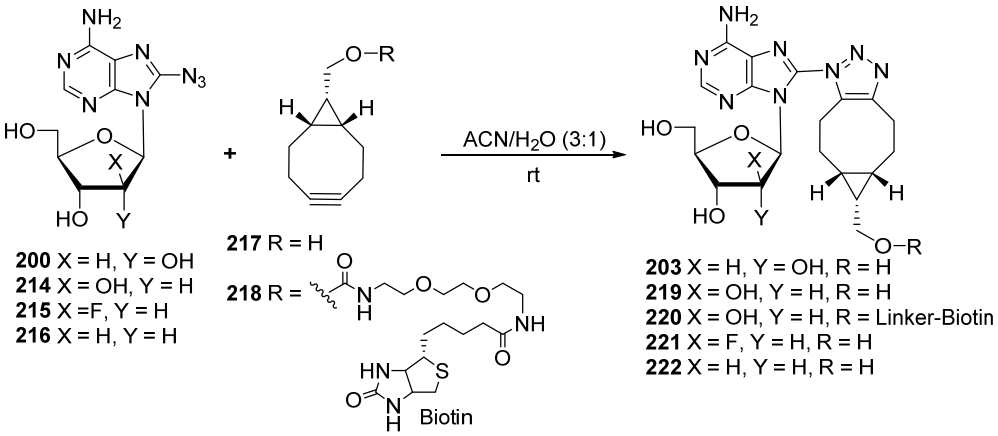

Scheme 41. SPAAC on 8-Azido Adenine Nucleosides

The kinetic analysis presented in Figure 31A showed that click reaction between **200** and **217** initially occurred very rapidly (60% conversion in 20 minutes) and then plateaued forming little new product after 70 minutes. Sequential ^{1}H NMR scans of this reaction showed that it proceeded without the formation of any byproducts. The profile for the reaction was measured by integrating disappearance of H2 of **1** at 8.07 ppm and appearance of H2 at 8.28 ppm for product **7** on ^{1}H NMR spectra. The reaction has a second order rate constant of 0.11 $M^{-1}s^{-1}$, Figure 31B, which is similar to the previously published reaction of OCT **217** with benzyl azide.[162]

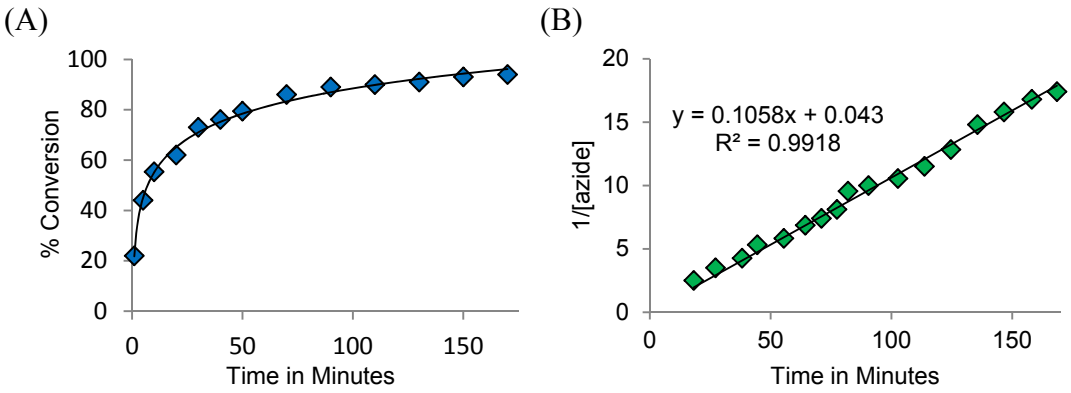

Figure 31. (A) The kinetics profile of the SPAAC of a 23 mM solution of 8-azidoadenosine **200** and cyclooctyne **217** in ACN-d6/D2O (3:1, *v/v*) as monitored by 1H NMR. (B) The rate plot for SPAAC of **200** and **217**. The second order rate constant was calculated by plotting 1/[azide] as a function of time. Data are plotted to within 90% conversion to the triazole products.

The click reaction of 8-azidoadenosine **200** with more complex cyclooctynes including strain modulated dibenzylcyclooctyne[251] **223** or electronic modulated monofluorocyclooctyne **227** in MeOH produced the triazoles modified with a terminal amine **224**, Scheme 42, or typically "reactive" *N*-hydroxysuccinimide (NHS) ester **228**, quantitatively as 1:1 mixture of regioisomers, Scheme 43. The reaction of **200** with **223** was sluggish and required overnight heating at 50 °C, while coupling of **200** and **227** was completed at ambient temperature overnight. Goddard and Bertozzi noted that although the aryl ring fusion may enhance the cyclooctyne ring strain; however, the sluggish reactivity of DBCO **223** with azides can be attributed to the "flagpole" hydrogen atoms *ortho* to the aryl/cyclooctyne ring junction which decrease reactivity by steric interference with the azide in the transition state.[44, 252]

Furthermore, 8-azidoadenine nucleosides **201** or **203** react efficiently with **223** to give the corresponding triazole products **225** and **226**. Even though **223** is not immediately soluble in acetonitrile and water (3:1 *v/v*), overnight heating at 50 °C of **200** with **223** similarly afforded **224** in high yields. Thus, after 16 h, the crude reaction mixture was purified using RP-HPLC. The HPLC column was eluted with an isocratic mobile phase mixture of 40% CH_3CN/H_2O at a flow rate of 1.0 mL/min to give **224** as a mixture of inseparable regioisomers t_R = 15.5 – 23.0 min.

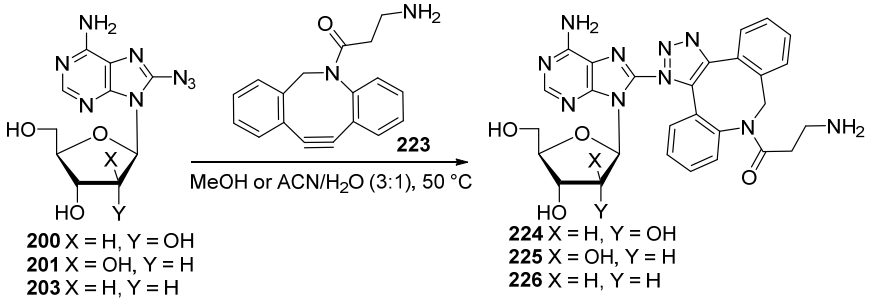

Scheme 42. SPAAC on 8-Azidoadenosine and Analogues with Dibenzyl Cyclooctyne

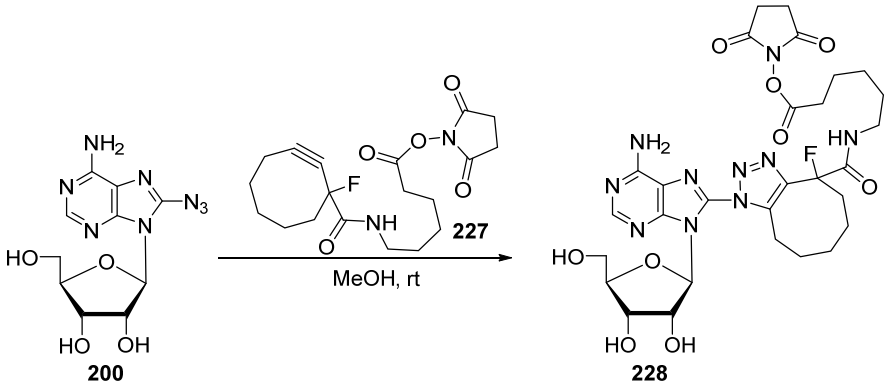

Scheme 43. SPAAC on 8-azidoadenosine with Monofluoro Cyclooctyne

Since click chemistry for labeling oligonucleotides is an emerging field,[103] I established a protocol for the SPAAC of azido base modified nucleotides with cyclooctynes. Thus, the click reaction of commercially available 8-azidoadenosine 5'-triphosphate tetralithium salt **229** and symmetrically fused cyclopropyl cyclooctyne **217** (OCT) in aqueous ACN efficiently gave the triazole product **230** in 92% yield, Scheme 44. The reaction was conducted at ambient temperature in an NMR tube, with no stirring, inside of the NMR spectrophotometer to study the kinetic profile of the reaction; therefore, the reaction would have probably occurred faster under typical reaction conditions that include constant vigorous stirring.

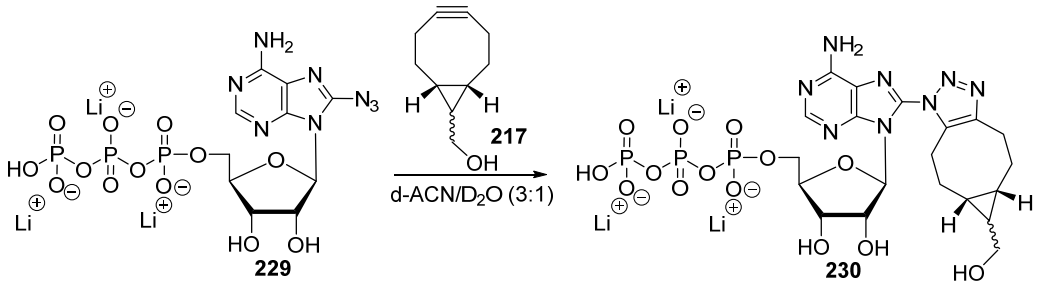

Scheme 44. SPAAC on 8-azidoadenosine 5'-triphosphate tetralithium salt

A ^{1}H NMR kinetic analysis of the click reaction between is depicted in Figure 32 and showed that reaction also occurred rapidly (46% in 20 minutes, 87% in 2 h) and did

not yield any undesired byproducts. The kinetic study shows a similar reaction profile and rate constant to the reaction between azide **200** and cyclooctyne **217** which initially occurred very rapidly and then plateaued forming little new product after 70 minutes. Thus, this reaction also has a second order rate constant of 0.07 $M^{-1}s^{-1}$, Figure 32B.

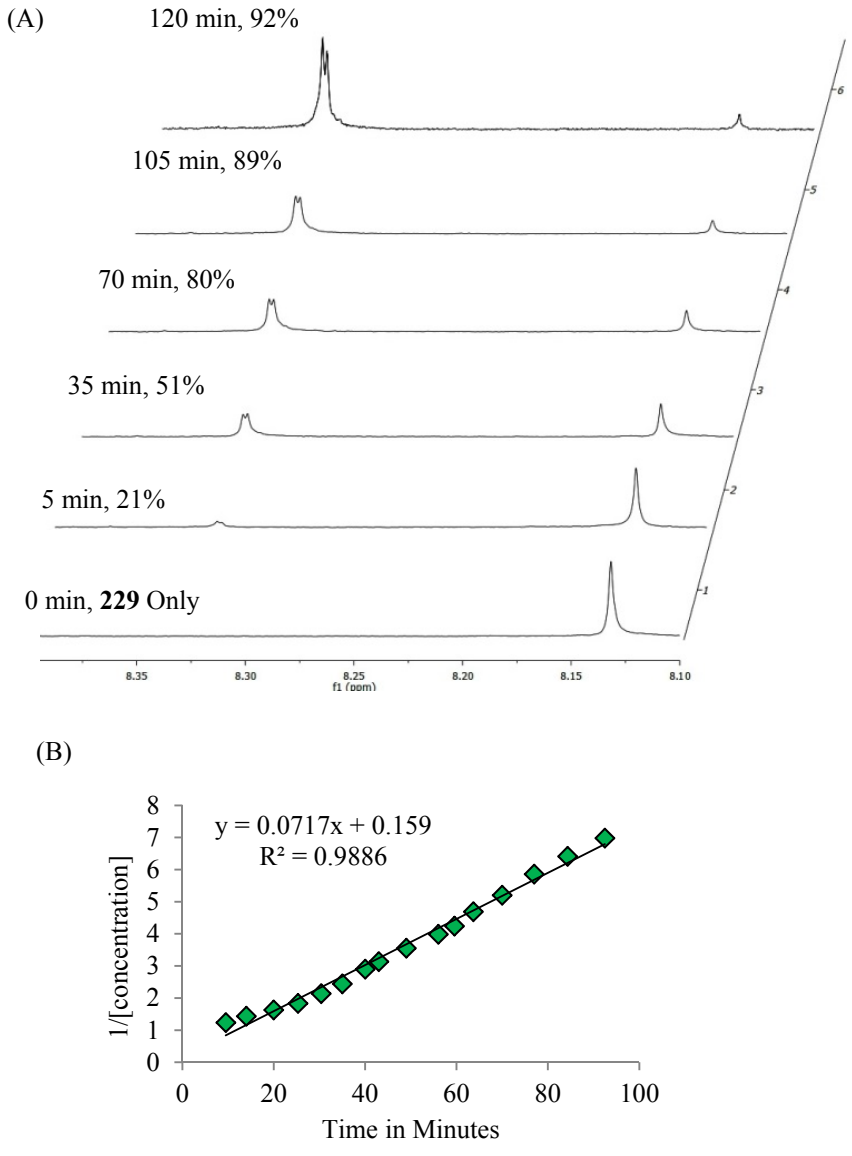

Figure 32. (A) Monitoring of the ^{1}H NMR kinetic profile of the reaction between 8-azidonucleotide **229** and cyclooctyne **217**. (B) The rate plot for SPAAC of **229** and **217**.
The second order rate constant was calculated by plotting 1/[azide] as a function of time. Data are plotted to within 90% conversion to the triazole products.

Azide	Cyclooctyne	Product	Time	Temp	Solvent	Yield [%][a]
200	**217**	**203**	3 h	rt	ACN/H_2O (3:1)	98 (96)[b]
200	**217**	**203**	3 h	rt	MeOH	98
200	**217**	**203**	3 h	rt	EtOH	98
200	**217**	**203**	3 h	rt	Cell Culture Media	98
214	**217**	**219**	3 h	rt	ACN/H_2O (3:1)	100 (93)
214	**218**	**220**	3 h	rt	ACN/H_2O (3:1)	100 (71)[b]
215	**217**	**221**	2 h	rt	ACN/H_2O (3:1)	98
216	**217**	**222**	3 h	rt	ACN/H_2O (3:1)	100 (96)[b]
200	**223**	**224**	16 h	50 °C	ACN/H_2O (3:1)	100 (98)[b]
214	**223**	**225**	16 h	50 °C	MeOH	100 (95)[b]
216	**223**	**226**	16 h	50 °C	MeOH	100 (95)[b]
200	**227**	**228**	16 h	rt	MeOH	98

[a] Based on ^{1}H NMR. Yields for the products purified on a silica gel column are in parenthesis.
[b] Purified by RP HPLC

Table 2. Summary of the click reaction conditions between 8-azido adenine nucleosides and cyclooctynes

3.1.2 SPAAC of 2-Azidoadenosine

The CuAAC for the introduction of 1,2,3-triazole at the C8 position or on the sugar in the adenosine scaffold is very popular; however, CuAAC on 2-azido adenine nucleosides (e.g., **201**) is sparsely known with very few examples shown in literature.[105-107, 253] Moreover, the SPAAC reaction of 2-azidoadenosine **201** is currently unknown.

3.1.2.1 Preparation of Substrates

The 2-azidoadenosine **201** can be prepared using a modified version of the Schaeffer procedure, Scheme 45,[104, 254] or is commercially available. Thus, commercially available 2,6-dichloropurine **232** is coupled to 1-*O*-acetyl-2,3,5-tri-*O*-benzoyl-β-D-ribose **231** in the presence of stannic chloride to give the corresponding 2-chloro modified nucleoside **233** which after treatment with hydrazine and sodium nitrite in an acid

solution gives target azide **201**, Scheme 45. Cladribine **233** is commercially and can also be used as a convenient precursor for azide **201**.

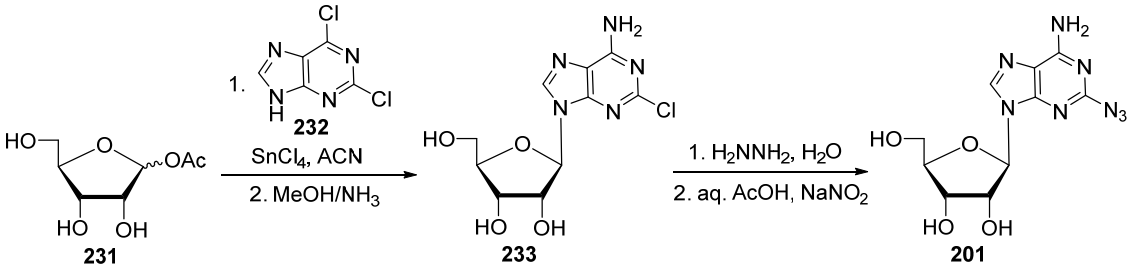

Scheme 45. Synthesis of 2-azidoadenosine[254]

3.1.2.2 SPAAC Reactions

The adenosine modified with azido group at the C2 position **201** also undergoes SPAAC reaction efficiently. Thus, **201** reacts with cyclooctyne **217** in aqueous media at ambient temperature for 3 h to yield a lower moving spot by TLC. The ^{1}H NMR showed quantitative conversion to click adduct **234** without the need for further purification, Scheme 46. The reaction was also tracked with the help of the UV/Vis Spectrophotometer, Figure 33. The UV/Vis profile of starting azide **201** was quite complex exhibiting 2 peaks and 2 valleys including characteristic azido purine peak at λ_{max} 269 nm (ε 12 617). Throughout the course of the click reaction a hypochromic shift was seen until the starting material **201** had completely converted to adduct **234** λ_{max} 260 nm (ε 10 700).

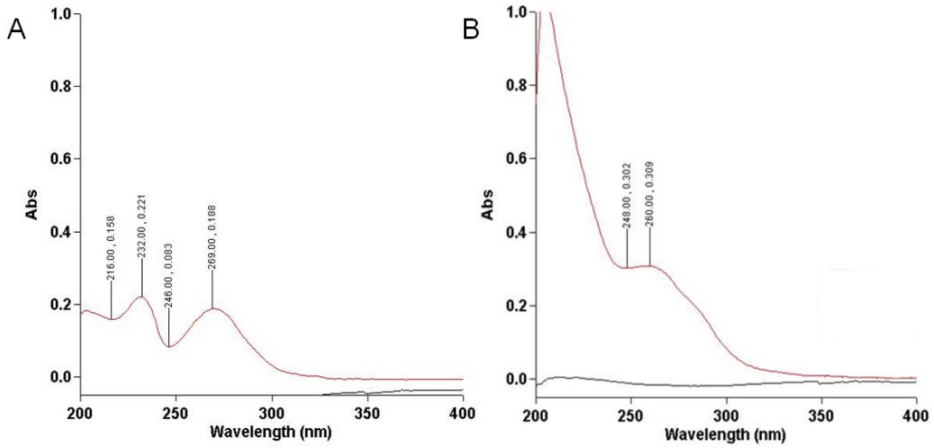

Figure 33. A. UV/Vis profile of 2-azidoadenosine **201**, **B.** UV/Vis profile of adduct 2-OCT-adenosine **233**

On the other hand, the SPAAC reaction of **201** with DBCO **223** proceeded smoothly to give the more polar triazole **235**. The purification of the reaction product was significantly more challenging and required HPLC. Thus, the crude reaction was passed through a 0.2 μm PTFE syringe filter, and then injected into a semipreparative HPLC column (Phenomenex Gemini RP-C18 column; 5 μ, 25 cm × 1 cm) via a 2 mL loop. The HPLC column was eluted with an isocratic mobile phase mixture of 40% CH_3CN/H_2O at a flow rate of 2.0 mL/min to give **235** in an 85% isolated yield as a mixture of inseparable regioisomers t_R = 13.0 – 16.2 min. A summary of the click reaction conditions between the 2-azidoadenosine and cyclooctynes can be seen in Table 3.

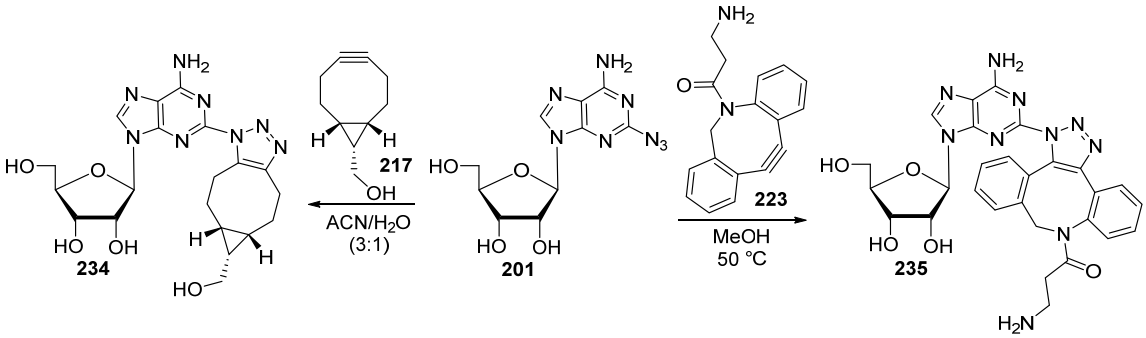

Scheme 46. SPAAC on 2-Azidoadenosine

Azide	Cyclooctyne	Product	Time	Temp	Solvent	Yield [%][a]
201	**217**	**233**	2 h	rt	ACN/H_2O (3:1)	100
201	**223**	**234**	16 h	50 °C	MeOH	98 (85)[b]

[a] Based on ^{1}H NMR. Yields for the products purified on a silica gel column are in parenthesis.

[b] Purified by RP HPLC

Table 3. Summary of the click reaction conditions between 2-azidoadenosine and cyclooctynes

3.1.3 SPAAC with 5-Azidouracil Nucleosides

3.1.3.1 Preparation of Substrates

The 5-azidouridine **202** is commercially available or can be prepared from parent nucleoside uridine **236**. Thus, **236** was treated with 0.55 equivalents of DBH in DMF for 10 minutes to afford less polar 5-bromo analogue **238**.[250] Conversion to the 5-amino analogue proceeded as described by Gourdain *et al.*[255] by heating with liquid ammonia at 70 °C overnight in a high pressure vessel. In the morning the reaction was cooled to -78 °C and the pressure was released allowing the ammonia to slowly boil off, leaving 5-amino derivative **240** as an oily brown residue. Direct treatment of amine **240** with triflic anhydride and sodium azide in a Sandmeyer azidation gave target azide **202**, Scheme 47. Treatment of 2'-deoxyuridine **237** in a similar reaction sequence of bromination, amination and Sandmeyer azidation gave the highly photolyzable 5-azido-2'-deoxyuridine **242**. The latter aromatic substitution reaction including all post reaction manipulations must be run in the dark in order to avoid the known photolysis of **242** caused by UV irradiation.[113]

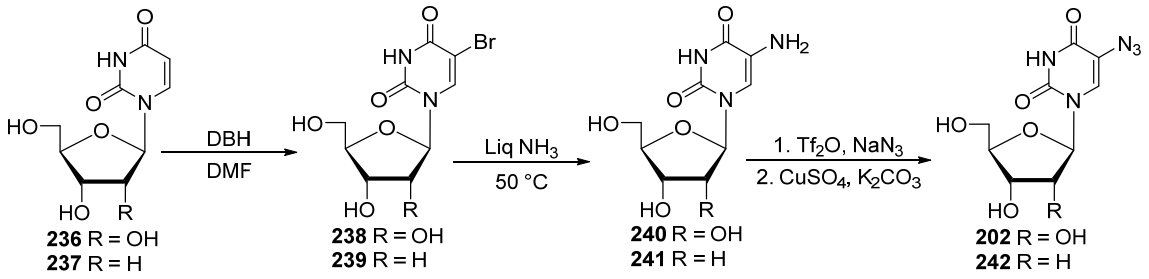

Scheme 47. Synthesis of 5-zzido Uracil Nucleosides

3.1.3.2 SPAAC Reactions

The click reaction between 5-azidouridine[256] **202** and several cyclooctynes including **217**, **218**, **223** or **227** proceeded quickly and very effectively yielding the corresponding click adducts **244**, **245**, **247** and **248**. Thus, treatment of 5-azidouridine **202** with hydroxyl modified cyclooctyne **217** in ACN:H_2O mixture (3:1, *v/v*) afforded **244** in 3 minutes at ambient temperature as a more polar spot on the TLC, Scheme 48. The crude reaction mixture was passed through a 0.2 μm PTFE syringe filter, and then injected into a semipreparative HPLC column (Phenomenex Gemini RP-C18 column; 5 μ, 25 cm × 1 cm) via a 2 mL loop. The HPLC column was eluted with an isocratic mobile phase mixture of 20% CH_3CN/H_2O at a flow rate of 2.0 mL/min to give **23** (5.8 mg, 77%) t_R = 5.2 – 8.0 min. Furthermore, treatment of azide **202** with biotin modified cyclooctyne **218** for 3 minutes at ambient temperature gave the corresponding triazole **245** as a white solid. Analogous treatment of 5-azidouridine **202** with DBCO-NH_2 **223** or NHS modified MFCO **227** in methanol at ambient temperature afforded complete conversion to triazoles **247** or **248** in less than 15 minutes, Figure 34.

The click reaction of the highly photolyzable 5-azido-2'-deoxyuridine[255] **242** with cyclooctyne **217**, in the ACN/H_2O/MeOH (3:1:1 *v/v/v*) gave corresponding triazole product **246** in excellent yield, Scheme 48. MeOH (~20%) must be added to the reaction

mixture to solubilize the starting nucleoside and allow the reaction to proceed efficiently. Additionally, the click reaction must be run in the dark in order to avoid photolysis of **242** caused by UV irradiation.[113] A summary of the click reaction conditions between the 5-azidouracil nucleosides and cyclooctynes can be seen in Table 4.

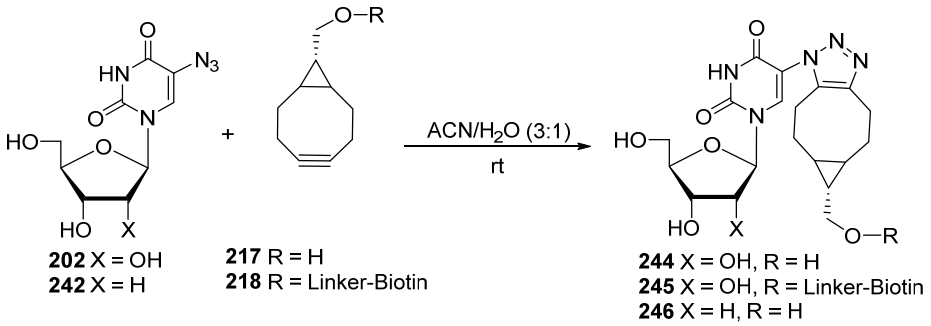

Scheme 48. SPAAC on 5-azido Uracil Nucleosides

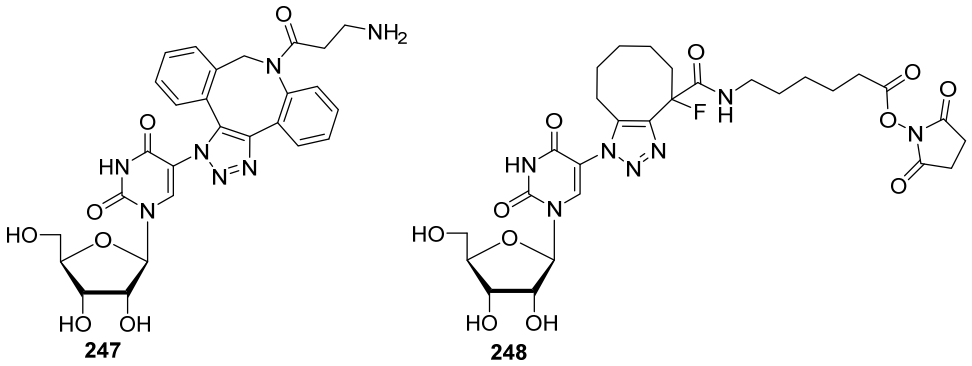

Figure 34. 5-Triazo-yl Uracil Click Adducts

Azide	Cyclooctyne	Product	Time	Temp	Solvent	Yield [%][a]
242	**217**	**244**	5 min	rt	ACN/H_2O (3:1)	95 (77)[b]
242	**218**	**245**	3 min	rt	ACN/H_2O (3:1)	98
243	**217**	**246**	15 min	rt	ACN/H_2O/MeOH (3:1:1)	100
242	**223**	**247**	15 min	rt	MeOH	100 (77)[b]
242	**227**	**248**	12 min	rt	MeOH	100

[a] Based on ^{1}H NMR. Yields for the products purified on a silica gel column are in parenthesis.

[b] Purified by RP HPLC

Table 4. Summary of the click reaction conditions between 5-azidouridine or 5-azido-2'-deoxyuridine and cyclooctynes

3.1.4 Fluorescence and Physical Properties of Triazole Adducts

Unsubstituted nucleosides are typically weakly fluorescent;[257-260] however, substitution at the C2 and C8 position of the purine ring or C5 of the pyrimidine ring with fluorogenic moieties results in nucleosides with fluorescent properties.[126, 261] While the 8-azidoadenosine **214** has no fluorescence, the click adduct **203** with triazole ring attached *directly* to the imidazolyl ring of purine via nitrogen atom emits at 300–500 nm with the maximum emission at 376 nm (Φ_{em} = 0.6%, B = 0.13 $M^{-1}cm^{-1}$). Similarly, 5-azidouridine **202** exhibits no noticeable fluorescence, whereas the triazole product **244** shows moderate emission between 285 nm and 550 nm with two emission peaks at 320 nm and 450 nm (Φ_{em} = 1.1%, B = 0.12 $M^{-1}cm^{-1}$). Interestingly, this triazole product showed an excitation maxima at 388 nm which was mainly observed in alkaline phosphate buffer (Figure 35d). A more moderate change in the absorption spectra was observed in MeOH and DMSO indicating a ground state deprotonation of the pyrimidine triazole scaffold.

The click adduct **235** of the 2-azidoadenosine and DBCO exhibited the highest fluorescence quantum yield (10.6%), the largest stokes shift (133 nm) and was the brightest (1.74 $M^{-1}cm^{-1}$) of the library of compounds that were prepared and tested, Figure 35. The 2-OCT-adenosine adduct **234** was the second brightest compound (0.38 $M^{-1}cm^{-1}$) and exhibited the second largest extinction coefficient, Table 5.

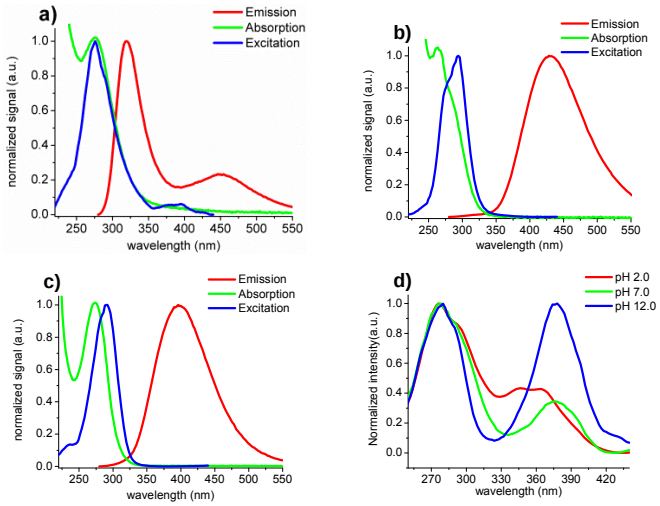

Figure 35. Normalized fluorescence emission, absorption and excitation spectra for the selected click adducts: a) **244**, b) **222**, and c) **235** in MeOH; (d) The pH effect on the excitation spectra of **244** in phosphate buffer.

The effect of solvent polarity was explored for derivatives **203**, **219**, **222**, **224**, **228**, **234**, **235**, **244** and **248** in DMSO and phosphate buffer pH 7.0, Figure 36. We observed a 10 nm and 17 nm bathochromic shift for **222** and **235** upon increasing solvent polarity (from DMSO to phosphate buffer at pH 7.0). Compound **244** showed a more complex spectra upon increase in solvent polarity, with peaks at 324 nm and 440 nm undergoing bathochromic shifts of 10 nm and 5 nm. The uncorrelated shift in emission likely arises from multiple glycosyl bond conformers of **23** each exhibiting different photophysical properties. Manderville found that compounds with different glycosyl bond conformations (*syn* vs *anti*) have different photophysical properties.[262-263] Thus, in solution **244** could exist as a monomer with a lifetime of 5 ns, but in a cell, π stacking with neighboring compounds could cause a broadening in the excitation spectra and a population with the shorter lifetime. The amplitude of the fluorescence emission was increased in DMSO for the uracil compounds, when compared to the intensity in MeOH and buffer. On the other hand, the intensity of the adenine derivatives was enhanced in

MeOH and quenched in buffer, with exception of analogues **203** and **224** which were enhanced in DMSO. The observed increase in fluorescence intensity in an aprotic solvent (i.e., DMSO) for the uridine derivatives correlates with the observed ground state deprotonation of the uracil triazole moiety. The solvent effect on **203** and **224** show distinct responses despite their similar structures, indicating that removal of the hydroxyl group at C2' likely induces a change in electron delocalization. Furthermore, introduction of a triazole ring at either the C2 or C8 positions likely causes a significant change in conformation (*syn* vs *anti*) thus changing the solvent sensitivity of the fluorophore, as shown by the OCT derivatives **203** and **234** and DBCO derivatives **224** and **235**.

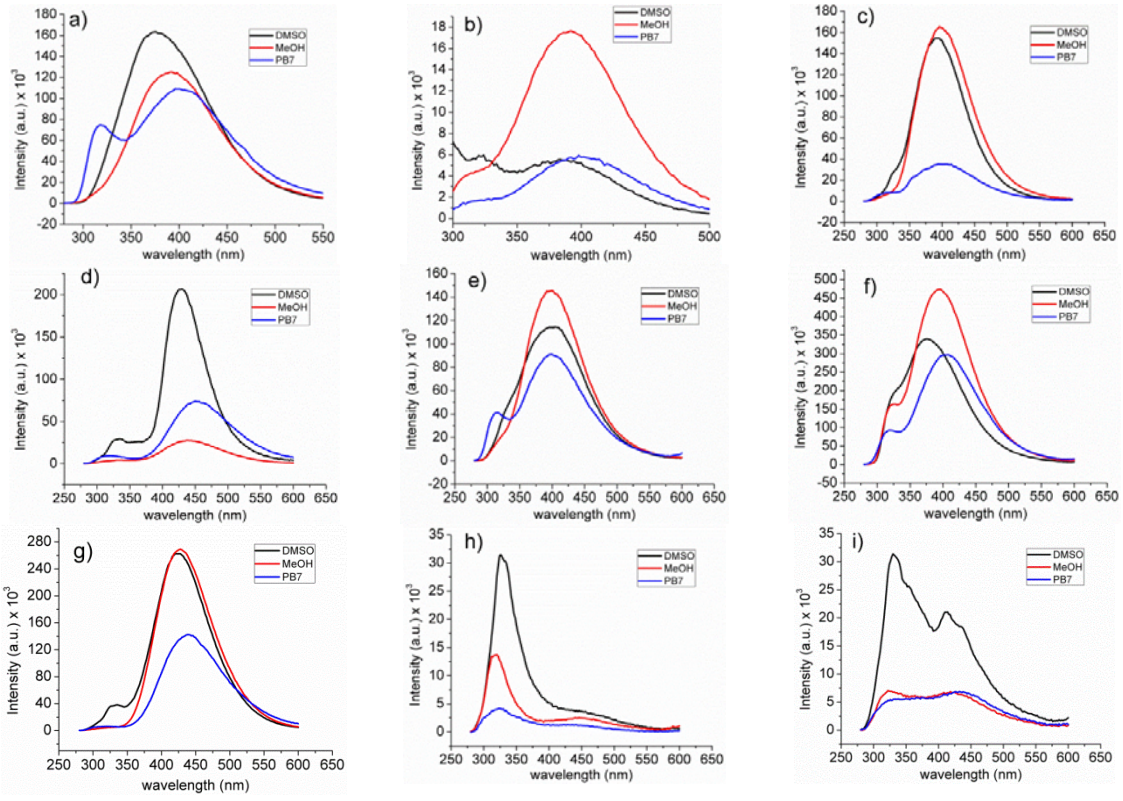

Figure 36. Fluorescence intensity of click adducts in DMSO, MeOH and 50 mM phosphate buffer at pH 7 (PB7) **solvents**: a) **203**, b) **219**, c) **222**, d) **224**, e) **228**, f) **234**, g) **235**, h) **244** and i) **248**.

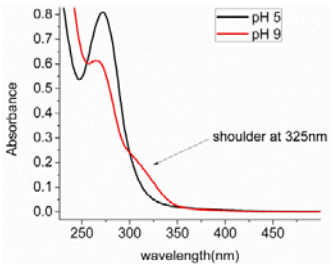

Figure 37. Absorption spectra of click adduct **244** in 50 mM phosphate buffer at pH 5 and 9.

All triazole products showed a complex fluorescence decay lifetime, with at least a triple discrete model needed to obtain a satisfactory fit (Figure 3), except analogue **219** which showed a biphasic decay. A fast lifetime of 0.1 ns to 0.6 ns was present in all compounds (Table 2). We hypothesize that the fast decay is likely the result of fluorescence decay of the adenine or uracil heterocyclic bases. In addition, 0.8 ns - 2.3 ns and 4.1 ns - 7.8 ns lifetime was recovered for all compounds, with **247** showing the longest lifetime (7.8 ns). The fractional contribution of each lifetime also varied among all triazole products; however, **222** (19%), **235** (40%) and **244** (38%) showed the largest contribution of the long lifetime (τ_3). The longest average lifetime was observed for **235** (2.8 ns), followed by **244** (2.7 ns), **247** (2.7 ns) and **222** (1.6 ns), Table 5. The recovered average fluorescence lifetime of the most fluorescent compounds is comparable to the lifetimes of current fluorescent proteins widely used in fluorescence lifetime imaging (FLIM),[264] indicating the potential utility of these fluorescent nucleoside analogs in FLIM for dynamic measuring and tracking of signaling events inside single living cells.

	203	**219**	**222**	**224**	**228**	**234**	**235**	**244**	**247**	**248**
$\varepsilon_{max}(M^{-1}cm^{1})$	21100	7500	8200	6000	6400	9100	6400	10100	7300	7100
$\lambda_{max}(abs)^{a}(nm)$	270	273	272	276	271	261	263	270	276	269
$\lambda_{max}(exc)^{a}(nm)$	280	278	290	293	288	270	295	276	312	-
$\lambda_{max}(exc)^{a,d}(nm)$	309	-	-	360	-	329	-	388	370	-
$\lambda_{max}(emi)^{a}(nm)$	392	390	397	440	399	395	428	312	361	327/412
$\lambda_{max}(emi)^{b}(nm)$	376	384	392	429	397	375	422	324/440	-	331/419
$\lambda_{max}(emi)^{c}(nm)$	403	400	402	452	399	405	439	334/445	-	339/434
$Stokes\ shift^{a}(nm)$	83	112	107	80	111	66	133	44/62	49	58
$\Phi_F{}^{a}$	0.006	0.006	0.014	0.017	0.006	0.02	0.106	0.011	0.013	0.009
$Brightness^{a}(M^{-1}cm^{1})$	0.13	0.11	0.25	0.27	0.10	0.38	1.74	0.12	0.09	0.06
$\tau_1{}^{a}(ns)$	0.10	0.60	0.10	-	0.10	0.30	0.10	0.30	0.30	-
$\tau_2{}^{a}(ns)$	0.80	4.90	0.90	-	0.90	1.0	2.0	1.30	2.30	-
$\tau_3{}^{a}(ns)$	5.90	-	5.60	-	5.30	5.80	4.10	5.70	7.80	-
$\tau_{average}(ns)$	0.70	1.60	1.60	-	1.20	0.80	2.80	2.70	2.70	-
$f_1{}^{a}(\%)$	0.63	0.77	0.28	-	0.46	0.64	0.02	0.22	0.11	-
$f_2{}^{a}(\%)$	0.30	0.23	0.53	-	0.39	0.30	0.58	0.39	0.78	-
$f_3{}^{a}(\%)$	0.07	-	0.19	-	0.15	0.05	0.40	0.38	0.11	-

[a] In MeOH. [b] In DMSO. [c] In 50 mM phosphate buffer pH 7.0. [d] Second maxima observed at the red edge of the excitation spectra.

Table 5. Photophysical data for the selected triazole adducts**.**

3.2 Application of Click Chemistry with Azido Nucleosides To Living Cell Fluorescent Imaging

Taking advantage that the click reaction between non-fluorescent azido nucleosides and cyclooctynes directly yields triazole products with fluorescence without necessity for additional modification for visualization, we have tested their application to *in vivo* studies and have demonstrated the viability of these reactions in living cells.

3.2.1 Cell Permeability Assay

The absorption of oral drugs is mainly determined by their ability to permeate through the GI tract and into the bloodstream. Faller *et al.* has shown a correlation between drug permeation across an alkane liquid membrane immobilized between two

aqueous phases and percent absorption in humans. A parallel artificial membrane permeation assay (PAMPA), was used to predict permeability of selected azides **201**, **214** and **216** and triazoles **222**, **235** and **244**. The results showed that approximately 20% of each compound was passively permeating in through the cellular membrane, Table 6. Typically, however, nucleoside transport proteins are also responsible for the cellular uptake of natural and modified nucleosides;[265] thus, although outside of the scope of this dissertation, these proteins might play a significant role in the uptake of these nucleoside-based theranostics.

Compound	% Fraction Absorbed	Log P_e (cm/s)[a]
201	22	-0.5
214[b]	18	-0.5
216	20	-0.5
222	21	-0.3
235	22	-0.03
244	20	-0.4

[a]Log of the effective permeability coefficient, Pe (cm·s −1), as assessed by a parallel artificial membrane permeability assay (HDM-PAMPA); [b]Permeability is independent of concentration as shown by assays performed at 150 μM and 75 μM concentrations.

Table 6. Cellular permeability data for the selected azides and triazole adduct

3.2.2 Cytotoxicity Assay

A cell toxicity assay was used to determine the non-toxic dose of triazoles **219** and **244** in MCF-7 cells, Figure 37. The effect of a single dose of azide **214** and azide **202** together with cyclooctyne **217** on the survival of MCF-7 cells cultured in a 96-well plate with DMEM/F12 media was assessed for a 24 h period. Under these conditions MCF-7 cells were subjected to the MTT assay that measured the ability of cells to reduce the tetrazolium dye. We measured activity of MCF-7 cells at the most active part of the cells growth phase 24 h after cell seeding (50% confluency). The *y*-axis of the dose-response graph represents cell viability correlated to metabolic activity. As shown in the dose-

response graph of both azide **202** and azide **214**, we determined that a 1 µM dose of both azides **202** and **214** were non-cytotoxic for a 24 h exposure in MCF-7 cells, Figure 38. I used 1 µM nucleoside treatments for my fluorescence imaging studies to determine whether the click reaction occurred inside cells that were not undergoing stress.

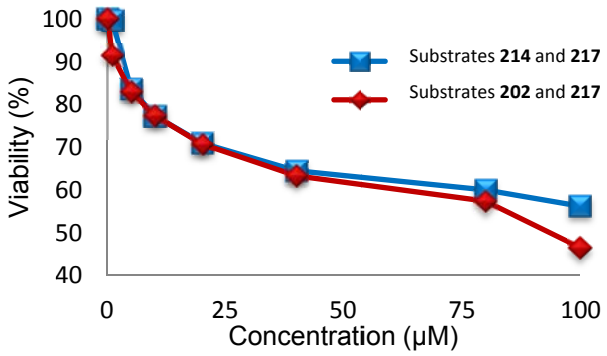

Figure 38. Viability of MCF-7 cells when exposed to SPAAC between azides **202** or **214** and cyclooctyne **217**

3.2.3 In Vivo Images in Living MCF-7 Cells

In our initial *in vivo* click-chemistry experiments to determine whether compounds **219** and **244** were generated within the cell we used liposomes to assure the delivery of the precursor molecules as shown by Ito *et al.*[124] Lipofectamine, a cationic-lipid transfection reagent typically used for the transfection of DNA/RNA into eukaryotic cells, was previously used in the experiments that observed the direct-light up of cyclic AMP derivatives by click chemistry in living cells. Thus, MCF-7 cells were incubated for 3 h at 37 °C in a CO_2 incubator after Lipofectamine transfection of azide **214** (100 µM). The click reaction commenced via the addition of DMEM cell media containing cyclooctyne **217** (100 µM). The blue fluorescence was observed using excitation and absorbance filters 360/40 and 470/40 nm, respectively, without washing and fixing cells (Figure 39 panels E and F). In our negative controls, background fluorescence was

indistinguishable in cells incubated without azide **214** (Figure 39 panels C and D) or cyclooctyne **217** (Figure 38 panels A and B).

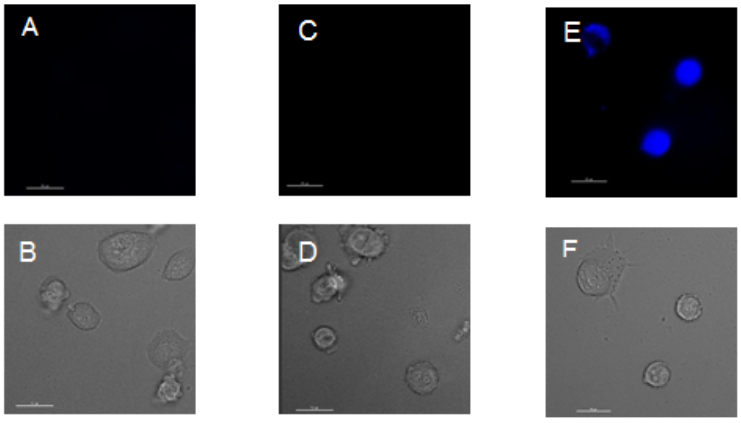

Figure 39. Fluorescence microscopy images
Brightfield photos (Panels A, C and E) and phase photos (Panels B, D and F) of live MCF-7 cells: (Panels A, B) MCF-7 cells after incubation with 8-azido-9-(β-D-arabinofuranosyl)adenine **214** (100 µM) as a negative control; (Panels C, D) MCF-7 cells after incubation with cyclooctyne reagent **217** (100 µM) as an another negative control; (Panels E, F) MCF-7 cells containing azide **2** after incubation with cyclooctyne **5** in cell culture media. Scale = 40 µm

A concentration-dependent experiment with Lipofectamine was also performed in live MCF-7 cells, which showed an increase in fluorescence intensity as the concentration of azide **214** increased, Figure 40.

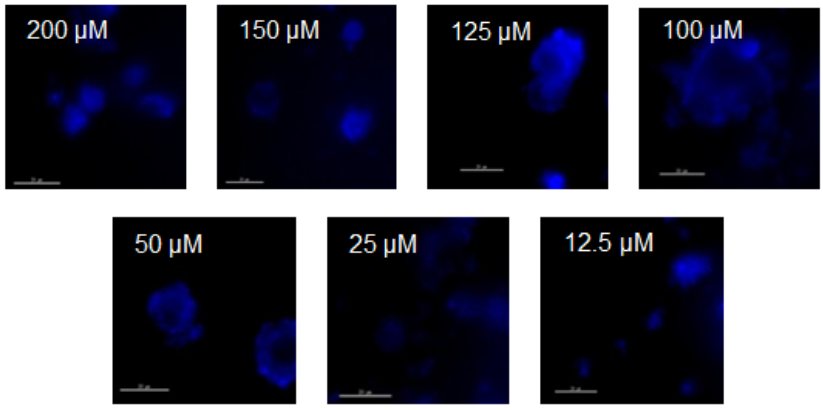

Figure 40. Dose response studies
with 12.5 µM to 200 µM (shown in white on each panel**)** of azide **242** and 125 µM cyclooctyne **217.** Scale = 40 µm

Furthermore, an *in vivo* assay of the click reaction between 5-azidouridine **242** and cyclooctyne **217** was performed. As expected, a direct light up of the live MCF-7 cells

was observed as click product **244** formed with fluorescence increasing as the concentration of azide **202** increased, Figure 41.

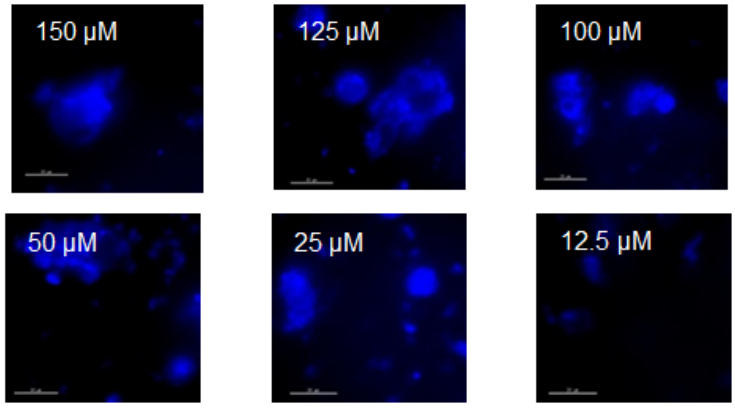

Figure 41. Dose response studies
with 12.5 µM to 200 µM (shown in white on each panel) of azide 244 and 125 µM cyclooctyne 217**.** Scale = 40 µm

The data from our fluorescent microscopy studies showed that the click reaction successfully occurred in MCF-7 cells treated with nucleosides and Lipofectamine at a concentration range from 12.5 - 200 µM as evidenced by the fluorescence of compounds **219** (Figure 40) and **244** (Figure 41). The fluorescence of both compounds occurred throughout the cytosol and nuclear regions which we suspect to be influenced by the Lipofectamine transfection reagent. The usefulness of these azido derivatives for imaging of nucleoside-based drugs in living cells by *direct* fluorescence light-up will depend on cell viability; however, the dose of Lipofectamine used in these experiments showed significant changes to the morphology of cells. The MCF-7 cells displayed signs of cell swelling and cytolysis as shown in the fluorescence and phase-contrast photos (Figure 38 Panels E and F). On the basis of our fluorescent imaging data, we showed that click-chemistry robustly occurred inside the cells via liposome delivery. Thus, we decided to

extend our studies to show that these azido nucleosides are able to undergo click-chemistry with cyclooctynes inside the cells without the aid of Lipofectamine.

The click chemistry between 8-azido-*arabino*-Ado **214** and cyclooctyne **217** was therefore carried out in MCF-7 breast cancer cells. The MCF-7 cells were incubated for 3 h at 37 °C in a CO_2 incubator with **214** (1 μM). The click reaction commenced via the addition of cyclooctyne **217** 1 μM containing DMEM cell media. We observed strong blue fluorescence in live cells using excitation and absorbance filters 360/40 and 470/40 nm, respectively (Figure 39) which was similar to the fluorescence that Ito *et al.,* observed during the reaction of azido modified cAMP and a difluorinated cyclooctyne in HeLa cells.[124] In our negative controls, background fluorescence was indistinguishable in cells incubated without azide **214** or cyclooctyne **217**. To distinguish between intracellular and extracellular fluorescent click reactions, cells were also treated with trypan blue to determine the presence or absence of extracellular fluorescence via a quenching mechanism.[266] Trypan blue cannot diffuse through the cell membrane of viable cells and hence can only quench fluorescence that occurs outside of the cell. Cells undergoing the click reaction and co-treated with trypan blue did not show any difference in fluorescent intensity compared to control (data not shown) and indicated that there was no extracellular triazole product fluorescence. Hence, we concluded that fluorescence was intracellular and not the result of the click reaction occurring on the surface of the cell membrane. As shown in Figure 42, the 1 μM dose of compounds **214** and **217** showed a strong fluorescent localization to the nucleus. Similarly, in Figures 43 and 44, the 1 μM dose of compounds **201** and **223** or **202** and **217** also showed a moderate fluorescent localized in the nucleus. Because MCF-7 cancer cells are undergoing rapid

cell division these nucleosides are being used as substrates to synthesize new DNA strands resulting in exclusive nuclear localization of these compounds

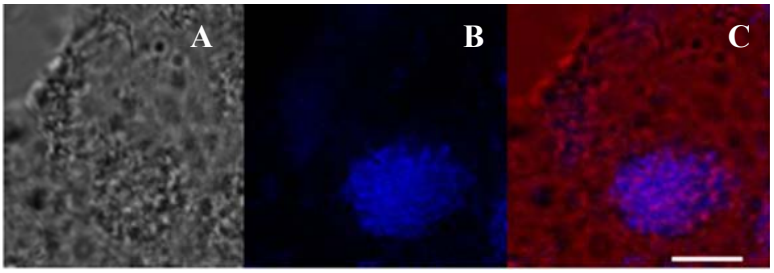

Figure 42. Fluorescence microscopy images and phase photos of live cells
(A) Phase photo of MCF-7 cells after the reaction of azide **214** with cyclooctyne **217**; (B) Fluorescent photo of the same MCF-7 cell; (C) Merged Photo of panels (A) and (B).

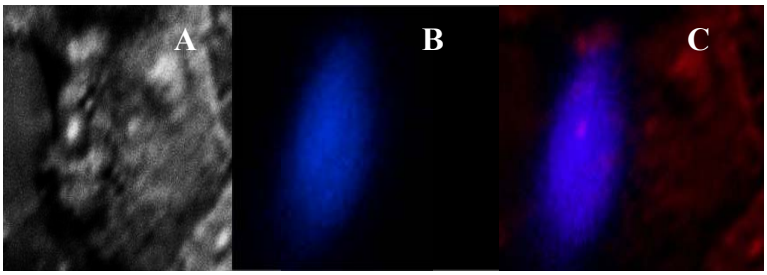

Figure 43. Fluorescence microscopy images and phase photos of live cells
(A) Phase photo of MCF-7 cells after the reaction of azide **201** with cyclooctyne **223**; (B) Fluorescent photo of the same MCF-7 cell; (C) Merged Photo of panels (A) and (B).

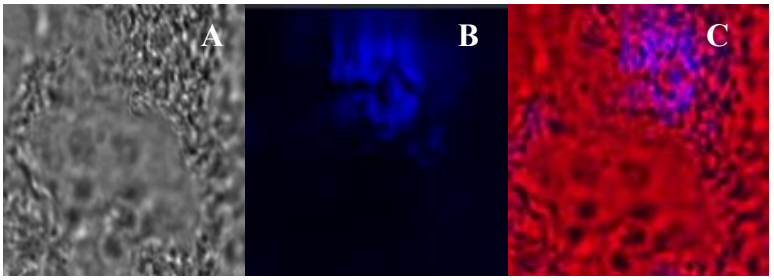

Figure 44. Fluorescence microscopy images and phase photos of live cells
(A) Phase photo of MCF-7 cells after the reaction azide **202** with cyclooctyne **217**; (B) Fluorescent photo of the same MCF-7 cell; (C) Merged Photo of panels (A) and (B).

The present *in situ* click chemistry drug delivery system represents a novel approach wherein both a therapeutic effect and drug uptake-related imaging information may be produced and readily monitored at the cellular level. Although it is beyond the

scope of my dissertation, the long-term implications of this *in situ* click chemistry drug delivery strategy embodied in click substrates **201**, **202** and **214** could allow for a more precise monitoring of dosage levels, as well as an improved understanding of cellular uptake and release mechanisms that could ultimately be translated to a more efficient treatment of diseases such as cancer.

3.2.4 Fluorescence Lifetime Imaging Microscopy

In order to determine fluorescence lifetime within living cells, frequency-domain fluorescence lifetime imaging microscopy (FD-FLIM) was conducted on MCF-7 cells incubated with the triazole products **219**, **235** or **244**, Figure 46. The FD-FLIM is an imaging technique capable of image acquisition rates that are compatible with *in vivo* imaging, while also offering a means to visualize the individual lifetime components of a sample (i.e. the polar plot histogram).[267] The technique allows one to compare the lifetime characteristics, τ value, of compounds *in vitro* and *in vivo*.

After incubation of MCF-7 cells with triazoles **219**, **235** or **244**, the fluorescent signal from cell nuclei were isolated for lifetime measurement and the average lifetime from multiple cells were calculated for each compound, Table 7. The lifetime value obtained for *arabino* triazole adduct **219** was much higher *in vivo* (2.66 ns) than that found *in vitro* (1.60 ns; Table 2). The discrepancy in lifetimes suggests that in a methanol solution **219** exists in base conformations (*syn* over *anti*, Figure 45A; as discussed above[268,269]) which populates the fast lifetime (0.6 ns); in the cell, however, when the compound has already been incorporated into a DNA strand and does not have the flexibility to rotate from the *anti* conformation needed for a Watson-Crick base pair to the

syn conformation (Figure 44B), the slow lifetime (4.9 ns) is more populated than the fast lifetime (0.6 ns). We also found that the mean lifetime of triazole **219** was not altered when **219** had been synthesized by an *in vivo* click reaction between azide **214** and cyclooctynes **217** in MCF-7 cells (Table 7, footnote *a*).

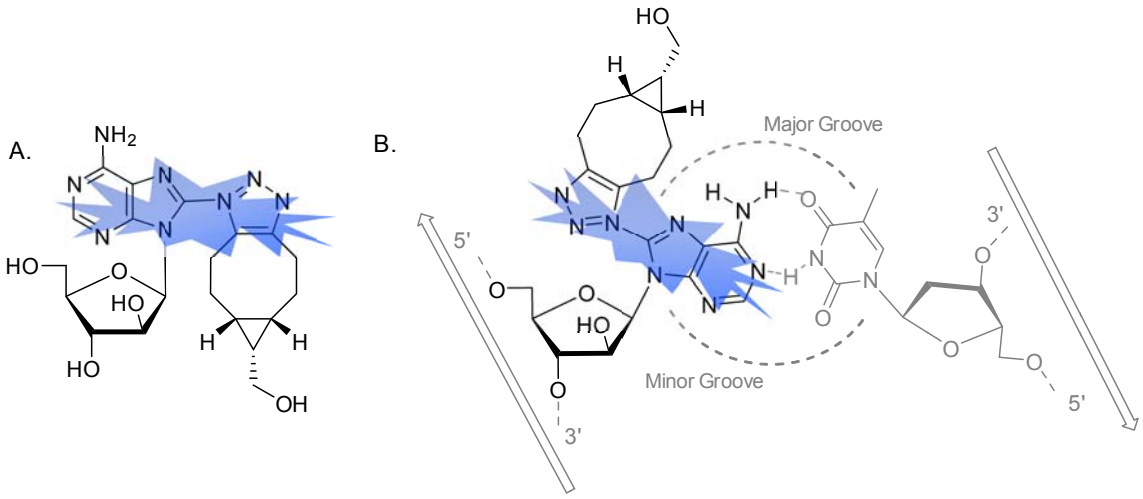

Figure 45. *Syn* and *Anti* Conformations of 8-OCT-Arabinoadenosine

The values for click adducts **235** (2.66 ns) and **244** (2.73 ns) were similar to those obtained through spectroscopic methods, although slightly lower. Polar plot analysis reveals that adduct **235** maintains its individual lifetime components, suggesting that the conformation found *in vitro* is also present *in vivo*, Figure 46 and Figure 47. We believe that this finding can be attributed to steric hindrance and the size of the bulky DBCO component.

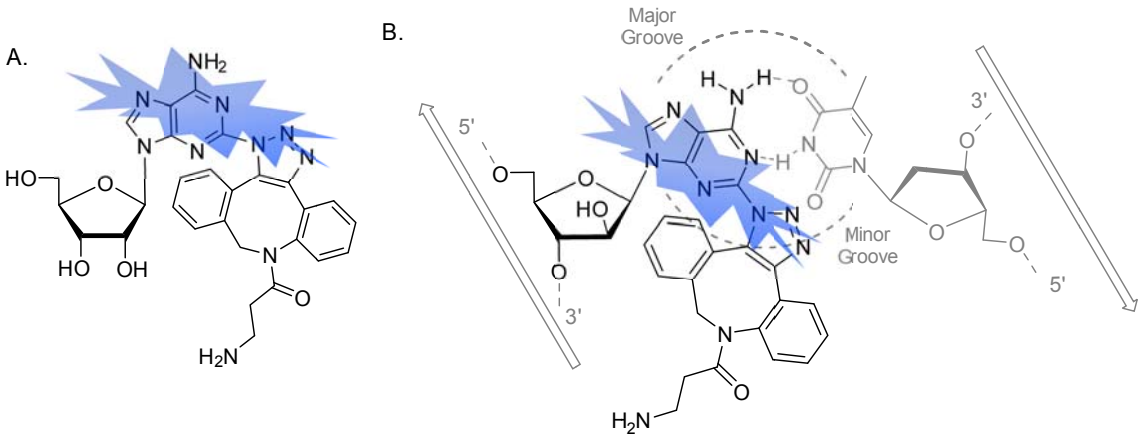

Figure 46. *Anti* Conformation of 2-DBCO-Adenosine

The histogram for adduct **244** indicates that its lifetime components undergo an alteration *in vivo* and in actuality only one lifetime population is observed in the live cells. As shown in Figure 34d, this compound is the most sensitive of all the compounds tested to pH and solvent polarity thus it is not entirely surprising to see differences between fluorescence lifetimes *in vitro* and within living cells. In addition to featuring a different solvent, the intranuclear environment may introduce a higher pH[270] or π-orbital stacking when compounds are DNA-bound (monomer vs dimer), both of which can alter the fluorescence lifetime characteristics of a given compound.[271-272]

Although the lifetime properties of **219** and **244** change slightly within cells (*in vivo* determination) compared to *in vitro* determination, we found that their intracellular lifetimes are also relatively consistent from cell to cell and thus prove unambiguously the formation and presence of **219**, **234** and **244** within the nucleus. Therefore, all three compounds can serve as viable fluorescent probes *in vivo*, with adduct **234** being the compound of choice when low environmental sensitivity (i.e., lifetime invariance) is desired.

Compound	Mean lifetime (ns)	SD	n (# nuclei)	SEM
219	2.66	0.159	13	0.044
219[a]	2.61	0.103	11	0.031
234	2.66	0.102	16	0.026
244	2.73	0.093	14	0.025

[a]Triazole adduct **219** synthesized by *in vivo* click reaction

Table 7. Mean lifetime of nucleoside triazole adducts within MCF-7 cells determined by Frequency-Domain Lifetime Imaging (FD-FLIM).

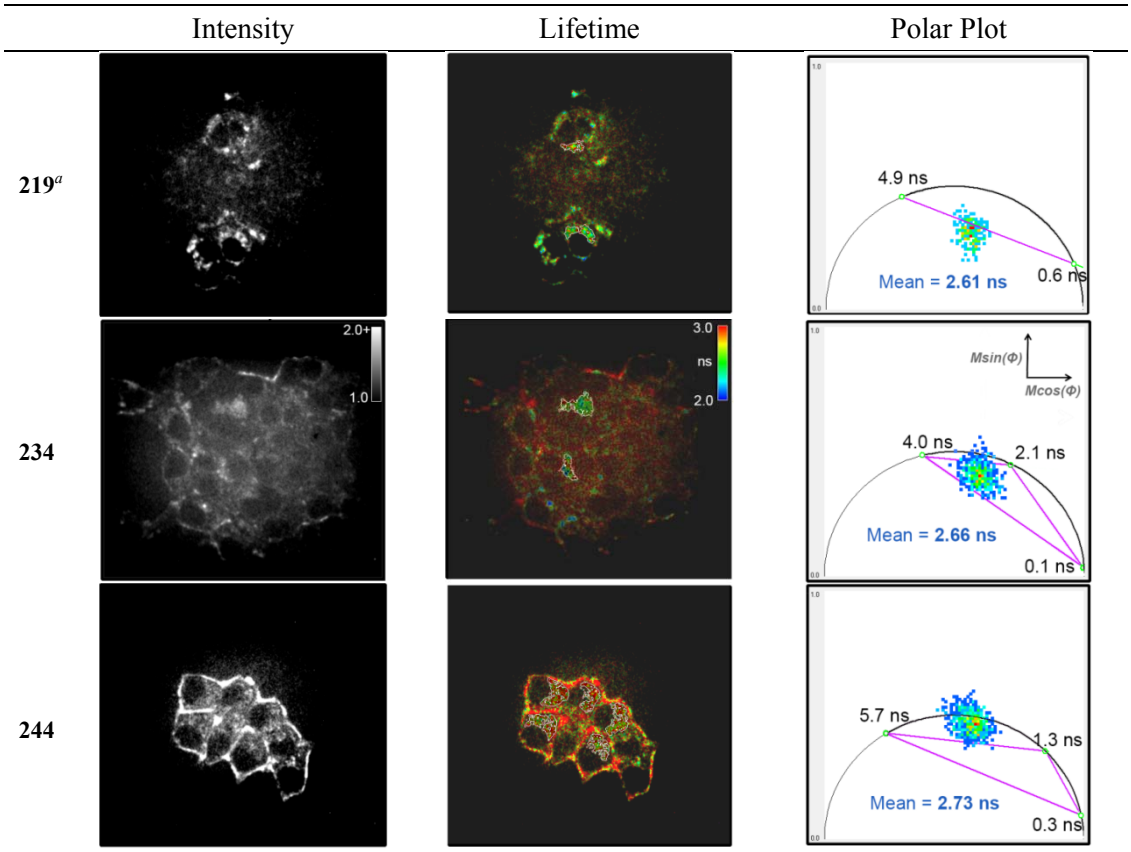

Figure 47. Representative images of fluorescence intensity (left), fluorescence lifetime (middle), and Polar Plot histogram (right) for triazole adducts **219, 235** or **244** (1 μM) in MCF-7 cells. Fluorescence intensity images display an intensity range from 1.0 (background intensity) to 2.0+ (2x background and greater). Fluorescence lifetime heat maps display lifetimes ranging from 2.0 ns (and below) in blue to 3.0 ns (and above) in red. Polar plot histograms depict the x,y coordinates [$M_{cos}(\Phi_F)$, $M_{sin}(\Phi_F)$] of pixels within nuclei (outlined in the corresponding lifetime image). Experimental component lifetimes are indicated on the semi-circle (green circles), as well as the group mean lifetime for the specific compound. [a] Images for **219** are for the triazole adduct synthesized using an *in vivo* click reaction.

3.3 Phosphorylation of Azido Modified Nucleosides

Nucleoside triphosphates (NTPs and dNTPs) are the building blocks of nucleic acids and are involved in many important processes including neurotransmission, DNA replications, metabolism and polysaccharide biosynthesis.[273] Typically NTPs and dNTPs are synthesized via one of two ways: chemically or enzymatically; however, no single chemical or enzymatic method has been reported thus far that can extend to all natural and unnatural nucleosides. Because of the presence of several reactive moieties (i.e., hydroxyl and amino groups) selective 5' phosphorylation often requires a protection/deprotection sequence and tedious purification to remove undesired byproducts or regioisomers.[273]

3.3.1 Survey of Chemical 5'-Phosphorylation of Nucleosides

Nucleotides were originally synthesized using phosphorochloridates which involved a complicated reaction sequence, fairly low selectivity and yields.[274-275] In 1967, Yoshikawa and coworkers were the first to directly use phosphoryl chloride for a nucleoside phosphorylation, Scheme 49.[276] They found that using a trialkylphosphate as the solvent accelerated the rate of the reaction of nucleosides with phosphoryl chloride at the 5' position of unprotected nucleosides. Thus, they were able to phosphorylate adenosine **249** with phosphoryl chloride and either triethyl or trimethyl phosphate to give **250** which was further phosphorylated with pyrophosphate to afford **251**.

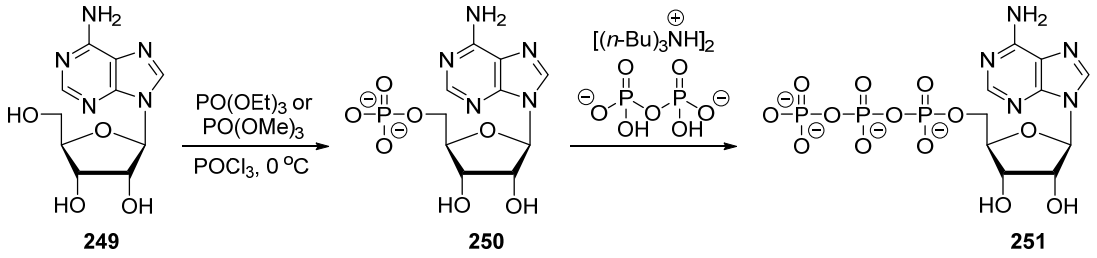

Scheme 49. Yoshikawa 5'- Phosphorylation Method

In 1984, Poulter and coworkers[277-278] described a protocol for the synthesis of nucleotide 5'-diphosphates (e.g., **253**), Scheme 50. Their strategy involved the nucleophilic displacement of 5'-*O*-tosyl nucleosides **252** by the tris(tetra-*n*-butylammonium) form of pyrophosphoric acid at ambient temperature. They also describe the synthesis of ATP using tetrakis(tetra-*n*-butylammonium) triphosphate.

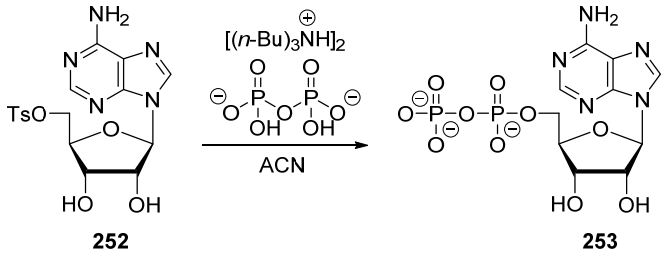

Scheme 50. Poulter Phosphorylation Method

Later, Ludwig and Eckstein[279] developed a procedure for the synthesis of nucleotide 5'-triphosphates using 2-chloro-4*H*-1,3,2-benzodioxaphosphorin-4-one **255**, Scheme 51. Thus, **255** phosphitylates the 5'-hydroxyl of a protected adenosine **254** to form intermediate **256**, which on subsequent reaction with pyrophosphate produces, in a double displacement, cyclic phosphite **257**. Oxidation with iodine and water gives 5'-triphosphate **251**.

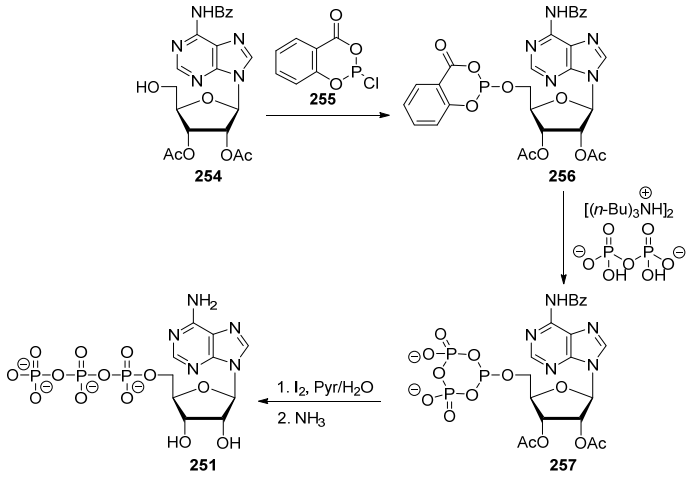

Scheme 51. Eckstein **5'**-Phosphorylation Method

3.3.2 Attempted Azidation of 2'-Deoxyadenosine-5'-triphosphate

Initially, we envisioned the installation of the azido group on the pre-made nucleotide through the insertion of a bromine atom at the C8 position and then a substitution with an azido group following a modified version of the procedure by Meffert *et al.*, Scheme 52.[280] Treatment of dATP **258** with bromine in potassium acetate followed by ion exchange purification with DEAE-Sephadex and lyophilization gave 8-bromo-dATP **259**. Thus, 8-bromo analogue **259** was reacted with sodium azide, instead of the prescribed hydrazoic acid[281-283] because hydrazoic acid is very toxic, explosive and not commercially available. Unfortunately however, I was never able to obtain azide **260** and only recovered what seemed to be intact 8-bromo starting material **259**.

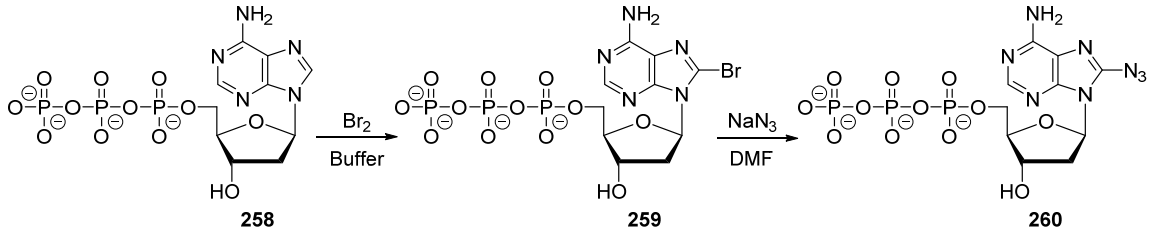

Scheme 52. Attempted Synthesis of 8-azido-dATP by Azidation of dATP

3.3.3 Attempted Phosphorylation of 8-azido-2'-deoxyadenosine

Next, I shifted my strategy from modifying the premade nucleotide (i.e. **258**) to phosphorylation of the azido nucleoside (i.e. **261**), Scheme 53. Thus, I employed the typical Yoshikawa procedure[276] in which the unprotected nucleoside **261** is treated with phosphoryl chloride in the presence of a trialkyl phosphate at 0 °C. Unfortunately, this method failed to show more than 5-10% conversion to the lower moving 5'-monophosphate **262** by TLC even after allowing the reaction to stir at ambient temperature overnight. Nevertheless, addition of 2 molar equivalents of pyrophosphate to this reaction mixture also failed to give the corresponding trinucleotide **260**. The TLC analysis of this reaction showed no significant change and mostly unreacted **261**.

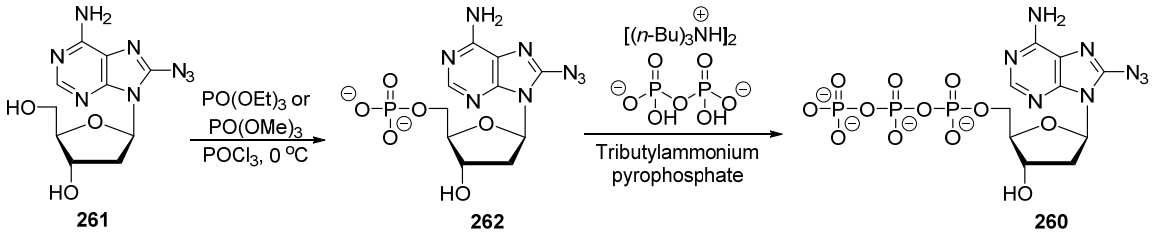

Scheme 53. Attempted Synthesis of 8-azido-dATP using the Yoshikawa procedure

Next, I tried phosphorylation using the Eckstein procedure, Scheme 54.[275] The 8-azido-2'-deoxyadenosine **261** was dissolved in a mixture of pyridine and dioxane in the presence of 2-chloro-4*H*-1,3,2-benzodioxaphosphorin-4-one **262** which should have yielded activated phosphite **263**; however, tracking the reaction by TLC showed that only traces of a more polar lower moving spot were formed. This new lower moving spot could have been the amino product of the reaction between the trivalent phosphorous of **262** and the azido group in a Staudinger reduction.[284-285]

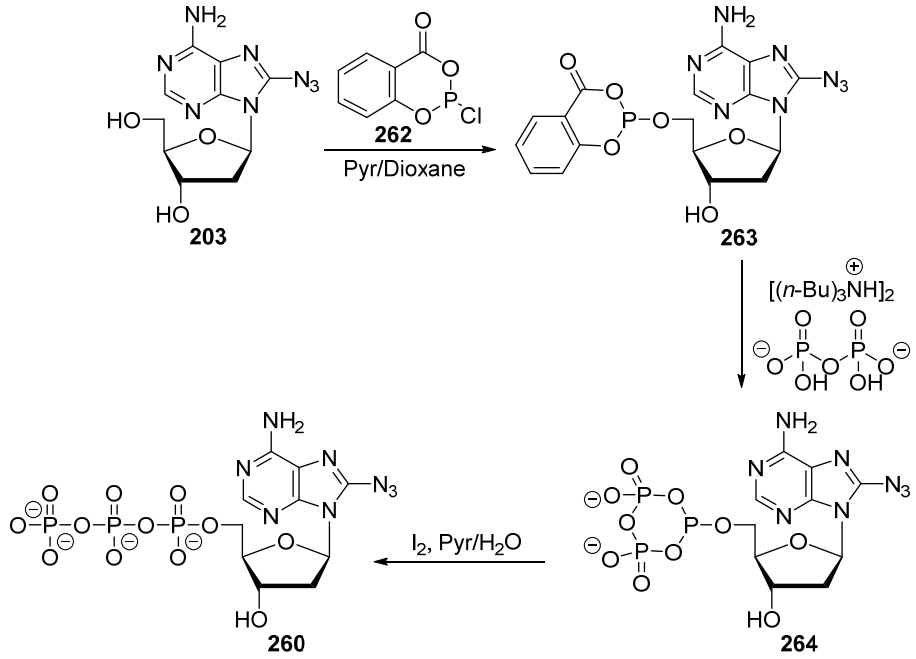

Scheme 54. Attempted Synthesis of 8-azido-dATP using the Eckstein procedure

The Poulter method[277-278] for phosphorylation was then attempted to synthesize nucleotide diphosphate **266**, Scheme 55. Tosylation of the azido stating material **261** proved to be troublesome and only provided 5'-tosyl analogue **B8** in very low yields. Nevertheless, treatment of activated analogue **265** with pyrophosphate in acetonitrile for 72 h failed to give the corresponding diphosphate analogue **266** and also resulted in the recovery of tosylated precursor **265**.

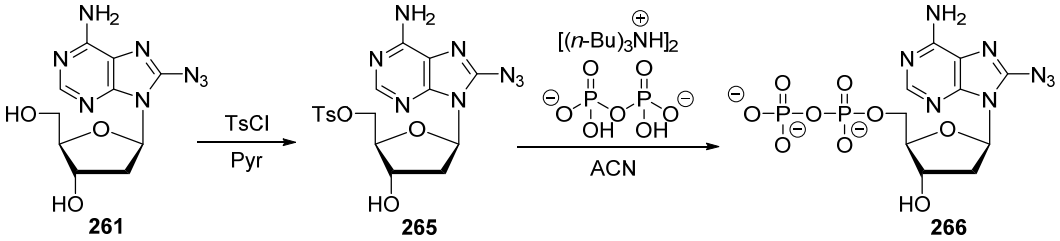

Scheme 55. Attempted Synthesis of 8-azido-dATP using the Poulter Procedure

3.3.4 Survey of Enzymatic 5'-Phosphorylation of Nucleosides

Enzymatic conversion of nucleosides and deoxynucleosides to their corresponding mono-, di- and triphosphate analogues requires the use of several kinases but is typically an effective method for synthesizing nucleotides.[286-287] Traditionally, kinases used for phosphorylation are typically specific for their natural substrates; however, there has been substantial work done on kinase mediated phosphorylation of modified nucleosides including nucleosides with azide modifications.[288]

Human deoxycytidine kinase (HdcK)[287, 289] is an enzyme that has been intensely studied for phosphorylation; it was found that deoxycytidine (dC), deoxyguanosine (dG) and deoxyadenosine (dA) are suitable substrates. Thus, HdcK has broad substrate specificity, and does not display selectivity on the basis of the chirality of the substrate. Cytidine (Uridine) monophosphate Kinase (CMP-UMPK)[290] is the enzyme that is most commonly used for the synthesis of diphosphates nucleotides. It normally catalyzes the phosphorylation of pyrimidine nucleoside monophosphates at the expense of ATP. As my azido nucleosides have an adenine base, the CMP-UMP kinase would not work, requiring another kinase. For adenine containing nucleosides, myokinase has been utilized in the past to obtain the corresponding diphosphate nucleotide.[291] For the synthesis of nucleoside triphosphates from diphosphates, pyruvate kinase (PK) is most commonly utilized.[292] It is typically robust, very flexible and not highly specific to substrates while using phosphoenolpyruvate as its phosphate source.

3.3.5 Enzymatic Phosphorylation of 8-azido-2'-deoxyadenosine

The phosphorylation of 8-azido-dATP **261** was attempted using enzymatic methods, Scheme 56. Hence, phosphorylation of **261** was achieved in the presence of human deoxycytidine kinase (hdCK)[289] enzyme using ATP as the phosphate donor to give 5'-monophosphate **262** in moderate yields. Treatment of **262** with cytidylate kinase[290] (UMP-CMP Kinase) did not give the corresponding diphosphate analogue; however, reaction of **262** with myokinase[291] (MK) and ATP did afford the 5'-diphosphate analogue **260**. Further treatment with pyruvate kinase (PK) and phosphoenolpyruvate (PEP) should give the desired 5'- triphosphate **260**.

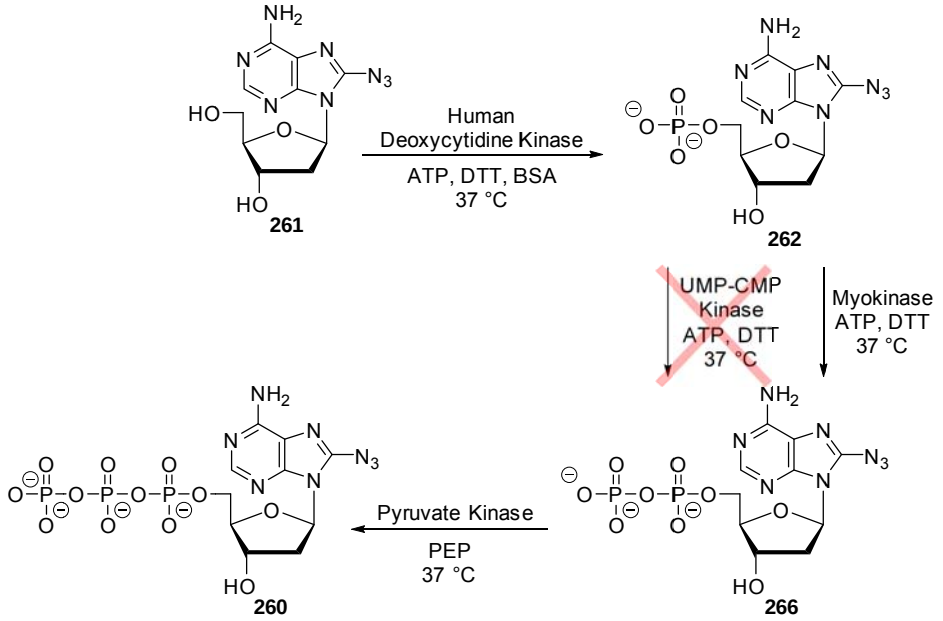

Scheme 56. Enzymatic synthesis of 8-azido-dATP

3.4 Design, Screening and Labeling of Nucleosides Against Protozoans

Taking advantage of the click chemistry of azido modified nucleosides that I developed above, we decided to explore the application this new protocol to identify the cellular targets of active nucleosides against *Trichomonas vaginalis and Tritrichomonos*

Foetus. Trichomonas vaginalis is a protozoal parasite that causes trichomoniasis, a common sexually transmitted disease in humans. The current FDA-approved treatments for this disease are 5-nitroimidazoles derivatives: metronidazole, also known as Flagyl, and tinidazole, which is also known as Tindamax. However, approximately 5% of all reported cases show some level of resistance to metronidazole.[226]

3.4.1 Screening of Compounds

In order to select the most promising candidate we screened a library of various purine **267**–**291**, Figure 48, and pyrimidine **292**–**299**, Figure 49, nucleoside analogues modified at C2', C3' or C5' of the ribose ring and at position C2 of adenine ring against *T. vaginalis*[232] *in vitro*. The most potent compounds were found to be 2'-modified adenosine derivatives, especially the analogues having an arabino configuration. Thus, we found that 9-(2-deoxy-2-fluoro-β,D-arabino-furanosyl)adenine (*arabino*-F-Ado) **272** is more potent against *T. vaginalis* than the FDA approved treatment, metronidazole. It inhibited the growth of *T. vaginalis* with an IC_{50} of 0.09 μM, whereas metronidazole inhibits growth of parasite with an IC_{50} of 0.72 μM, Table 8. Moreover, **272** is also active against the metronidazole resistant strain *T. vaginalis* with an IC_{50} value of 0.21 μM. Encouraged by these exciting results we decided it would be important to visualize the cellular localization and potential cellular targets of F-*arabino*adenosine **272**.

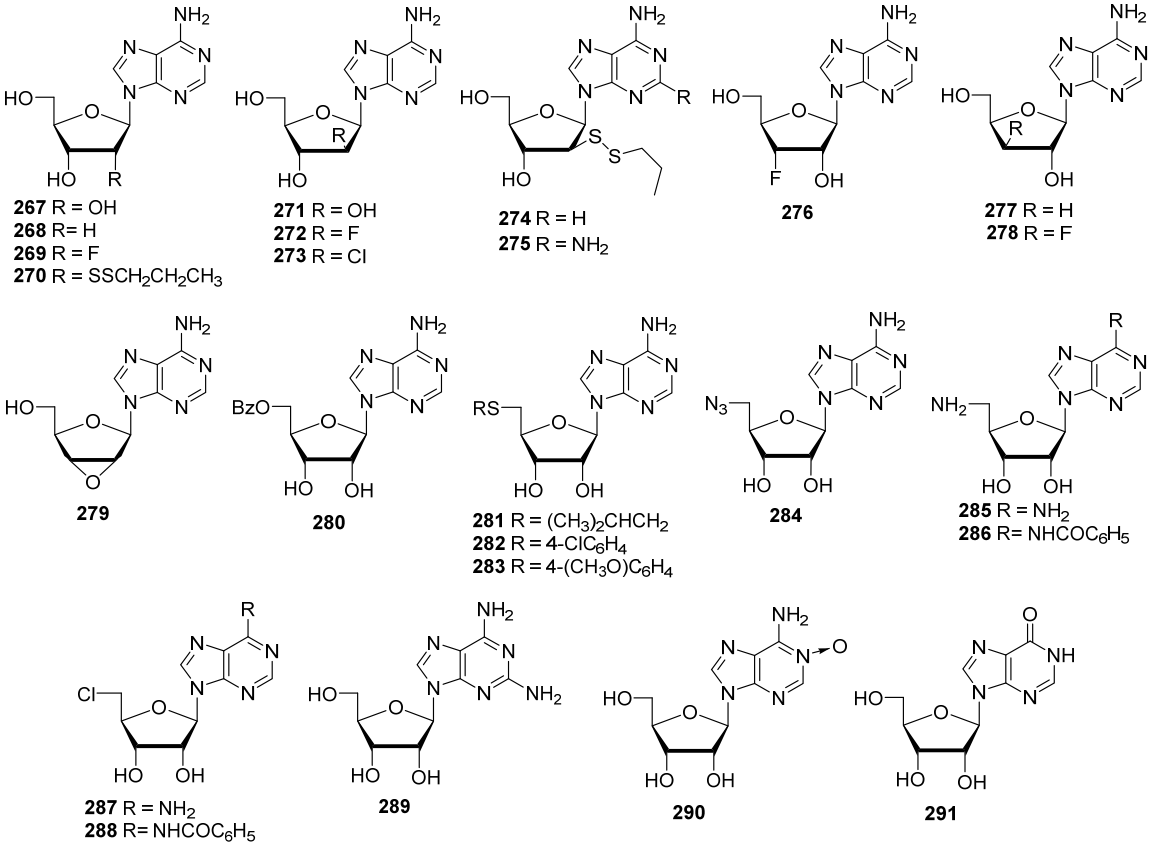

Figure 48. Modified adenosine analogues tested against *T. vaginalis*.

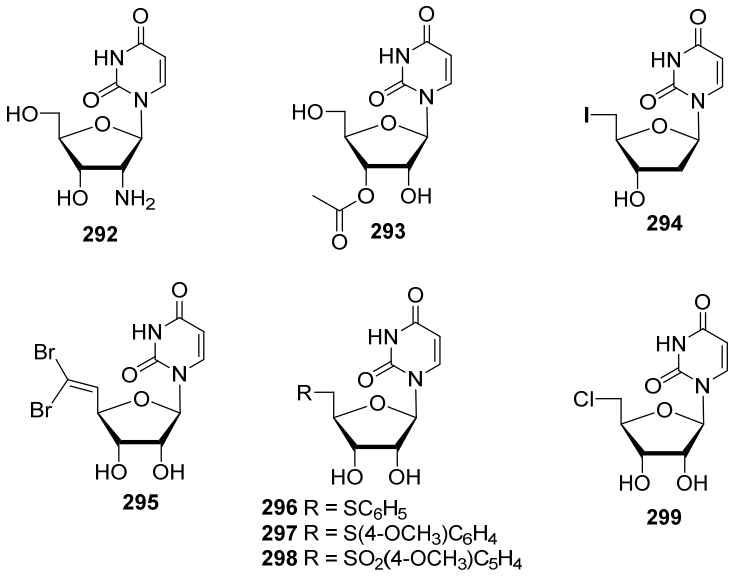

Figure 49. Modified uridine analogues tested against *T. vaginalis*

Compound	IC_{50} Value (μM)
Metronidazole	0.72
269	2.94
271	3.60
272	0.09
273	5.93
276	1.61
284	48.5
287	53.3
289	29.5

Table 8. Calculated IC_{50} values of the most potent compounds determined for *T. vaginalis* strain T1 and compared with metronidazole

3.4.2 Design of Tagging Experiments

Initially, I envisioned tagging at the 3' and 5' hydroxyl groups; however, the strategy was not advantageous because 3' and 5' hydroxyl phosphorylation might be an important step in the mechanism of action. Also, our attempts on coupling a carboxylic acid to incorporate a tag at the exocyclic amine (e.g., **300**) were unsuccessful with fluoro-arabinoadeosine, Figure 50.

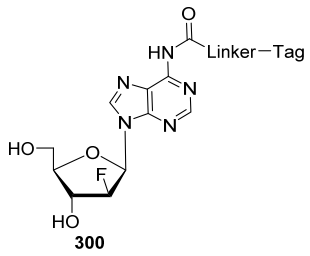

300

Figure 50. Tagging of Exocyclic Amine of F-*arabino*adenosine **272**

I then came across a publication detailing a procedure for visualizing the subcellular localization of K11777,[247] a protease inhibitor of *T. brucei*, a parasite similar to *T. vaginalis*. To visualize the location of K11777, live parasites were directly treated with an alkyne modified analogue of K11777, fixed, and reacted *in situ* with a fluorescent azide reporter, then imaged. I, therefore, developed our new experiment design, on a modified version of the proteomic profiling of K11777, in which live *T. vaginalis*

parasites are directly treated with azide modified fluoro-*arabino* analgoue, fixed, tagged, and then imaged.

3.4.3 Synthesis of Azide Modified Substrates

To accomplish this goal, I selected 8-azido-2'-fluoro-arabinoadenosine as our imaging probe because modifications at the C8 position remain in the major groove and do not affect the formation of DNA duplex.[248] Thus, I synthesized 8-bromo analogue **300** by direct bromination[250] of parent compound F-*ara*-Ado **272**. Further treatment of 8-bromo derivative **300** with sodium azide afforded azido modified clickable analogue **215**, Scheme 57. The identities of both novel compounds **215** and **300** were confirmed with UV-Vis, NMR and HRMS. The 8-bromo analogue **300** and 8-azido analogue **215** were also tested for *in vivo* inhibitory activity and showed 15.5 ± 0.9 and 19.6 ± 8.1 % inhibition at 100 μM, respectively.

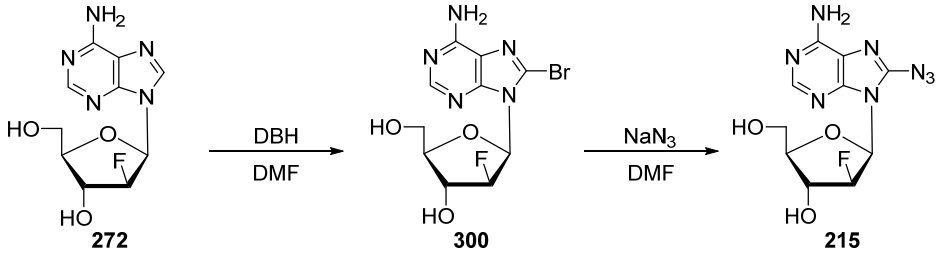

Scheme 57. Synthesis of 8-azido-fluoro-*arabino*adenosine **215**

3.4.4 Model Studies

I performed several model studies of the click reaction between azide **215** and commercially available cyclooctyne **218** that is conjugated via a linker to biotin before attempting the *in situ* labeling reaction, Scheme 58. Hence, the click reaction of **215** with unmodified cyclooctyne OCT **217** afforded derivative **221**; the identity of this compound was confirmed by NMR and LC-MS analysis. The labeling reaction with cyclooctyne

218 which is conjugated to biotin was successful albeit much messier on ^{1}H NMR showed a new peak on HPLC, corresponding to the labeled compound, **301**.

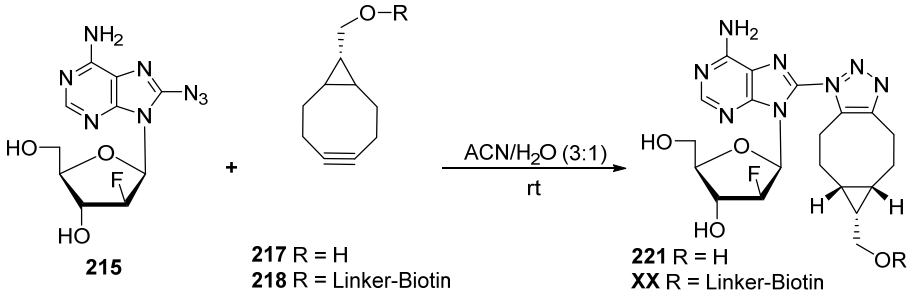

Scheme 58. Model click reactions on 8-azido-fluoro-*arabino*adenosine **215**

We intended to apply this new methodology for cellular localization and identification of potential cellular targets in collaboration with Dr. Kirkwood Land and Dr. Lisa Wrischnik at the University of the Pacific. This work is currently underway and may provide a basis for development of new drugs against this important human parasite

3.5 Synthesis of Azido-Modified α-Ketoglutarate

Next, we decided to take advantage of the click chemistry for subcellular localization that I developed previously; I decided to explore the application of this new methodology to identify the cellular targets of active compounds against the ubiquitous bacteria *Pseudomonas aeruginosa* in collaboration with Dr. Kalai Mathee from Florida International University's Department of Human and Molecular Genetics.

3.5.1 General Information about *Pseudomonas aeruginosa*

Pseudomonas aeruginosa is a gram negative, rod-shaped, asporogenous, and monoflagellated bacterium.[293] It uses aerobic respiration for metabolism but can respire anaerobically on nitrate or other electron acceptors. *P. aeruginosa* can catabolize a large

variety of organic molecules as carbon sources making it a pervasive microorganism usually found in soil, water, plants, sewage, and even immunocompromised humans.[294]

Analysis of *P. aeruginosa* shows the presence of a two component system (TCS), MifSR (MifS-Sensor and MifR-Response Regulator), which are upstream from the *pox*AB operon. It is has been postulated that the MifSR TCS is involved in β-lactam resistance (i.e. antipseudomonal penicillins) by the regulation of *pox*B.[295] In our study, te Mathee lab constructed mifR, mifS and mifSR deletion mutants, and compared to them to the wild type parent strain PAOl for differences in growth and phenotype.

3.5.2 General information about α-Ketoglutarate

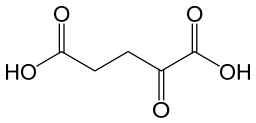

302

Figure 51. α-ketoglutarate

The α-ketoglutarate (α-KG) **302**, Figure 51, a member of the citric acid cycle, has been recognized as an intermediate for both carbon and nitrogen metabolism.[296] Campbell and Stokes noted that *P. aeruginosa* grown in acetate rich media displayed a significant lag when transferred into α-KG medium suggesting the possibility of an inducible α-KG transporter.[297] We found no *P. aeruginosa* growth, when the mifR, mifS, and mifSR deletion mutants were incubated with α-KG, indicating that either the α-KG was unable to cross the bacterial cell membrane because there is no transport protein or once the α-KG was inside the cell it was not metabolized and therefore could not be used as a carbon source. Interestingly, all the other components of the TCA cycle including citrate and isocitrate can be metabolized by the mifR, mifS and mifSR deletion mutants.

3.5.3 General information about 2,2-Difluoropentanedioic Acid

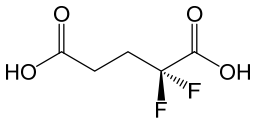

303

Figure 52. 2,2-Difluoropentanedioic acid

The 2,2-Difluoropentanedioic Acid (DFPA) **303**, Figure 52, a non-metabolizeable fluorinated derivative of α-KG, has been used to demonstrate the signaling functions of α-KG *in vivo*. Its cellular uptake and accumulation has studied by ^{19}F NMR.[298]

3.5.4 Synthesis of Azido-Modified α-Ketoglutarate

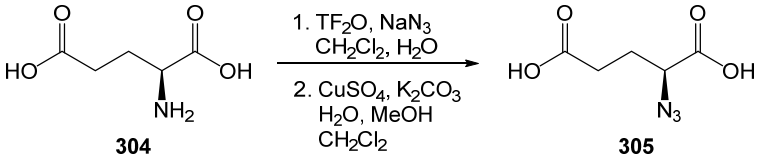

304 **305**

Scheme 59. Diazotization of α-ketoglutarate

The azido-modified α-glutarate **305** was prepared using a modified procedure described by Lundduist and Pelletier[299] for the synthesis of α-azide protected amino acids. First, the triflyl azide reagent was prepared from triflyl anhydride in a method similar to the one described previously by Wong.[300] Next, the unprotected glutamic acid **304** was combined with K_2CO_3 and $Cu^{II}SO_4$ pentahydrate in distilled water and MeOH. The freshly prepared triflyl azide was added and allowed to stir at ambient temperature and pressure overnight in a Morton flask. This reaction is a biphasic reaction with two liquid (aqueous and organic) phases; therefore, a Morton flask with a small magnetic stirrer must be used to maximize the turbulence and shear of the mixture. In the morning, the organic solvents were removed *in vacuo*, the aqueous slurry was diluted with H_2O and acidified to pH 6 with conc. HCl.

The product can be extracted using two different methods: A) *Buffered Extraction*: Phosphate buffer (0.25 M pH 6.2) was added and extracted with EtOAc to remove the sulfonamide byproduct. The aqueous phase was once again acidified to pH 2 and the extracted with EtOAc. B) *Acidification Extraction*: The aqueous layer was washed (4x) with EtOAc to remove the sulfonamide byproduct. The aqueous phase was once again acidified to pH 2 and the extracted with EtOAc. These extracts were pooled together, dried with $MgSO_4$ and evaporated to dryness to give **305** as a pale oil which was used directly in a click reaction. Although, the buffered extraction method gave pure **305**, the yields were low when compared to the method requiring acidification only.

3.5.5 Proposed testing on *Pseudomonas aeruginosa*

We proposed using SPAAC to study the inhibitory concentration and localization of azido modified glutaric acid **305** *in vivo* in *P. aeruginosa*. Growth curves for cells that have been infected with *P. aeruginosa* and treated with **305** were constructed to test if **305** can be utilized as an alternative carbon source and what is its minimum inhibitory concentration. We postulated that it should be similar to that of α-KG **304**. Second, we envisioned a tagging study which will utilize my previously developed SPAAC method and a fluorogenic cyclooctyne to prove that azido-KG **305** is not getting across the inner membrane of the cell when pcaT has been knocked down and is not present, Figure 53A. Thus, we should only see fluorescence outside of the cell or between the outer and inner membrane. This experiment will also be done with cells that that express pcaT to prove that it is a transporter of α-KG and only then should we see fluorescence inside of the cell and not in the cell membrane, Figure 53B. Lastly, an antibiotic resistance assay will be

performed to determine if the azido derivatized α-KG **305** has antibacterial properties and if it works synergistically with other known antibiotics.

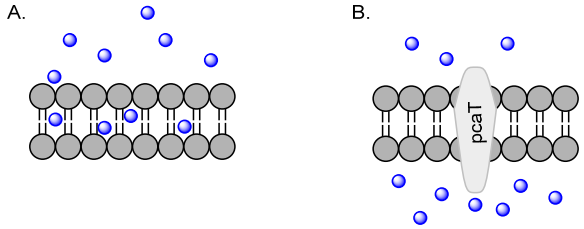

Figure 53. α-KG tagging study

3.5.6 Model Click Reactions with Azido-Modified α-Ketoglutarate

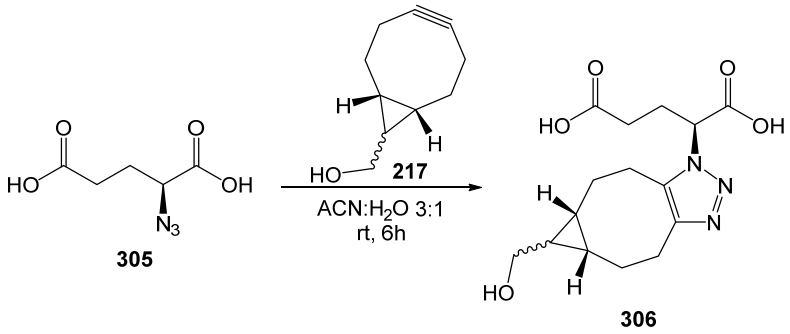

Scheme 60. Model SPAAC of α-azidoketoglutarate and OCT

The α-ketoglutarate modified with azido group at the C2 position **305** undergoes SPAAC reaction efficiently *in vitro*, Scheme 60. Thus, equivalent amounts of **305** reacts with OCT **217** in aqueous media at ambient temperature for 6 h to give **306** in a high yield (82%). This work is currently ongoing in the Mathee laboratory.

3.6 Synthesis of SAM Analogues for Probing TRMD

3.6.1 General Information about TRMD Enzyme

The tRNA(m^1G37)methyltransferase (TrmD) enzyme catalyzes the transfer of a methyl group from SAM to guanosine at position 37 within a division of bacterial tRNA. This function is essential in preventing frameshift errors thereby maintaining the correct reading frame during translation.[301-302] TrmD is made up of two separate domains, a

larger NTD domain and a smaller CTD domain connected by an extended flexible linker, Figure 54.[301, 303] The flexible linker appears to play a central role as the possible lid to cover the active site upon binding the cognate tRNA.[301]

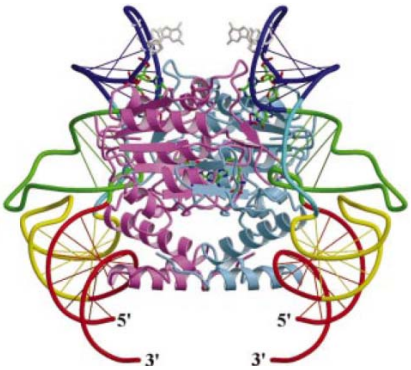

Figure 54. tRNA(m^1G37)methyltransferase (TrmD) Enzyme

The adenine portion of SAM is bound in one part of the trefoil binding pocket, and the amino acid portion is buried in another portion of the pocket with the positively charged methyl group jutting out of the binding pocket. A total of nine H-bonds suspend SAM in the TrmD binding pocket.[301] Typically, the O4'-C4'-C5'-SR dihedral angle in most SAM dependent methyltransferase is -170° to -180° and 160° to 180° which places the amino acid moiety in an extended conformation, Figure 55A.[304] However, when SAM is bound in the TrmD binding pocket it adopts a novel, bent conformation with its O4'-C4'-C5'-SD dihedral angle -62°, Figure 55B.[301]

A. **B.**

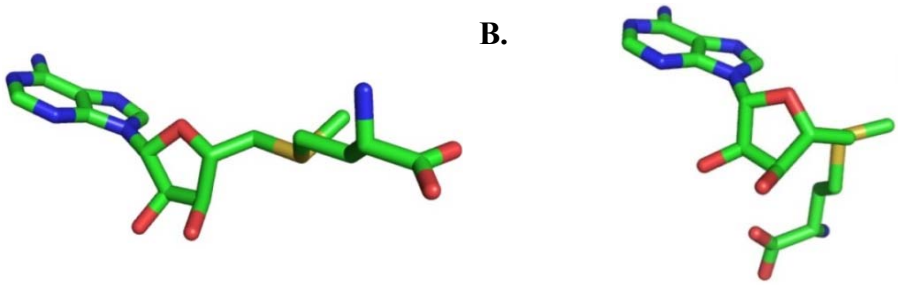

Figure 55. A. Typically conformation of SAM in methyltransferase enzyme active site. **B.** Conformation of SAM in the TrmD active site.

3.6.2 Synthesis and Tagging of EnYn Analogue of SAM

Methyltransferases (MTases) catalyze highly specific transfers of methyl groups from the ubiquitous cofactor S-adenosyl-*L*-methionine to various nucleophilic positions in biopolymers like DNA, RNA, and proteins. Doubly activated SAM analogue **20** was synthesized for use in reactions with methyltansferases, enzymatic tagging and click chemistry for eventual introduction of a fluorophore.[305-306]

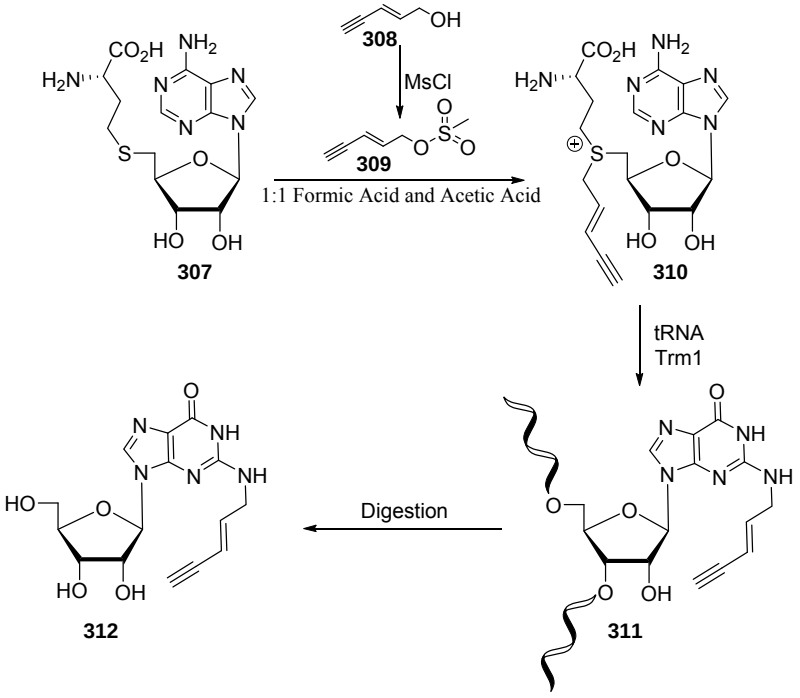

Scheme 61. Synthesis of AdoEnYn and application with Trm1

Doubly activated AdoEnYn **310** was synthesized using the procedure by published Weinhold and coworkers, which reacted SAH **307** with mesyl activated (*E*)-pent-2-en-4-yn-1-ol **309**, Scheme 61.[307] Thus, treatment of freshly distilled (*E*)-pent-2-en-4-yn-1-ol **308** with 1.1 equivalents of mesyl chloride gave mesyl activated analogue **309**. The activated alcohol **309** was dissolved in a mixture of formic and acetic acid (1:1) and

added directly to SAH **307**. After 14 h, the reaction was quenched by the addition of water and purified with RP-HPLC to give **310**.

Initial reactions with enzyme Trm1 showed that AdoEnYn **310** can inhibit AdoMet-dependent methylation of tRNA, indicating that there is competition with the authentic methyl donor. An inhibition analysis revealed that AdoEnYn has a similar affinity to the methylation enzyme in the range of K_d of 11-17 μM. Furthermore, AdoMet-methylated tRNA synthesized in the presence of AdoEnYn has reduced physical blockage to reverse transcriptase at the expected site on the tRNA, indicating that there is inhibition of methylation to the expected site. This suggests that AdoEnYn can be incorporated into tRNA in place of AdoMet. LC-MS/MS analysis of a reaction between tRNA, Trm1 and AdoEnYn showed EnYn2G **311** as well as expected fragmentation (e.g., **312**) indicating that the EnYn group was transferred from AdoEnYn **310** by methyltransferase Trm1 to guanosine on tRNA **21**.

3.6.3 Design and Attempts at Synthesis of Cyclic Analogues

The research aim of this section was the synthesis of constrained *S*-adenosyl-L-methionine analogues which will mimic the naturally occurring bent conformation of SAM in the tRNA(m^1G37)methyltransferase (TrmD) binding pocket, Figure 53. These analogues will serve as probes to study the transfer of the protruding methyl group and possibly as tRNA inhibitors. To achieve this goal I designed bicyclic nucleoside derivatives having 9, 10, or 11 membered rings bridging from the C5' thioether to either the 3' OH or 2' OH groups which will mimic the naturally occurring bent conformation of SAM in the TrmD binding pocket. Numerous synthetic pathways including lactonization, lactamization and ring closure metathesis (RCM) were explored in attempts

at the synthesis of novel constrained SAM analogues. Preliminary docking studies of lactone derivatives, conducted in the laboratory of Dr. Ya Ming Hou at Thomas Jefferson University, suggested that derivatives with either xylo or arabino conformations are better accommodated by the TrmD binding pocket.

3.6.3.1 Lactonization

In this approach, I targeted the synthesis of macrolactone **316** that featured an ester linkage to the 3'-OH and a thioether linkage to the 5'-S forming a 9 membered ring, Scheme 62. Thus, **314** was prepared via a substitution reaction of 5'analogue **313** with the open form of γ-butyrothiolactone. Deprotection of methyl ester **314** with NaOMe gave acid **315**. Macrocyclization of thioether **315** was attempted using an HOBt coupling protocol;[308] however, my attempts at this procedure were unsuccessful. This could be attributed to the instability of the resulting ester; because an ester linkage is prone to hydrolysis and therefore too unstable to use as my key linkage.

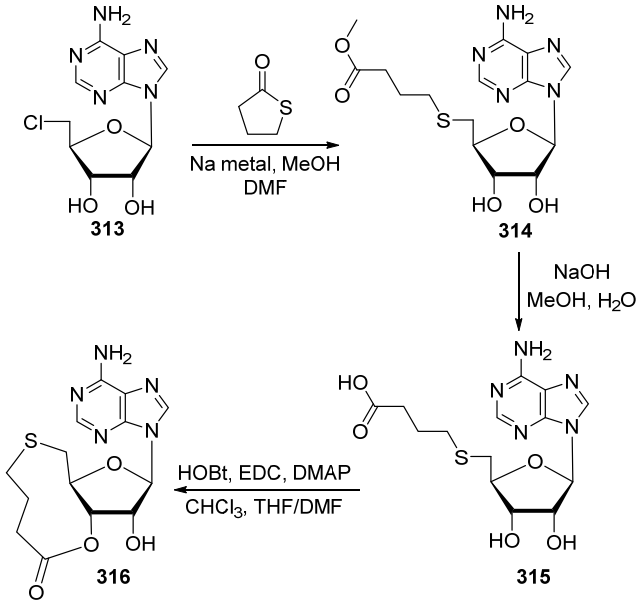

Scheme 62. Synthesis and attempted cyclization of model SAM analogue **315**

3.6.3.2 Lactamization

I subsequently turned my attention to the synthesis of macrolactam **317**, Figure 56, an analogue of aminonucleoside antibiotic, Puromycin **318**, which is an analogue of the 3' end of a tyrosyl-tRNA since it is comprised of a molecule of adenosine, linked at the 3' position to a molecule of tyrosine via a stable non-hydrolysable amide bond. For this reason, I designed macrolactam **317** which is an analogue of both *S*-Adenosyl-*l*-Homocysteine and Puromycin since it combines a molecule of adenosine and one of homocysteine linked via a non-hydrolysable amide linkage at the 3' position.

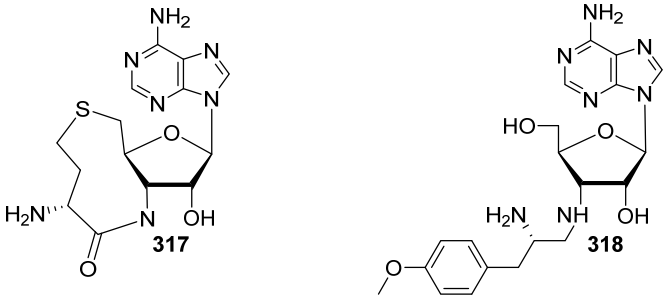

Figure 56. SAH macolactam and Puromycin

Lactam **317** can be synthesized from key intermediate azide **320** which I synthesized in 7 steps from adenosine, Scheme 63.[309-310]

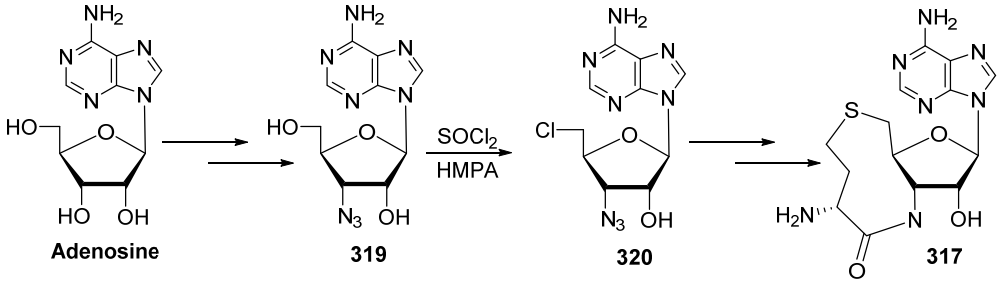

Scheme 63. Overview of the synthetic pathway for the synthesis of macrolactam **317**

The synthesis of lactam **317** was attempted several different ways, Scheme 64. Substitution of the 5' chloro- group of **320** with the sodium salt of homocysteine afforded

derivative **321** in a fair yield. In an attempt to optimize this yield the reaction was repeated with homocysteine lactone and by *in situ* reduction of *N*-Boc protected homocystine with Dithiothreitol (DTT); only the latter strategy yielded the corresponding Boc-protected analogue **323** in low yields. This method was later abandoned because of the very low yields of each of the synthetic manipulations.

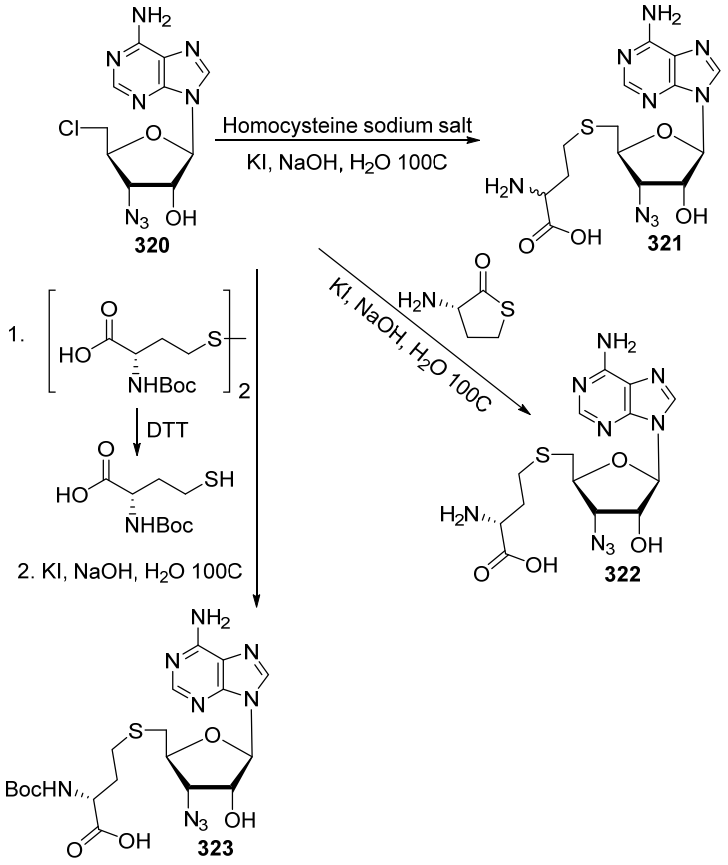

Scheme 64. Homocysteine substitution of 5'-chloroadenosine analogue **321**

Cyclization was then attempted in the opposite way, Scheme 65. Azide **320** was condensed with the oxybenzotriazolyl ester of *N*-Boc-*S*-Trityl-Homocysteine, which was formed *in situ* by the treatment of commercial *N*-Boc-*S*-Tr-Hcy with HOBt and DIC at 0 °C,[311] to afford amide **324**. The *tert*-Butyloxycarbonyl (Boc) protection on the amino group was easily deprotected using a mixture of trifluoroacetic acid and dichloromethane

at ambient temperature;[312] however, deprotection of the *S*-trityl group was unsuccessful and led to significant glycosidic bond cleavage. Furthermore, staining of a TLC of the reaction mixture with Ellman's reagent, a stain used to visualize free thiol groups, showed no yellow color, thus proving that no free thiol was present. Several attempts at this reaction all showed similar results, glycosidic cleavage and no free thiol. Thus, this method was also abandoned.

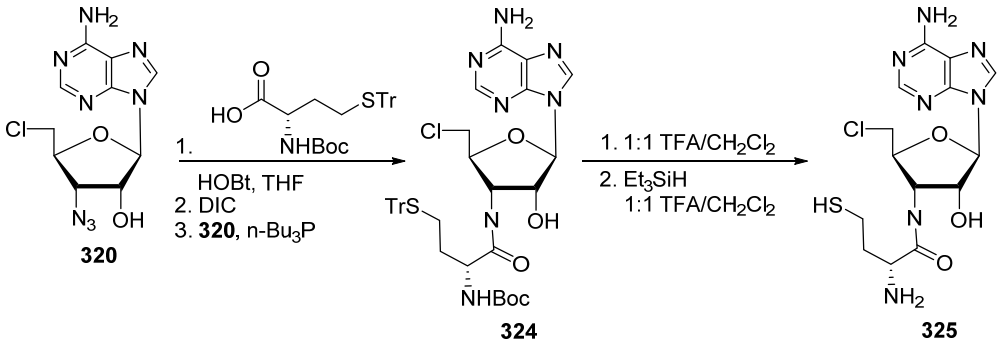

Scheme 65. Synthesis of amide linked homosysteine-adenosine conjugate **324**

3.6.3.3 Ring Closure Metathesis

Ring closure metathesis (RCM) has been used to the past to synthesize previously difficult to assemble rings. RCM is an alkene synthesis which uses a Grubbs' catalyst, yielding the cycloalkene and a volatile alkene. Thus, allylation of 5'-chloro analogue **313** with dibutyltin oxide and allyl bromide yielded a mixture of 2' and 3' O-allyl isomers **327** and **326**, respectively, which were chromatographically separated to yield pure 3' O-allyl derivative **326**, Scheme 66.[313-315] Unfortunately, only trace amounts of pure **326** were recovered indicating that **327** was the major allyl compound formed because the 2' hydroxyl is more reactive since it is adjacent to the glycosidic bond and electron withdrawing base. Treatment of **327** with allyl mercaptan should lead to the di-allyl

compound; however, NMR analysis of the product showed that the 5'-allyl group had isomerized to a vinyl moiety affording **330** instead.[316] Treatment of **313** with allyl mercaptan gave **328** in very low yields. Also, subjection of di-allyl derivative **329** to a RCM reaction using the *second*-generation Grubbs' catalyst[317] should yield the unsaturated bicyclic derivative as expected on the basis of literature precedence for the synthesis of other bicyclic nucleoside analogues. This approach, however, was never attempted because of the low preparative yields of key di-allyl starting material **329** most probably as a result of isomerization of the 5' S-allyl group.

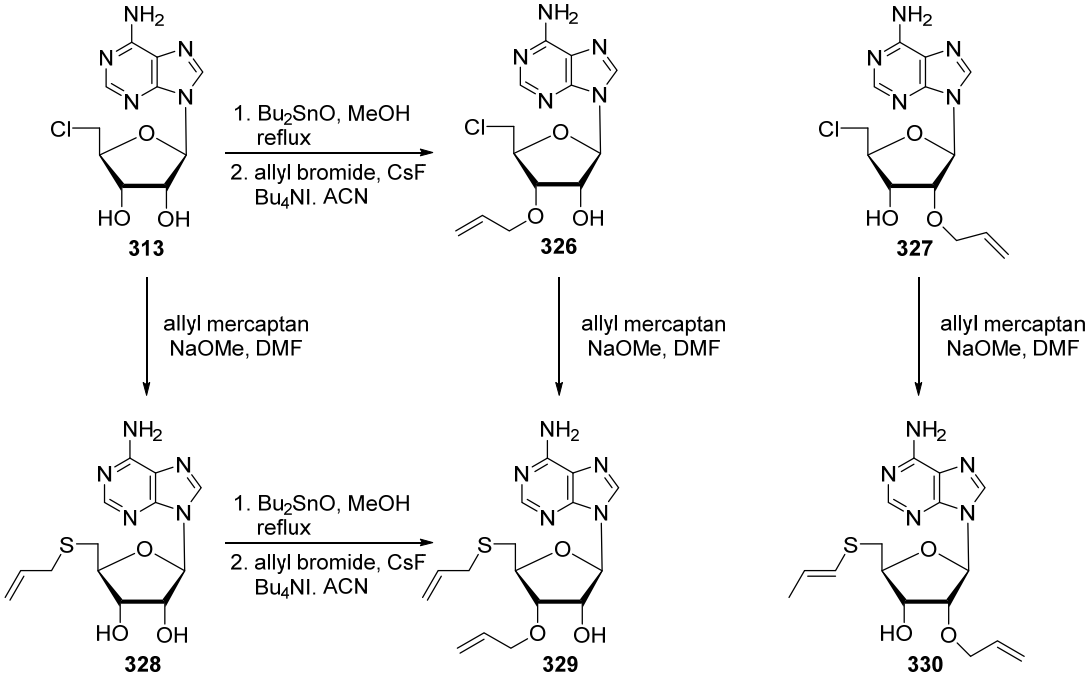

Scheme 66. Synthesis of 3',5' diallylated adenosine **329**

4 Experimental

4.1 General Procedure

Materials and General Methods. Detailed methods and characterization can be found in the Supporting Information. The ^{1}H (400 MHz), ^{19}F NMR (376.4 MHz) and ^{13}C

(100.6 MHz) were recorded at ambient temperature in solutions of ACN-d_3, D_2O, or DMSO-d_6, as noted. The reactions were followed by TLC with Merck Kieselgel 60-F254 sheets, and products were detected with a 254nm light. Column chromatography was performed using Merck Kieselgel 60 (230−400 mesh). Reagent-grade chemicals were used, and solvents were dried by reflux distillation over CaH_2 under nitrogen gas unless otherwise specified. Azido nucleoside substrates were prepared as described in literature (**200**,[249] **214**,[318] **216**,[319] and **243**[255]**)** or in experimental section (**215)**, or are commercially available (**201**, **202** and **229)** from Carbosynth. Cyclooctynes **217**, **218**, **223** and **227** are commercially available from Kerafast, SynAffix, Sigma Aldrich or Berry & Associates. Lipofectamine LTX and Plus reagent was purchased from Invitrogen. HPLC analysis was performed on a semi-preparative Phenomenex Gemini RP-C18 column (5 μ, 25 cm × 1 cm) with UV detection at 254 nm.

4.2 Synthesis of Novel Azido Nucleosides

8-Bromo-9-(2-deoxy-2-fluoro-β-D-arabinofuranosyl)adenine (212). 1,3-Dibromo-5,5-dimethylhydantoin (DBH; 29.1 mg, 0.10 mmol) was added to a stirred solution of 9-(2-deoxy-2-fluoro-β-D-arabinofuranosyl)adenine[S320] (**208** 41 mg, 0.15 mmol) in DMF (1.5 mL). The resulting pale-yellow solution was stirred at ambient temperature for 5 h. Volatiles were evaporated *in vacuo* and the resulting residue was purified on silica gel column chromatography (EtOAc → 4% MeOH/EtOAc) to give **212** (27.8 mg, 54%) as a white solid: UV λ_{max} 262 nm (ε 15 400); ^{1}H NMR (DMSO-d_6) δ 3.73-3.80 (m, 2H, H5' & 5''), 3.82-3.86 (m, 1H, H4'), 4.76 (ddd, J = 22.3 Hz, 7.7 Hz, 5.7 Hz, 1H, H3'), 5.33 (dt, J = 54.3 Hz, 5.7 Hz, 1H, H2'), 6.47 (dd, J = 8.3 Hz, 6.5 Hz, 1H,

H1'), 8.10 (s, 1H, H2); ^{19}F NMR (DMSO-d_6) δ -197.94 (ddd, J = 53.7, 21.3, 8.4 Hz); ^{13}C NMR δ 60.58 (C5'), 72.66 (d, J = 22.2 Hz, C3'), 81.75 (d, J =8.9 Hz, C4'), 83.32 (d, J = 17.4 Hz, C1'), 96.07 (d, J = 195.6, C2'), 118.98 (C5), 125.76 (C8), 150.36 (C4), 152.49 (C6), 154.52 (C2); HRMS (ESI$^+$) *m/z* calcd $C_{10}H_{11}BrFN_5O_3$ $(M+H)^+$: 348.0102, found: 348.0095.

8-Azido-9-(2-deoxy-2-fluoro-β-D-arabinofuranosyl)adenine (215). NaN_3 (18.0 mg, 0.30 mmol) was added to a stirred solution of **212** (20 mg, 0.06 mmol) in DMF (2.0 mL). The resulting pale-yellow solution was stirred at 70 °C overnight. After 16 h, the volatiles were evaporated *in vacuo* and the resulting residue was purified on column chromatography (EtOAc → 4% MeOH/EtOAc) to give **215** (10.3 mg, 61%) as a white solid: UV λ_{max} 280 nm (ε 14 500); ^{1}H NMR (DMSO-d_6) δ 3.70-3.78 (m, 3H, H5', H5" & OH), 4.74-4.82 (m, 1H, H4'), 5.10 (t, J = 6.3 Hz, 1H, H3'), 5.31 (dt, J = 54.5 Hz, 6.1 Hz, 1H, H2'), 5.90 (d, J = 4.7 Hz, 1H, OH), 6.29 (t, J = 6.96, 1H, H1'), 7.29 (bs, 2H, NH_2), 8.09 (s, 1H, H2); ^{19}F NMR (DMSO-d_6) δ -199.06 (ddd, J = 53.9, 21.7, 7.1 Hz, 1F); ^{13}C NMR δ 60.99 (C5'), 72.56 (d, J = 21.7 Hz, C3'), 80.22 (d, J = 17.5 Hz, C1'), 81.82 (d, J = 9.4 Hz, C4'), 96.08 (d, J = 195.4 Hz, C2'), 116.61 (C5), 143.93 (C8), 149.70 (C4), 151.76 (C6), 154.29 (C2); HRMS (ESI$^+$) *m/z* calcd $C_{10}H_{11}FN_8NaO_3$ $(M+Na)^+$: 333.0830, found: 333.0825.

4.3 Synthesis Of Nucleoside Click Adducts

8-(1,2,3-Triazol-1*H*-yl)adenosine-OCT adduct (203). Typical Procedure. Cyclooctyne **217** (*endo*; 7.6 mg, 0.05 mmol) was added to a stirred solution of 8-azidoadenosine[249] **200** (15.0 mg, 0.05 mmol) in a mixture of ACN/H_2O (3:1, 1 mL) at ambient temperature. After 3 h, the volatiles were evaporated *in vacuo* and the resulting

residue was purified on silica gel column chromatography (EtOAc → 20% MeOH/EtOAc) to give **7** as mixture of regioisomers (1:1; 21.0 mg, 96%) as a white solid. Alternatively the crude reaction mixture was passed through a 0.2 μm PTFE syringe filter, and then purified on the semipreparative HPLC column (17% ACN/H_2O, 2.0 mL/min) to give **203** (1:1; 21.0 mg, 96%) as a white solid (t_R = 4.5–8.2 min): UV λ_{max} 270 nm (ε 21 100), λ_{min} 241 nm (ε 12 100); ^{1}H NMR (DMSO-d_6) δ 0.84-0.95 (m, 2H, Hγ), 0.99 ("q", *J* = 9.4 Hz, 0.5H, CH cyclopropyl), 1.00 (q, *J* = 9.4 Hz, 0.5H, CH cyclopropyl), 1.51-1.74 (m, 2H, Hβ), 2.00-2.19 (m, 2H, Hβ), 2.57-2.67 (m, 1H, Hα), 2.77-2.87 (m, 1H, Hα), 2.87-2.99 (m, 1H, Hα), 3.09-3.15 (m, 1H, Hα), 3.42-3.53 (m, 3H, CH_2 & H5'), 3.58 ("dd" *J* = 12.2, 4.2 Hz, 1H, H5"), 3.85-3.93 (m, 1H, H4'), 4.00-4.07 (m, 1H, H3'), 4.35 (t, *J* = 4.9 Hz, 1H, OH), 4.93 ("q", *J* = 5.2 Hz, 0.5H, H2'), 5.00 ("q", *J* = 5.2 Hz, 0.5H, H2'), 5.12-5.23 (m, 2H, H1' & OH), 5.36-5.52 (m, 2H, 2 x OH), 7.78 (br s, 2H, NH_2), 8.23 (s, 1H, H2); ^{13}C NMR (CD_3CN) δ 18.44, 18.58, 18.62, 20.14, 20.22, 20.82, 20.88, 21.21, 21.30, 22.33, 22.44, 25.04, 58.02, 58.81, 62.08, 69.18, 70.83, 71.01, 72.39, 72.44, 72.56, 86.96, 87.05, 89.39, 90.92, 138.39, 138.42, 138.47, 144.87, 144.93, 148.52, 152.01, 153.35, 156.31; HRMS (ESI$^+$) *m/z* calcd $C_{20}H_{27}N_9O_5$ $(M+H)^+$: 459.2054, found: 459.2050

Note: Analogous treatment of **200** (7.0 mg, 0.023 mmol) with **217** (4.7:1, *exo-endo*; 3.4 mg, 0.023 mmol) also gave **203** (~1:1; 10.0 mg, 96%).

9-(β-D-Arabinofuranosyl)-8-(1,2,3-triazol-1*H*-yl)adenine-OCT adduct (219). Cyclooctyne **217** (4.7:1, *exo-endo*; 4.9 mg, 0.02 mmol) was added to a stirred solution of **214**[318] (10.0 mg, 0.02 mmol) in a mixture of ACN/H_2O (3:1, 1 mL) at ambient temperature. After 1 h, the volatiles were evaporated *in vacuo* and the resulting residue

was purified by column chromatography on silica gel (EtOAc → 20% MeOH/EtOAc) to give **219** as mixture of regioisomers (~1:1; 12.8 mg, 93%) as a white solid: UV λ_{max} 273 nm (ε 17 500), λ_{min} 248 nm (ε 8700); ^{1}H NMR (DMSO-d_6) δ 0.83-0.96 (m, 2H, 2 x Hγ), 0.96-1.07 (m, 1H, CH cyclopropyl), 1.50-1.70 (m, 2H, 2 x Hβ), 2.01-2.19 (m, 2H, 2 x Hβ), 2.56-2.71 (m, 1H, Hα), 2.78-2.95 (m, 2H, 2 x Hα), 3.11 ("q", *J* = 3.3 Hz, 0.5H, Hα), 3.15 ("q", *J* = 3.6 Hz, 0.5H, Hα), 3.46-3.53 (m, 1H, H5'), 3.58-3.66 (m, 3H, H5" & CH_2OH), 4.20 (q, 1H, *J* = 5.6 Hz, H4'), 4.26-4.37 (m, 1H, H2' & H3'), 5.08-5.15 (m, 1H, OH), 5.41 (br s, 1H, OH), 5.63-5.67 (m, 1H, OH), 5.69 (d, *J* = 6.7 Hz, 0.5H, H1'), 5.71 (d, *J* = 6.8 Hz, 0.5, H1'), 7.61 (s, 2H, NH_2), 8.23 (s, 1H, H2); ^{13}C NMR (DMSO-d_6) δ 13.34, 17.42, 17.49, 19.31, 19.84, 19.87, 20.36, 20.38, 21.65, 24.12, 24.17, 30.09, 35.23, 56.57, 59.73, 73.17, 73.28, 75.17, 75.24, 81.61, 81.69, 84.24, 84.27, 115.79, 137.15, 137.18, 137.42, 137.43, 143.29, 143.34, 148.43, 152.46, 154.95, 162.35; HRMS (ESI$^+$) *m/z* calcd $C_{20}H_{26}N_8NaO_5$ $(M+Na)^+$: 481.1918, found: 481.1927.

9-(β-D-Arabinofuranosyl)-8-(1,2,3-triazol-1*H*-yl)adenine-OCT-biotin adduct (220). Cyclooctyne **218** (*endo*; 5.5 mg, 0.01 mmol) was added to a stirred solution of **214** (3.1 mg, 0.01 mmol) in a mixture of ACN/H_2O (3:1, 1 mL) at ambient temperature. After 2 h (TLC showed complete conversion to the more polar product), the volatiles were evaporated *in vacuo* and the resulting residue was purified by HPLC (as described for **7**) to give **220** (5.4 mg, 71%) as a white oil: HRMS (ESI$^+$) *m/z* calcd $C_{20}H_{26}N_8NaO_5$ $(M+Na)^+$: 481.1918, found: 481.1927.

9-(2-Deoxy-2-fluoro-β-D-arabinofuranosyl)-8-(1,2,3-triazol-1*H*-yl)adenine-OCT adduct (221). Cyclooctyne **217** (*exo:endo,* 4.7:1; 3.7 mg, 0.025 mmol) was added to a stirred solution of **215** (7.6 mg, 0.025 mmol) in a mixture of ACN/H_2O (3:1, 1 mL) at

ambient temperature. After 2 h (TLC and NMR showed complete conversion of **215** to **221**) the volatiles were evaporated *in vacuo* to give **221** as mixture of regioisomers (~1:1; 11 mg, 95%) as a white solid: ^{1}H NMR (DMSO-d_6) δ 0.84-0.97 (m, 2H, 2 x Hγ), 0.98-1.07 (m, 1H, CH cyclopropyl), 1.52-1.71 (m, 2H, 2 x Hβ), 2.00-2.19 (m, 2H, 2 x Hβ), 2.56-2.72 (m, 1H, Hα), 2.73-2.95 (m, 2H, 2 x Hα), 3.09-3.16 (m, 1H, Hα), 3.46-3.53 (m, 2H, CH_2OH), 3.54-3.67 (m, 2H, H5' & H5"), 3.69-3.75 (m, 1H, OH), 4.31-4.38 (m, 1H, OH), 4.63-4.77 (m, 1H, H4'), 5.06-5.12 (m, 1H, H3'), 5.23 (dt, *J* = 53.9, 5.7 Hz, H2'), 5.86-5.95 (m, 2H, H1' & OH), 7.00 (br s, 2H, NH_2), 8.27 (s, 0.5H, H2), 8.28 (s, 0.5H, H2); ^{19}F NMR (DMSO-d_6) δ -198.52 (ddd, *J* = 53.9, 21.4, 8.2 Hz, 0.5F), -199.01 (ddd, *J* = 53.9, 21.5, 7.3 Hz, 0.5F); HRMS (ESI$^+$) *m/z* calcd $C_{20}H_{26}FN_8O_4$ $(M+H)^+$: 461.2056, found: 461.2059.

2'-Deoxy-8-(1,2,3-triazol-1*H*-yl)adenosine-OCT adduct (222). Cyclooctyne **217** (*endo*; 15.7 mg, 0.1 mmol) was added to a stirred solution of **216**[319] (29.5 mg, 0.1 mmol) in a mixture of ACN/H_2O (3:1, 1 mL) at ambient temperature. After 3 h, the crude reaction mixture was passed through a 0.2 μm PTFE syringe filter, and then purified on the semipreparative HPLC column (17% ACN/H_2O, 2.0 mL/min) to give **222** as mixture of regioisomers (1:1; 49.3 mg, 96%) as a white solid (t_R = 13.0–16.2 min): UV λ_{max} 272 nm (ε 18 200), λ_{min} 238 nm (ε 8500); ^{1}H NMR (DMSO-d_6) 0.82-0.95 (m, 2H, 2 x Hγ), 0.96-1.07 (m, 1H, CH cyclopropyl), 1.53-1.72 (m, 2H, 2 x Hβ), 2.03-2.19 (m, 3H, H2' & 2 x Hβ'), 2.60-2.72 (m, 2H, 2 x Hα), 2.81-2.97 (m, 2H, 2 x Hα), 3.03-3.18 (m, 3H, H2" & 2 x Hα), 3.37-3.45 (m, 1H, H5'), 3.47-3.59 (m, 3H, H5' & CH_2OH), 3.76-3.82 (m, 1H, H4'), 4.30-4.37 (m, 2H, H3' & OH), 5.26 (d, *J* = 4.0 Hz, 1H, OH), 5.27-5.34 (m, 1H, OH), 5.71 (dd, *J* = 6.4, 3.1 Hz, 0.5H, H1'), 5.73 (dd, *J* = 6.4, 3.2 Hz, 0.5H, H1'), 7.72 (br

s, 2H, NH_2), 8.26 (s, 1H, H2); HRMS (ESI^+) *m/z* calcd $C_{20}H_{27}N_8O_4$ $(M+H)^+$: 443.2150, found: 443.2142.

8-(1,2,3-Triazol-1*H*-yl)adenosine-DBCO adduct (224). Cyclooctyne **223** (15.0 mg, 0.055 mmol) was added to a stirred solution of **200** (16.4 mg, 0.055 mmol) in a mixture of ACN/H_2O (3:1, 1.5 mL) at 50 °C. After 16 h, the crude reaction mixture was passed through a 0.2 μm PTFE syringe filter, and then injected into a semipreparative HPLC column (40% ACN/H_2O 1.0 mL/min) to give **224** (10.6 mg, 98%) as a mixture of several inseparable regioisomers (t_R = 15.5–23.0 min): UV λ_{max} 276 nm (ε 16 000), λ_{sh} 307 nm (ε 11 200), λ_{min} 270 nm (ε 14 500). Two major isomers (~85-90% of total isomeric composition) had: ^1H NMR (DMSO-d_6) δ 1.64-1.78 (m, 2H, NH_2), 2.08-2.33 (m, 2H, CH_2CO), 2.67-2.81 (m, 2H, C$H_2$$NH_2$), 3.31-4.18 (m, 4H, H3', H4', H5' & H5"), 4.59 ("dm", *J* = 17.1 Hz, 1H, CH_2), 5.08-5.18 (m, 1H, H2'), 5.19-5.55 (m, 3H, 3 x OH), 5.72 (d, *J* = 7.5 Hz, 0.5H, H1'), 5.83 (d, *J* = 7.0 Hz, 0.5H, H1'), 5.96 (br d, *J* = 17.6 Hz, 1H, CH_2), 6.09 (br d, *J* = 17.4 Hz, 1H, CH_2), 7.26-7.56 (m, 8H, H_{ar}), 8.25 (s, 0.5H, H2), 8.28 (s, 0.5H, H2); HRMS (ESI^+) *m/z* calcd $C_{28}H_{29}N_{10}O_5$ $(M+H)^+$: 585.2317, found: 585.2330.

9-(β-D-Arabinofuranosyl)-8-(1,2,3-triazol-1*H*-yl)adenine-DBCO adduct (225). Cyclooctyne **223** (5.72 mg, 0.02 mmol) was added to a stirred solution of **201** (4.0 mg, 0.02 mmol) in MeOH (1 mL) at 50 °C. After 16 h, the crude reaction mixture was passed through a 0.2 μm PTFE syringe filter, and then injected into a semipreparative HPLC column (Phenomenex Gemini RP-C18 column; 5 μ, 25 cm × 1 cm) (40% ACN/H_2O, 1.5 mL/min) to give **225** (8.52 mg, 95%) as a mixture of several inseparable regioisomers (t_R = 5.5–10.0 min): ^1H NMR (DMSO-d_6) δ Two major isomers (~85-90%

of total isomeric composition) had: ^{1}H NMR (DMSO-d_6) δ 1.42-1.78 (m, 2H, NH_2), 2.01-2.17 (m, 2H, CH_2CO), 2.60-2.78 (m, 2H, CH_2NH$_2$), 3.17-3.24 (m, 2H, H4' & H5'), 3.28 (dd, J = 11.5 Hz, 4.6 Hz, 1H, H5''), 3.83-3.87 (m, 1H, H3'), 4.10 (t, J = 6.0 Hz, 0.5H, H2'), 4.11 (t, J = 5.9 Hz, 0.5H, H2'), 4.49 (br s, 2H, CH_2), 5.72 (d, J = 5.1 Hz, 1H, H1'), 7.26-7.56 (m, 8H, H_{ar}), 8.09 (s, 1H, H2); HRMS (ESI$^+$) *m/z* calcd $C_{28}H_{29}N_{10}O_5$ $(M+H)^+$: 585.2317, found: 585.2425.

2'-Deoxy-8-(1,2,3-triazol-1*H*-yl)adenosine-DBCO adduct (226). Cyclooctyne **223** (4.7 mg, 0.015 mmol) was added to a stirred solution of **203** (4.9 mg, 0.015 mmol) in MeOH (1.5 mL) at 50 °C. After 16 h, the crude reaction mixture was passed through a 0.2 μm PTFE syringe filter, and then injected into a semipreparative HPLC column (Phenomenex Gemini RP-C18 column; 5 μ, 25 cm × 1 cm (40% ACN/H_2O, 2.0 mL/min) to give **226** (9.5 mg, 95%) as a mixture of several inseparable regioisomers (t_R = 8.5–5.0 min): UV λ_{max} 273 nm (ε 12 550); ^{1}H NMR (DMSO-d_6) δ 1.64-1.81 (m, 2H, NH_2), 2.11-2.15 (m, 1H, H2'), 2.15-2.30 (m, 2H, CH_2CO), 2.60-2.79 (m, 2H, CH_2NH$_2$), 3.34-3.95 (m, 4H, H3', H4', H5' & H5''), 4.51-4.60 (m, 2H, CH_2), 4.91 (dd, J = 5.8, 2.3 Hz, 1H, H2'), 5.18-5.48 (m, 3H, 3 x OH), 5.74 (d, J = 6.7 Hz, 0.5H, H1'), 5.76 (d, J =6.2 Hz, 0.5H, H1'), 5.94 (br d, J = 15.8 Hz, 1H, CH_2), 6.12 (br d, J = 16.4 Hz, 1H, CH_2), (6.86-7.84 (m, 8H, H_{ar}), 8.4 (s, 0.5H, H2), 7.94 (s, 0.5H, H2); HRMS (ESI$^+$) m/z calcd $C_{28}H_{29}N_{10}O_4$ $(M+H)^+$: 569.2368, found: 569.2411.

8-(1,2,3-Triazol-1*H*-yl)adenosine-MFCO adduct (228). Cyclooctyne **227** (6.25 mg, 0.02 mmol) was added to a stirred solution of **200** (6.25 mg, 0.02 mmol) in MeOH (1 mL) at ambient temperature. After 16 h, the volatiles were evaporated *in vacuo* to give cycloadduct **228** (1:1; 12.3 mg, 98%) as a clear oil: UV λ_{max} 271 nm (ε 16 400), λ_{min} 242

nm (ε 8000); ^{1}H NMR (DMSO-d_6/D_2O) δ 1.43-1.50 (m, 6H, 3 x CH_2), 1.56-1.67 (m, 4H, 2 x CH_2), 1.67-1.75 (m, 2H, CH_2), 2.23-2.34 (m, 2H, CH_2), 2.54-2.60 (m, 2H, CH_2), 2.60-2.67 (m, 2H, CH_2), 2.76-2.82 (br s, 4H, 2 x CH_2), 3.04-3.13 (m, 2H, CH_2), 3.45 ("dd", *J* = , 10.8, 2.3 Hz, 1H, H5'), 3.51 ("dd", *J* = 2.2 Hz, 10.9 Hz, 1H, H5"), 3.87-3.90 (m, 0.5H, H4'), 3.91-3.95 (m, 0.5H, H4'), 4.03 (m, 0.5H, H3'), 4.09 (m, 0.5H, H3'), 4.97 (t, *J* = 4.9 Hz, 0.5H, H2'), 4.98 (t, *J* = 5.1 Hz, 0.5H, H2'), 5.27 (d, *J* = 7.0 Hz, 0.5 H, H1'), 5.28 (d, *J* = 7.1 Hz, 0.5 H, H1'), 8.27 (s, 0.5H, H2), 8.28 (s, 0.5H, H2); HRMS (ESI^+) *m/z* calcd $C_{29}H_{37}FN_{10}NaO_9$ $(M+Na)^+$: 711.2621, found: 711.2543.

2-(1,2,3-Triazol-1*H*-yl)adenosine-OCT adduct (234). Cyclooctyne **217** (4.7:1 *exo-endo* mixture; 3.13 mg, 0.020 mmol) was added to a stirred solution of 2-azidoadenosine[104] **201** (6.25 mg, 0.020 mmol) in a mixture of ACN/H_2O (3:1, 1 mL) at ambient temperature. After 2 h, the volatiles were evaporated *in vacuo* to give **234** (9.3 mg, 100%) as a white solid: UV λ_{max} 261 nm (ε 19 100), λ_{min} 246 nm (ε 16 600); ^{1}H NMR (DMSO-d_6) δ 0.81-0.89 (m, 2H, 2 x Hγ), 0.94-1.04 (m, 1H, CH cyclopropyl), 1.56-1.72 (m, 2H, 2 x Hβ), 2.06-2.22 (m, 2 H, 2 x Hβ), 2.81-2.90 (m, 1H, Hα), 2.99-3.14 (m, 2H, 2 x Hα), 3.15-3.19 (m, 1H, Hα), 3.44-3.58 (m, 3H, H5' & CH_2), 3.59-3.69 (m, 1H, H5"), 4.11-4.16 (m, 1H, H4'), 4.35 (t, *J* = 5.0 Hz, 1H, H3'), 4.59 ("quin", *J* = 6.0 Hz, 1H, H2'), 4.99-5.04 (m, 1H, OH), 5.21 (d, *J* = 4.9 Hz, 1H, OH), 5.45-5.53 (m, 2H, 2 x OH), 5.89 (d, *J* = 5.8 Hz, 1H, H1'), 7.89 (br s, 2H, NH_2), 8.52 (s, 1H, H8); HRMS (ESI^+) *m/z* calcd $C_{20}H_{27}N_9O_5$ $(M+H)^+$: 459.2099, found: 459.2098.

2-(1,2,3-Triazol-1*H*-yl)adenosine-DBCO adduct (235). Cyclooctyne **223** (9.67 mg, 0.035 mmol) was added to a stirred solution of **201** (10.93 mg, 0.035 mmol) in MeOH (1 mL) at ambient temperature. After 16 h, the volatiles were evaporated *in vacuo*

and the residue was passed through a 0.2 μm PTFE syringe filter, and then purified on the semipreparative HPLC column (17% ACN/H_2O, 2.0 mL/min) to give **235** (17.5 mg, 85%) as a mixture of several inseparable isomers (t_R = 13.0–16.2 min): UV λ_{max} 263 nm (ε 16 400), λ_{sh} 274 nm (ε 9 600), λ_{min} 253 nm (ε 15 200); Two major isomers (~85-90% of total isomeric composition) had: ^{1}H NMR (DMSO-d_6) δ 1.58-1.62 (m, 2H, NH_2), 2.03-2.09 (m, 2H, CH_2CO), 2.57-2.72 (m, 2H, C$H_2$$NH_2$), 3.49-3.50 (m, 1H, H5'), 3.69 (dd, *J* = 11.8 Hz & 3.3 Hz, 1H, H5''), 3.83-3.94 (m, 1H, H4'), 4.07-4.16 (m, 1H, H3'), 4.38 (t, *J* = 5.1 Hz, 0.5H, H2'), 4.44 (t, *J* = 5.0 Hz, 0.5H, H2'), 4.53 ("dm", *J* = 17.0 Hz, 1H, CH_2), 4.86-5.47 (m, 3H, 3 x OH), 5.67 (d, *J* = 7.1 Hz, 0.5H, H1'), 5.82 (d, *J* = 7.2 Hz, 0.5H, H1'), 5.96 (br d, *J* = 19.7 Hz, 2H, CH_2), 7.06-7.52 (m, 8H, H_{ar}), 8.54 (s, 0.5H, H8), 8.55 (s, 0.5H, H8); HRMS (ESI$^+$) *m/z* calcd $C_{28}H_{29}N_{10}O_5$ $(M+H)^+$: 585.2317, found: 585.2318.

5-(1,2,3-Triazol-1*H*-yl)uridine-OCT adduct (244). Cyclooctyne **217** (4.0 mg, 0.025 mmol) was added to a stirred solution of 5-azidouridine **202** (7.3 mg, 0.025 mmol) in a mixture of ACN/H_2O (3:1, 1 mL) at ambient temperature. After 15 min, the volatiles were evaporated *in vacuo*, and the oily residue was passed through a 0.2 μm PTFE syringe filter, and then purified on the semipreparative HPLC column (20% ACN/H_2O, 2.0 mL/min; t_R = 5.2 – 8.0 min) to give **244** (6.2 mg, 77%) as a 1:1 mixture of isomers: UV λ_{max} 270 nm (ε 10 100) λ_{min} 248 nm (ε 6 800); ^{1}H NMR (DMSO-d_6) δ 0.85-0.93 (m, 2H, 2 x Hγ), 0.95-1.02 (m, 1H, CH cyclopropyl), 1.46-1.56 (m, 2H, 2 x Hβ), 1.99-2.14 (m, 2H, 2 x Hβ), 2.72-2.83 (m, 2H, 2 x Hα), 3.00-3.04 (m, 0.5H, Hα), 3.05-3.08 (m, 0.5H, Hα), 3.16-3.18 (d, *J* = 5.2 Hz, 1H, Hα), 3.50 (dd, *J* = 2.5, 12.0 Hz, 1H, H5'), 3.59-3.62 (m, 1H, H5''), 3.85-3.89 (m, 1H, H4'), 3.95-4.01 (m, 1H, H3'), 4.10 ("q", *J* = 4.6 Hz, 1H, H2'), 4.36 (t, *J* = 4.9Hz, 1H, OH), 5.09-5.14 (m, 2H, 2 x OH), 5.51-5.55 (m, 1H,

OH), 5.78 (d, *J* = 4.0 Hz, 0.5H, H1'), 5.79 (d, *J* = 3.9 Hz, 0.5H, H1'), 8.52 (s, 0.5H, H2), 8.53 (s, 0.5H, H2); HRMS (ESI^+) m/z calcd $C_{19}H_{27}N_5O_7$ $(M+H)^+$: 436.1827, found: 436.1829.

5-(1,2,3-Triazol-1*H*-yl)uridine-biotin adduct (245). Cyclooctyne **218** (11.0 mg, 0.02 mmol) was added to a stirred solution of 5-azidouridine **202** (5.6 mg, 0.02 mmol) in a mixture of ACN/H_2O (3:1, 1 mL) at ambient temperature. After 3 min, the volatiles were evaporated *in vacuo* to give cycloadduct **245** (16.0 mg, 98%) as a white solid: HRMS (ESI^+) *m/z* calcd $C_{36}H_{53}N_9O_{12}S$ $(M+H)^+$: 836.3607, found: 836.3562.

2'-Deoxy-8-(1,2,3-triazol-1*H*-yl)uridine-OCT adduct (246). Cyclooctyne **217** (4.7:1 *exo-endo* mixture; 14.3 mg, 0.1 mmol) was added to a stirred solution of **242**[255] (26.7 mg, 0.1 mmol) in a mixture of ACN/H_2O/MeOH (3:1:1, 1 mL) at ambient temperature. After 15 min, the volatiles were evaporated *in vacuo* to give cycloadduct **246** as mixture of isomers (~1:1; 15.3 mg, 100%) as a white solid: ^1H NMR (DMSO-d_6) δ 0.83-0.94 (m, 2H, 2 x Hγ), 0.95-1.05 (m, 1H, CH cyclopropyl), 1.42-1.59 (m, 2H, 2 x Hβ), 1.98-2.14 (m, 2H, 2 x Hβ), 2.20 ("t", *J* = 5.2 Hz, 2H, H2' & H2"), 2.46-2.56 (m, 1H, Hα), 2.70-2.83 (m, 2H, 2 x Hα), 3.00-3.05 (m, 0.5H, Hα), 3.05-3.09 (m, 0.5H, Hα), 3.44-3.54 (m, 3H, H5' & CH_2), 3.54-3.61 (m, 1H, H5"), 3.80 (q, *J* = 3.2 Hz, 1H, H4'), 4.17-4.26 (m, 1H, H3'), 4.34 (m, 1H, OH), 5.02 (m, 1H, OH), 5.28 (m, 1H, OH), 6.15 (t, *J* = 6.3 Hz, 0.5H, H1'), 6.16 (t, *J* = 6.3 Hz, 0.5H, H1'), 8.43 (s, 0.5H, H6), 8.44 (s, 0.5H, H6); HRMS (ESI^+) *m/z* calcd $C_{19}H_{26}N_5O_6$ $(M+H)^+$: 420.1878, found: 420.1878.

5-(1,2,3-Triazol-1*H*-yl)uridine-DBCO adduct (247). Cyclooctyne **223** (5.6 mg, 0.02 mmol) was added to a stirred solution of **202** (5.5 mg, 0.02 mmol) in MeOH (1 mL) at ambient temperature. After 15 min, the volatiles were evaporated *in vacuo* and the

residue was passed through a 0.2 μm PTFE syringe filter, and then injected into a semipreparative HPLC column (40% ACN/H_2O, 1.0 mL/min; t_R = 7.0–12.0 min) to give **247** as an inseparable mixture of isomers (5.1 mg, 77%): UV λ_{max} 276 nm (ε 7300), 291 nm (ε 7100), λ_{sh} 309 nm (ε 5400), λ_{min} 265 nm (ε 6750), 283 nm (ε 7000), 303 nm (ε 5000); HRMS (ESI^+) *m/z* calcd $C_{27}H_{28}N_9O_7$ $(M+H)^+$: 562.2045, found: 526.2040.

5-(1,2,3-Triazol-1*H*-yl)uridine-MFCO adduct (248). Cyclooctyne **227** (7.6 mg, 0.02 mmol) was added to a stirred solution of 5-azidouridine **202** (5.6 mg, 0.02 mmol) in MeOH (1 mL) at ambient temperature. After 12 min, the volatiles were evaporated *in vacuo* to give complete conversion to cycloadduct **248** as mixture of regioisomers (1:1; 12.9 mg, 100%) as a white solid: UV λ_{max} 269 nm (ε 7100), λ_{min} 244 nm (ε 5000); ^1H NMR (DMSO-d_6) δ 1.40-1.50 (m, 6H, 3 x CH_2), 1.73-1.81 (m, 2H, CH_2), 2.27-2.34 (m, 2H, CH_2), 1.57-1.67 (m, 6H, 3 x CH_2), 2.48-2.53 (m, 2H, CH_2), 2.62-2.69 (m, 2H, CH_2), 2.78-2.86 (s, 4H, 2 x CH_2), 3.01-3.13 (m, 2H, CH_2), 3.47-3.54 (m, 1H, H5'), 3.60-3.65 (m, 1H, H5''), 3.94-3.99 (m, 1H, H4'), 4.08-4.15 (m, 1H, H3'), 4.27-4.36 (m, 1H, H2'), 5.06-5.11 (m, 2H, OH (2') & OH (3')), 5.51 (t, *J* = 6.7 Hz, 1H, OH (5')), 5.78 (d, *J* = 4.9 Hz, 0.5 H, H1'), 5.79 (d, *J* = 4.6 Hz, 0.5 H, H1'), 8.57 (s, 1H, H6); HRMS (ESI^+) *m/z* calcd $C_{28}H_{36}FN_7O_{11}$ $(M+H)^+$: 666.2530, found: 666.2518.

8-(1,2,3-Triazol-1*H*-yl)adenosine-OCT adduct triphosphate (230). Cyclooctyne **217** (5.6 mg, 0.01 mmol) was added to a stirred solution of 8-azidoadenosine 5'-triphosphate tetralithium salt **229** (3.2 mg, 0.01 mmol) in a mixture of ACN/H_2O (3:1, 1 mL) at ambient temperature. After 2 h, the volatiles were evaporated *in vacuo* to give **230** (3.2 mg, 92%) as a 1:1 mixture of regioisomers: ^1H NMR (ACN-d_3/D_2O) δ 0.80-0.88 (m, 2H, 2 x Hγ), 0.95-1.06 (m, 1H, CH cyclopropyl), 1.46-1.6 (m,

2H, 2 x Hβ), 2.06-2.28 (m, 2H, 2 x Hβ), 2.62-2.74 (m, 1H, Hα), 2.82-3.00 (m, 2H, 2 x Hα), 3.11-3.21 (m, 1H, Hα), 3.56-3.64 (m, 4H, H5', H5'' & CH_2), 4.17-4.32 (m, 2H, H3' & H4'), 4.89 (t, *J* = 5.8 Hz, 0.5H, H2'), 4.97 (t. *J* = 5.7 Hz, 0.5H, H2'), 5.47 (d, *J* = 5.6 Hz, 0.5H, H1'), 5.51 (d, *J* = 5.5 Hz, 0.5H, H1'), 8.32 (s, 0.5H, H2), 8.33 (s, 0.5H, H2); HRMS (ESI^-) *m/z* calcd $C_{20}H_{28}N_8O_{14}P_3$ $(M+H)^-$ 697.0943, found: 697.0962.

4.4 NMR Kinetic Analysis of Selected SPAAC Reactions

General Procedures. Kinetic data for the reactions between azides **200** or **229** and cyclooctyne **229** were acquired by 1H NMR at ambient temperature using a 400 MHz Bruker NMR. A 23 mM solution of azide **200** or 6 mM solution of azide **229** was each prepared in deuterated acetonitrile (CD_3CN) and water (D_2O) (3:1, *v/v*). For each experiment, three NMR tubes were prepared, each containing 700 μL of the azide solution. The solid cyclooctyne was added to one of the prepared NMR tubes and quickly shaken to dissolve. The resulting solution contained cyclooctyne and azide in a 1:1 ratio and was scanned every minute over 120 minutes. This procedure was repeated for each of the remaining prepared NMR tubes.

For each of the azides tested, proton spectra showed formation of the desired click adducts without formation of any byproducts. The profile for the reaction was measured by integrating disappearance of the signal of H2 of substrate **200** or **229** at 8.07 ppm and appearance of H2 signal at 8.28 ppm for the product **203** or **230**, respectively. Second order rate constants were calculated by plotting 1/[azide] as a function of time. The y-intercept of each plot was set to 1/[starting azide concentration]. Plots show data collected to ~90% conversion to the triazole product

4.5 Synthesis of Phosphorylated Azides

8-Azido-2'-deoxyadenoesine monophosphate (262). Azide **203** (5.0 mg, 0.017 mmol), ATP (2 mM), DTT (2 mM), and BSA (0.5 mg/mL) were added to a solution of TRIS (50 mM, pH 7.6) containing KCl (100 mM) and $MgCl_2$ (5 mM) for a final volume of 6 mL. The reaction was initiated by the addition of 6 x His -HdCK (1.33 mg/mL) and incubated at 37 °C. After 45 min, the reaction was quenched by cooling for 10 min at 0 °C and then applied onto a DEAE Sephadex A-25 column (10 mL, 1 × 5.0 cm for a 17 μmol synthesis). The column was eluted using a linear gradient of 0.1 – 0.4 M triethylammonium bicarbonate (TEAB) pH 7.5 in dH_2O. The fractions eluting at 0.2 M TEAB were pooled together. Excess TEAB was removed with repeated cycles of dilution and concentration *in vacuo* from a 1:1 mixture of water and ethanol to give **262** as a triethylammonium salt: ^{1}H NMR (D_2O) δ 2.26 (dd, J = 14.0 Hz, 6.0 Hz, 1H, H2'), 2.76-2.83 (m, 1H, H2''), 3.02-3.09 (m, 2H, H5' & 5''), 4.03-4.09 (m, 1H, H4'), 4.23 (bs, 1H, H3'), 6.50 (dd, J = 9.3 Hz, 6.0 Hz, 1H, H1'), 8.06 (s, 1H, H2); ^{31}P NMR (D_2O) δ 3.48 (s); MS (ESI^+) *m/z* 369 $(M+H)^+$.

8-Azido-2'-deoxyadenoesine diphosphate (**266**). Monophosphate **262** (2.0 mg, 0.005 mmol) ATP (4 mM) and DTT (2 mM) were added to a solution of TRIS (50 mM pH 8.0) containing $MgCl_2$ (5 mM) for a final volume of 6 mL. The reaction was initiated by the addition of Myokinase (S.A. 3400 units/mL) and incubated at 37 °C. After 45 min, the reaction was quenched by cooling for 10 min at 0 °C and then applied onto a DEAE Sephadex A-25 column (15 mL, 1 × 5.0 cm for a 5 μmol synthesis). The column was eluted using a linear gradient of 0.005 – 0.6 M triethylammonium bicarbonate (TEAB) pH 7.5 in dH_2O. The fractions eluting at 0.4 M TEAB were pooled together. Excess

TEAB was removed with repeated cycles of dilution and concentration *in vacuo* from a 1:1 mixture of water and ethanol to give **266** as a triethylammonium salt: ^{1}H NMR (D_2O) δ 2.30 (ddd, *J* =14.1 Hz, 6.2 Hz, 2.3 Hz, 1H, H2'), 2.75-2.81 (m, 1H, H2''), 4.21-4.38 (m, 4H, H3',4',5',5''), 6.47 (dd, *J* = 8.7 Hz, 6.3 Hz, 1H, H1'), 8.06 (s, 1H, H2); ^{31}P NMR [^{1}H] (D_2O) δ -11.02 (s), -7.40 (s).

8-Azido-2'-deoxyadenoesine triphosphate (260). Diphosphate **266** (2.0 mg, 0.005 mmol) and PEP (4 mM) were added to a solution of TRIS (50 mM pH 8.0) containing $MgCl_2$ (5 mM) for a final volume of 6 mL. The reaction was initiated by the addition of Pyruvate Kinase (S.A. 3400 units/mL) and incubated at 37 °C. After 45 min, the reaction was quenched by cooling for 10 min at 0 °C and then applied onto a DEAE Sephadex A-25 column (15 mL, 1 × 5.0 cm for a 5 μmol synthesis). The column was eluted using a linear gradient of 0.1 – 0.8 M triethylammonium bicarbonate (TEAB) pH 7.5 in dH_2O. The fractions eluting at 0.6 M TEAB were pooled together. Excess TEAB was removed with repeated cycles of dilution and concentration *in vacuo* from a 1:1 mixture of water and ethanol to give **260** as a triethylammonium salt.

4.6 Synthesis of Azido Modified α-Ketoglutarate

***(S)*-2-Azidopentanedioic acid (305).** *Triflic azide preparation:* A solution of sodium azide was prepared by dissolving sodium azide (890 mg, 13.73 mmole) in deionized water (3.0 mL) and CH_2Cl_2 (4.0 mL) in a Morton flask. This solution was cooled to 0 °C in an ice bath for 5 min. Triflyl anhydride (0.465 mL, 2.78 mmole) was added slowly with a syringe over 5 min with very vigorous stirring. This was allowed to stir as an emulsion for an additional 2 h. The mixture was placed in a separatory funnel and the organic layer was removed. The aqueous portion was washed with CH_2Cl_2 (2 x

20 mL). The organic fractions containing triflic azide were pooled, washed with $NaHCO_3$ and used directly without further purification. *Diazo transfer reaction:* α-Ketoglutarate **304** (205 mg, 1.4 mmole) was combined with K_2CO_3 (289 mg, 2.1 mmole) and $Cu^{II}SO_4$ pentahydrate (4.0 mg, 14 μmole) in distilled water (4.5 mL) and MeOH (9 mL) The freshly prepared triflyl azide in CH_2Cl_2 was added and allowed to stir at ambient temperature and pressure overnight in a Morton flask. After 16h, the reaction had turned a bright blue color. The organic volatiles were evaporated *in vacuo* and the aqueous portion was diluted with H_2O (25 mL) and acidified to pH 6 with conc. HCl (6M). The aqueous layer was washed four times with EtOAc to remove the sulfonamide byproduct. Then, the aqueous phase was once again acidified to pH 2 and the extracted with EtOAc (3 x 20 mL). These extracts were pooled together, dried with $MgSO_4$ and evaporated to dryness to give **305**[299] (90 mg, 75%) as a pale oil: ^{1}H NMR (D_2O) δ 1.78-1.91 (m, 1H, H3), 1.95-2.06 (m, 1H, H3), 2.28-2.42 (m, 2H, H4), 4.09 (dd, *J* = 8.4 Hz, 5.0 Hz, 1H, H2).

2-(1,2,3-Triazol-1*H*-yl)pentanedioic acid OCT adduct (306). Cyclooctyne **217** (14.0 mg, 0.095 mmol) was added to a stirred solution of *(S)*-2-azidopentanedioic acid **305** (15.0 mg, 0.087 mmol) in a mixture of ACN/H_2O (3:1, 1 mL) at ambient temperature. After 6 h, the volatiles were evaporated *in vacuo*, the residue was taken up in $CHCl_3$ and washed with H_2O to give **306** (23.0 mg, 92%) in the aqueous layer: ^{1}H NMR (DMSO) δ 0.74-0.84 (m, 2H, 2 x Hγ), 0.97 (quin, *J* = 16 Hz, 1H, CH cyclopropyl), 1.46-1.64 (m, 2H, 2 x Hβ), 2.00-2.12 (m, 4H, 2 x Hβ & CH_2(3)), 2.30-2.68 (m, 3H, CH(2) & CH_2(4)), 2.54-2.68 (m, 1H, Hα), 2.72-2.90 (m, 2H, 2 x Hα), 2.92-3.02 (m, 1H, Hα), 3.47 (d, *J* = 7.9 Hz, 2H, CH_2), 5.23 (bs, 1H, OH); MS (ESI^-) *m/z* 324 $(M+H)^-$.

4.7 Synthesis of SAM Analogues for TrmD

5'-[(S)-[(3S)-3-Amino-3-carboxypropyl](E)-pent-2-en-4-ynylsulfonio]-5'-deoxyadenosine (AdoEnYn) (310). Mesyl chloride (395 μL, 584 mg, 5.09 mmol) was added to a suspension of NaOH (222 mg, 5.57 mmol) in dichloromethane (6 mL), and the suspension was cooled to 0 °C. Freshly distilled (E)-pent-2- en-4-yn-1-ol **308** (380 mg, 4.63 mmol) was added and the mixture stirred at ambient temperature overnight. After 16 h, the crude reaction was washed with saturated $NaHCO_3$ solution until the aqueous phase remained basic. Volatiles were evaporated *in vacuo* to give **309**[321] (600 mg, 81%) as a yellow oil. Mesylated alcohol **309** (600 mg, 3.75 mmol) was directly dissolved in a mixture (1 mL) of formic and acetic acid (1:1 *v/v*). The solution was added to *S*-adenosyl-*L*-homocysteine **307** (10 mg, 26 μmol) and the reaction mixture stirred in the dark at ambient temperature overnight. After 14 h, the reaction was quenched with water (30 mL) and the aqueous phase was extracted with diethylether (3 × 60 mL). The aqueous layer was passed through a 0.2 μm PTFE syringe filter, and then purified on the semipreparative HPLC column (5% ACN, 0.01% TFA/H_2O, 1.0 mL/min) to give **310**[307] as mixture of regioisomers (1:1; 1.0 mg, 9%) as a white solid (t_R = 22.5–23.8 min): ^{1}H NMR (D2O, pD 3.5): δ 2.38 (q, *J* = 5.9 Hz, 2H, CH_2 β), 3.81-3.91 (m, 2H, H5' & H5"), 3.56-3.68 (m, 2H, CH_2 γ), 3.95-3.99 (m, 1H, Hα), 4.21 (d, *J* = 7.6Hz, 0.5H, H1"), 4.25 (d, *J* = 7.6Hz, 0.5H, H1"), 4.40-4.52 (m, 1H, H4'), 4.56 (t, J = 5.9 Hz, 0.5H, H3'), 4.65 (t, J = 6.0 Hz, 0.5H, H3'), 4.78-4.85 (m, 1H, H2'), 5.65 (dd, *J* = 13.8 Hz, 2.2 Hz, 0.5H, H3"), 5.85 (dd, *J* = 14.2 Hz, 2.3 Hz, 0.5H, H3"), 5.94-6.04 (m, 0.5H, H2"), 6.05-6.11 (m, 1.5H, H1' & H2"), 8.36 (s, 1H, H2), 8.37 (s, 0.5H, H8), 8.39 (s, 0.5H, H8); MS (ESI^+) *m/z* 450 $(M+H)^+$.

5'-S-Adenosyl-4-thiobutyric Acid Methyl Ester (314). γ-Thiobutyrolactone (35 μL, 53 mg, 0.52 mmol) was added dropwise to a stirred solution of NaOMe in MeOH [prepared *in situ* by dissolving Na metal (13 mg, 0.56 mmol) in MeOH (3 mL) under N_2 for 15 min] at ambient temperature. The 5'-chloro-5'-deoxyadenosine[322] **313** (100 mg, 0.35 mmol) was then added to the resulting solution was refluxed for 3 h. The reaction was then allowed to continue stirring overnight at room temperature. After 24 h, the additional amount of freshly prepared thiolate (thiolactone (23 μL, 35.7 mg, 0.35 mmol) and Na metal (8.6 mg, 0.37 mmol) in 0.5 mL MeOH) was added and refluxed was continued for another 2 h. The MeOH was evaporated and the crude materials was dissolved in EtOAc, washed twice with $NaHCO_3$ then with dilute HCl and lastly with brine. The organic layer was dried with $MgSO_4$ and evaporated to give thick yellow oil which was chromatographed (100% $CHCl_3$ → 15% MeOH in $CHCl_3$) to give **314**[323] (35 mg, 27%) as a light yellow oil: ^{1}H NMR δ 1.61-1.69 (m, 2H, H8',8''), 2.22 (t, *J* = 7.3 Hz, 2H, H9',9''), 2.42 (m, 2H, H7',7''), 2.83 (dd, *J* = 14.5 Hz, 6.5 Hz, 1H, H5'), 2.91 (dd, *J* = 14.5 Hz, 5.0 Hz, 1H, H5''), 3.54 (s, 3H, CH_3), 4.23 (q, *J* = 4.5 Hz, 1H, H4'), 4.35 (t, *J* = 6.0 Hz, 1H, H3'), 4.82 (t, *J* = 5.6 Hz, 1H, H2'), 5.98 (d, *J* = 4.9 Hz, 1H, H1'), 8.15 (s, 1H, H8), 8.26 (s, 1, H2). MS (ESI$^+$) *m/z* 384 $(M+H)^+$.

5'-S-Adenosyl-4-thiobutyric Acid (315). NaOH (0.08 mmol, 160 μL of 0.5M NaOH solution) was added to a stirred solution of **314** (10.0 mg, 0.026 mmol) in MeOH (0.5 mL). The reaction was quenched after 2 h with 1M HCl and evaporated to give **315**[323] (9 mg, 94%) as a clear oil: ^{1}H NMR δ 1.64-1.71 (m, 2H, H8' & 8''), 2.11 (t, *J* = 7.6 Hz, 2H, H9',9''), 2.44-2.51 (m, 2H, H7',7''), 2.86 (dd, *J* = 15.2 Hz, 6.5 Hz, 1H, H5'), 2.95 (dd, *J* = 14.9 Hz, 4.7 Hz, 1H, H5''), 4.26 (q, *J* = 5.1 Hz, 1H, H4'), 4.36 (t, *J* = 5.1 Hz, 1H,

H3'), 4.80 (t, *J* = 5.1 Hz, 1H, H2'), 5.99 (d, *J* = 5.11 Hz, 1H, H1'), 8.15 (s, 1H, H2), 8.28 (s, 1H, H8). MS (ESI^+) *m/z* 369 $(M+H)^+$.

3'-Azido-5'-chloro-3',5'-dideoxyadenosine (320). 3'-Azido-3'-deoxyadenosine **319**[324] (40 mg, 0.13 mmol) was added to a precooled solution of thionyl chloride (51 µL, 92.8 mg, 0.78 mmol) in HMPA (4 mL). The reaction was allowed to stir at ambient temperature for 1.5 h and then quenched with water (1.5 mL) decolorizing the reaction. The reaction mixture was applied to a Dowex column (H+), washed with 2 column volumes of water and eluted with 2N aqueous NH_4OH and 2N aqueous NH_4OH/MeOH (*v/v* 1:1). The fractions that contained UV were collected and extracted with ethyl acetate, dried over sodium sulfate and evaporated to yield **320**[310] (40 mg, 95%) as a white solid: ^{1}H NMR δ 3.71 (dd, *J* = 11.8 Hz, 4.0 Hz, 1H, H5"), 3.80 (dd, *J* = 11.8 Hz, 4.0 Hz, 1H, H5'), 4.12 ("q", *J* = 4.6 Hz, 1H, H4'), 4.21 (t, *J* = 4.3 Hz, 1H, H3'), 4.99 (t, *J* = 5.3 Hz, 1H, H2'), 5.86 (d, *J* = 5.9 Hz, 1H, H1'), 8.05 (s, 1H, H2), 8.12 (s, 1H, H8),

3'-Azido-3'-deoxy-5'-S-Adenosyl-*D/L*-Homocysteine (321). *D/L*-Homocysteine (9.7 mg, 0.057 mmol), NaOH (2 mg, 0.054 mmol) and KI (4 mg, 0.024 mmol) were added to a suspension of 3'-azido-5'-chloro-3',5'-dideoxyadenosine **320**[310] in 1 mL deoxygenated water [which had been boiled for 1 hour and then quickly cooled]. The reaction was allowed to sir at 100 °C for 5 h and then immediately cooled in ice bath. The pH was adjusted to 3.5 with 1N $HCl_{(aq)}$ and then applied directly to a Dowex (NH_4+) column, washed with 2 column volumes of water and eluted with 1N aqueous NH_4OH. The fractions that contained UV were collected and evaporated yield **321** (2.0 mg, 10%) as an ivory oil. ^{1}H NMR δ 1.99-2.14 (m, 3, H8', H8" & H9'), 2.61 (t, *J* = 7.3 Hz, 2H, H7' & H7"), 2.91-3.02 (m, 2H, H5' & H5"), 3.96-4.10 (m, 1H, H4'), 4.28 (q, *J* = 12.0 Hz, 1H,

H3'), 5.05 (q, *J* = 7.2 Hz, 1H, H2'), 5.99 (d, *J* = 3.8 Hz, 1H, H1'), 7.97 (s, 1, H2), 8.11 (s, 1H, H8), MS (ESI^+) *m/z* 410 $(M+H)^+$.

5'-Chloro-3'-(*N*-Boc-*S*-trityl-homocystylamino)-3',5'-dideoxyadenosine (324). *N*-Boc-*S*-trityl-homocysteine (61 mg, 0.13 mmol) was coevaporated 3 times with dry THF (2 mL) and then dissolved in dry THF (1.75 mL) at 0°C. HOBt (21 mg, 0.17 mmol) was added to this solution and allowed to stir at 0 °C for 10 min. Then DIC (26 μL, 0.17 mmole) was added drop wise and again allowed to stir for 10 min at 0°C. 3'-azido-5'-chloro-3',5'-dideoxyadenosine **320** (20 mg, 0.065 mmol) and *n*-Bu_3P were added and the temperature was allowed to warm up to room temperature over 30 min. At 4 h, all starting material had been consumed so volatiles were evaporated to yield an oil which was dissolved in $CHCl_3$ and washed with water and brine. The residue was purified on silica gel column chromatography (EtOAc → 20% MeOH/EtOAc) to give **324** (6.1 mg, 13%). ^1H NMR δ 0.78-0.89 (m, 15H, t-Bu), 1.55-1.97 (m, 2H, CH_2 β), 2.19-2.25 (m, 2, CH_2 γ), 3.72-3.80 (m, 2H, H5' & H5''), 4.00 (q, *J* = 9.2 Hz, 1H, H4'), 4.21 (t, *J* = 3.2, 1H, Hα), 4.50-4.58 (m, 1H, H3'), 4.76-4.81 (m, 1H, H2'), 5.86 (d, *J* = 2 Hz, 1H, H1'), 6.23 (bs, 2H, NH_2), 6.81 (d, *J* = 3 Hz, 1H, NH), 8.05 (s, 1H, H8), 8.17 (s, 1H, H2). MS (ESI^+) *m/z* 744 $(M+H)^+$.

4.8 Biological Evaluation of Azido Nucleosides and Click Adducts

4.8.1 **Parallel Artificial Membrane Permeability Assay (PAMPA)**

Permeability Measurements Typical Procedure: Parallel artificial membrane permeability assay (PAMPA) was used to determine effective permeability coefficients P_e (centimeters per second), in a 96-well microtiter filter plates, on polycarbonate filter of

.45 μm pore size, 10 μm thickness (Millipore AG, Volketswil, Switzerland), according to the procedure of Wohnsland and Faller.[325]

Each well was coated with 15 μL of lecitin (1% or 4% in dodecane solution) for 5 minutes avoiding pipette tip contact with the membrane. Each compound, dissolved in 5% DMSO in PBS solution (concentration of 75 μM and 150 μM) was tested at least in triplicate. The compound containing solutions (300 μL each) was added to each well of the donor plate. Aqueous buffer (PBS) (300 μL) was added to each well of the acceptor plate and then the donor plate was placed upon the acceptor plate. The resulting chamber was incubated at room temperature for 16 h at ambient temperature under gentle shaking. After incubation, it was carefully disassembled and each well of the acceptor plate was analyzed using UV-Vis for compound concentration. A solution of each compound at its theoretical equilibrium (i.e., the resulting concentration of the donor and acceptor phases were simply combined) was similarly analyzed. The effective permeability (Log P_e) was calculated from the equation as reported by Faller *et al.*[325]

4.8.2 MTT Assay

MTT Typical Procedure: MCF-7 cells were seeded in 96-well plates at a density of $1x10^4$ cells/well and treated with different concentrations of azides **2** or **21** and cyclooctyne **5** for 24 h at 37 °C in a 5% CO_2 incubator. Methylthiazoletetrazolium (MTT) solution (5 mg/ml) was added to the assay mixture and incubated for 4 h. The culture media was removed prior to addition of DMSO. The optical density of the solution was measured at 595 nm, using an absorbance microplate reader (Bio-Tek). Cells without the treatment of the compounds were used as the control. The cell viability percentage was

calculated by the following formula: Cell viability percentage (%) = OD sample/OD control × 100%

4.8.3 Fluorescent Cell Microscopy Studies

Fluorescent Spectroscopy Typical Procedure: The MCF-7 cells (5×10^5 cells/mL) were seeded in an eight chambered coverglass system (1.5 German borosilicate coverglass, Lab-Tek II) and incubated at 37 °C overnight in Dulbecco's modified Eagle's medium (DMEM/F12 (1:1) 1X, 1.5 ml) containing 5% fetal bovine serum (FBS). The media was removed and reduced serum medium (OPTI-MEM I, 1X, Gibco, Invitrogen) was added to the cells and allowed to incubate at 37 °C for 3 h.

The 8-azido-9-(β-D-arabinofuranosyl)adenine **2** in the reduced serum medium (1 μM) was added to the cells. After 4h, the cells were washed three times with fresh DMEM/F12 (1:1) 1X media to remove any azide from the exterior portions of the cells. The cyclooctyne reagent **5** in the reduced serum medium (1 μM) was then added to the the cells and incubated at 37 °C for 16 h. The cells were then washed three times with fresh DMEM/F12 (1:1) 1X media to remove any click adduct from the exterior portions of the cells and then observed with a DLITE-microscope (Fisher Scientific) using excitation and absorbance filters were 360/40 and 470/40 nm, respectively.

In the first negative control, the MCF-7 cells were just incubated with azide **2** without the cyclooctyne reagent added. In the second negative control, the MCF-7 cells were just incubated with cyclooctyne **5** without the azide **2**. Also, in the positive control the cells were treated with click adduct (e.g., **11)** dissolved in culture media. We used 0.1% trypan blue in the culture media before imaging the cells in DV ELITE microscope.

Note: In parallel experiments Lipofectamine LTX was used as liposome carrier.

4.9 Photophysical Screening and Evaluation of Triazole Adducts

4.9.1 Photophysical Characterization

The fluorescent properties of the triazole products were determined using samples of varying concentration but whose absorbance at the excitation wavelength did not exceed 0.1 absorbance units. For determination of Φ_F the absorbance was kept below 0.06 and quinine sulfate in 100mM sulfuric acid was used as reference standard (Φ_F = 0.55).[326] All samples were prepared in HPLC grade MeOH, DMSO or 50mM phosphate buffer, and placed in a 2 x 10 mm quartz cuvette at 18 °C. Absorption spectra were measured using a single beam UV–Vis spectrophotometer (Cary 50, Varian). Steady-state excitation and emission spectra were measured on a PC1 spectrofluorometer with bandwidth and slit width for excitation/emission set at 2 nm. Frequency-domain fluorescence lifetime measurements were performed using a ChronosFD spectrofluorometer. Samples were excited with a frequency modulated 280 nm LED and emission was collected using a 305 nm long pass filters (Andover); 2,5-Diphenyloxazole (PPO) solubilized in ethanol was used as a lifetime reference (τ =1.4 ns).[327] Modulation-phase data were fitted by a multiple-exponential decay model using GlobalsWE software and the residual and χ^2 parameter was used as criterion for goodness of fit.

4.9.2 Fluorescent Lifetime Imaging Microscopy

Typical Procedure: Synthetically prepared triazole adduct **8**, **20** or **23** as well as *in vivo* generated **8** [0.5 mL of 1 μM solution in DMEM/F12 (1:1) 1X media] were added to MCF-7 cells (~50% cell confluency) cultured on slides mounted with 1-tissue culture

well. After 24 h, the cells were washed twice with fresh (DMEM/F12 (1:1) 1X, 0.5 ml). The cells were then imaged at ambient temperature in fresh DMEM/F12 (~0.2 mL). Ex vivo lifetime measurements were acquired using a custom-assembled frequency-domain upright FLIM system from Intelligent Imaging Innovations Inc. (3i). A continuous–wave excitation source (488 nm Argon laser) was modulated by a Pockels cell electro-optic modulator, which was synchronized with a Lambert Instruments II18MD gated image intensifier and CoolSnap EZ camera. A Yokogawa CSU-X1 spinning disk provided confocal scanning for fast image acquisition. A Zeiss W Plan-Apochromat 63x (n.a. 1.0) water-immersion objective lens and a Semrock 520 emission filters with a Semrock Di10 T488/568 diochroic were also used. Image intensification was maintained at 2800 units across all experiments. Exposure times were set to acquire enough signal to span approximately 75% of the CCD's dynamic range, however this time was never extended to more than 40 seconds (as such samples typically have low signal-to-noise. System calibration was performed with the fluorescent dye, 1-hydroxypyrene-3,6,8-trisulfonate (HPTS), in solution (PBS at pH 7.5) for a standard lifetime of 5.4 ns. We found HPTS to be a reliable standard and superior to fluorescein, owing to its greater stability over time and pH shifts.

5 Conclusion

In this dissertation, I have developed a protocol for the efficient strain promoted click chemistry of 2- or 8-azidoadenine and 5-azidouracil nucleosides as well as 8-azidoadenosine triphosphate with various cyclooctynes. The reactions were performed in aqueous solution at ambient temperature without the assistance of copper and/or microwave heating. These triazole analogues were designed to have fluorescent, light-up, properties and were utilized for direct fluorescent imaging in living cells. As analogues of natural nucleosides, the synthesized click adducts are less likely to result in undue cellular stress and allow for a dynamic real-time view inside the cell.

The azido nucleoside precursors were prepared either by substitution (e.g., **200**, **214**-**216**) or diazo transfer (e.g., **202** and **243**). These azido purine and pyrimidine modified nucleosides underwent stain promoted click chemistry (SPAAC) with several different cyclooctynes including some modified with fused cyclopropyl cyclooctyne (e.g., **217** and **218**), dibenzylcyclooctyne (e.g., **223**) or monofluorocyclooctyne (e.g., **227**) to produce triazole click products functionalized with hydroxyl, amino, *N*-hydroxysuccinimide, or biotin moieties. Photophysical studies of the triazole adducts synthesized demonstrated complex fluorescence decay lifetimes with at least two or three lifetime components.

The synthesized triazole adducts induced fluorescent properties which were used for direct imaging in MCF-7 cancer cells without the need for traditional fluorogenic reporters. Thus, the viability of these click reactions to produce fluorescent nucleoside analogues was demonstrated inside living cancer cells. From a cell cytotoxicity assay (MTT), it was determined that a 1 μM dosage of azides **202** and **214** were non-toxic. We

utilized this dosage for subsequent fluorescent studies. Additionally, a parallel artificial membrane (PAMPA) was used to predict the passive cellular permeability of selected azides and triazole adducts, which demonstrated that approximately 20% of each of the compounds tested passively permeated in through the cellular membrane.

Fluorescence at the lower concentrations without the aid of liposome delivery was localized to the nucleus. Thus, fluorescence lifetime imaging microscopy (FD-FLIM) was used to determine the lifetime of each fluorophore from the fluorescent signal localized in the cellular nuclei using frequency-domain The observed FLIM values for the click adducts **234** and **244** were similar to those obtained through spectroscopic methods; however, the value found for **219** was much higher *in vivo* than that found *in vitro*. The discrepancy between fluorescence lifetimes *in vitro* and within living cells can be attributed to different solvent conditions. Furthermore, the intranuclear solvent may exist at a higher or lower pH or π-orbital stacking may occur.

The present *in situ* click chemistry drug delivery system represents a novel theranostics approach wherein both a therapeutic effect and drug uptake-related imaging information may be produced and readily monitored at the cellular level. The long-term implications of this *in situ* click chemistry drug delivery strategy embodied in the synthesized click substrates could allow for a more precise monitoring of dosage levels as well as an improved understanding of cellular uptake. It is also noteworthy that our nucleobase-derived triazole adducts can be visualized using fluorescent microscopy and FLIM without reliance on auxiliary fluorescent reporters such as green-fluorescent protein[328] or Alexa Fluor.[329]

Through the screening and evaluation of a library of numerous nucleoside analogues, I have demonstrated that 9-(2-deoxy-2-fluorob,D-arabinofuranosyl)adenine **215** is more active against protozoan parasite *T. vaginalis* (IC_{50} 0.09 μM) than the current FDA approved drug for treatment of trichomoniasis, metronidazole (IC_{50} 0.72 μM). Furthermore, fluoro-arabinoadenosine **215** was also active against the metronidazole resistant strain of *T. vaginalis* (IC_{50} 0.21 μM), but shows no effect on non-infected mammalian cells. Further investigation of this compound may provide a basis for development of new drugs against this important human parasite. Tagging and subcellular localization studies using azido modified fluoro-arabinoadenosine **272** could provide insight into the cellular targets of fluoro-arabinoadenosine **215**.

An activated analogue of SAM with an EnYn group on the sulfur instead of a methyl was prepared. Ivestigation with the Trm1 enzyme showed that AdoEnYn **310** can inhibit AdoMet-dependent methylation of tRNA which indicates that it is a competitive inhibitor of the natural methyl donor, SAM. Furthermore, since the EnYn group was transferred from the sulfur on AdoEnYn **310** by methyltransferase Trm1 to guanosine on tRNA **311**, it was determined that AdoEnYn can be incorporated into tRNA in place of AdoMet.

References

1. Jordheim, L. P.; Durantel, D.; Zoulim, F.; Dumontet, C. *Nature Reviews Drug Discovery* **2013,** *12*, 447-464.

2. Parker, W. B. *Chem. Rev.* **2009,** *109*, 2880-2893.

3. Cano-Soldado, P.; Pastor-Anglada, M. *Med. Res. Rev.* **2012,** *32*, 428-457.

4. Minuesa, G.; Huber-Ruano, I.; Pastor-Anglada, M.; Koepsell, H.; Clotet, B.; Martinez-Picado, J. *Pharmacol. Ther.* **2011,** *132*, 268-279.

5. Damaraju, V. L.; Damaraju, S.; Young, J. D.; Baldwin, S. A.; Mackey, J.; Sawyer, M. B.; Cass, C. E. *Oncogene* **2003,** *22*, 7524-7536.

6. Elion, G. B. *Annu. Rev. Pharmacool. Toxicol.* **1993,** *33*, 1-23.

7. Elion, G. B. *J. Med. Virol.* **1993**, 2-6.

8. De Clercq, E. *Annu. Rev. Pharmacol. Toxicol.* **2011,** *51*, 1-24.

9. Holy, A. *Antiviral Res.* **2006,** *71*, 248-253.

10. Young, I.; Young, G. J.; Wiley, J. S.; van der Weyden, M. B. *Eur. J. Cancer Clin. Oncol.* **1985,** *21*, 1077-1082.

11. Li, F.; Maag, H.; Alfredson, T. *J. Pharm. Sci.* **2008,** *97*, 1109-1134.

12. Moyle, G. *Drug Saf.* **2000,** *23*, 467-481.

13. Wang, W.-S.; Tzeng, C.-H.; Chiou, T.-J.; Liu, J.-H.; Hsieh, R.-K.; Yen, C.-C.; Chen, P.-M. *Jap. J. Clin. Oncol.* **1997,** *27*, 154-157.

14. Renis, H. E. *Antimicrob. Agents Chemother.* **1973,** *4*, 439-444.

15. Lauter, C. B.; Bailey, E. J.; Lerner, A. M. *Antimicrob. Agents Chemother.* **1974,** *6*, 598-602.

16. Dennison, J. B.; Shanmugam, M.; Ayres, M. L.; Qian, J.; Krett, N. L.; Medeiros, L. J.; Neelapu, S. S.; Rosen, S. T.; Gandhi, V. *Blood* **2010,** *116*, 5622-5630.

17. Frey, J. A.; Gandhi, V. *Mol. Cancer Ther.* **2010,** *9*, 236-245.

18. Lange-Carter, C. A.; Vuillequez, J. J.; Malkinson, A. M. *Cancer Res.* **1993,** *53*, 393-400.

19. Gu, Y. Y.; Zhang, H. Y.; Zhang, H. J.; Li, S. Y.; Ni, J. H.; Jia, H. T. *Biochem. Pharmacol.* **2006,** *72*, 541-550.

20. Yang, S. Y.; Jia, X. Z.; Feng, L. Y.; Li, S. Y.; An, G. S.; Ni, J. H.; Jia, H. T. *Biochem. Pharmacol.* **2009,** *77*, 433-443.

21. Cummings, J.; Langdon, S. P.; Ritchie, A. A.; Burns, D. J.; Mackay, J.; Stockman, P.; Leonard, R. C. F.; Miller, W. R. *Ann. Oncol.* **1996,** *7*, 291-296.

22. Stellrecht, C. M.; Vangapandu, H. V.; Le, X. F.; Mao, W.; Shentu, S. *J. Hematol. Oncol.* **2014,** *7*, 23.

23. Pinto, A.; Aldinucci, D.; Gattei, V.; Zagonel, V.; Tortora, G.; Budillon, A.; Cho-Chung, Y. S. *Proc. Natl. Acad. Sci. U. S. A.* **1992,** *89*, 8884-8888.

24. Dennison, J. B.; Balakrishnan, K.; Gandhi, V. *Br. J. Haematol.* **2009,** *147*, 297-307.

25. Kolb, H. C.; Finn, M. G.; Sharpless, K. B. *Angew. Chem. Int. Ed.* **2001,** *40*, 2004-2021.

26. Huisgen, R. *Angew. Chem. Int. Ed.* **1963,** *2*, 565-598.

27. Smith, P. A. S. Scriven, E. F. V., Ed. Academic Press: 1984; pp 95-204.

28. Scriven, E. F. V.; Turnbull, K. *Chem. Rev.* **1988,** *88*, 297-368.

29. Tornøe, C. W.; Christensen, C.; Meldal, M. *J. Org. Chem.* **2002,** *67*, 3057-3064.

30. Rostovtsev, V. V.; Green, L. G.; Fokin, V. V.; Sharpless, K. B. *Angew. Chem. Int. Ed.* **2002,** *41*, 2596-2599.

31. Xi, W.; Scott, T. F.; Kloxin, C. J.; Bowman, C. N. *Adv. Funct. Mater.* **2014,** *24*, 2572-2590.

32. Hein, C. D.; Liu, X. M.; Wang, D. *Pharm. Res.* **2008,** *25*, 2216-2230.

33. Nwe, K.; Brechbiel, M. W. *Cancer Biother. Radiopharm.* **2009,** *24*, 289-302.

34. Yang, P. Y.; Wang, M.; He, C. Y.; Yao, S. Q. *Chem. Commun. (Camb.)* **2012,** *48*, 835-837.

35. Hong, V.; Steinmetz, N. F.; Manchester, M.; Finn, M. G. *Bioconjugate Chem.* **2010,** *21*, 1912-1916.

36. Chiou, S. H. *J. Biochem.* **1983,** *94*, 1259-1267.

37. Kennedy, D. C.; McKay, C. S.; Legault, M. C. B.; Danielson, D. C.; Blake, J. A.; Pegoraro, A. F.; Stolow, A.; Mester, Z.; Pezacki, J. P. *J. Am. Chem. Soc.* **2011,** *133*, 17993-18001.

38. Presolski, S. I.; Hong, V. P.; Finn, M. G. John Wiley & Sons, Inc.: 2009.

39. Agard, N. J.; Prescher, J. A.; Bertozzi, C. R. *J. Am. Chem. Soc.* **2004,** *126*, 15046-15047.

40. Baskin, J. M.; Bertozzi, C. R. *QSAR & Comb. Sci.* **2007,** *26*, 1211-1219.

41. Baskin, J. M.; Prescher, J. A.; Laughlin, S. T.; Agard, N. J.; Chang, P. V.; Miller, I. A.; Lo, A.; Codelli, J. A.; Bertozzi, C. R. *Proc. Natl. Acad. Sci. U.S.A.* **2007,** *104*, 16793-16797.

42. Codelli, J. A.; Baskin, J. M.; Agard, N. J.; Bertozzi, C. R. *J. Am. Chem. Soc.* **2008,** *130*, 11486-11493.

43. Laughlin, S. T.; Bertozzi, C. R. *ACS Chem. Biol.* **2009,** *4*, 1068-1072.

44. Gordon, C. G.; Mackey, J. L.; Jewett, J. C.; Sletten, E. M.; Houk, K. N.; Bertozzi, C. R. *J. Am. Chem. Soc.* **2012,** *134*, 9199-9208.

45. Chang, P. V.; Prescher, J. A.; Sletten, E. M.; Baskin, J. M.; Miller, I. A.; Agard, N. J.; Lo, A.; Bertozzi, C. R. *Proc. Natl. Acad. Sci. U.S.A.* **2010,** *107*, 1821-1826.

46. Sletten, E. M.; Bertozzi, C. R. *Org. Lett.* **2008,** *10*, 3097-3099.

47. Fernandez-Suarez, M.; Baruah, H.; Martinez-Hernandez, L.; Xie, K. T.; Baskin, J. M.; Bertozzi, C. R.; Ting, A. Y. *Nat. Biotechnol.* **2007,** *25*, 1483-1487.

48. Laughlin, S. T.; Baskin, J. M.; Amacher, S. L.; Bertozzi, C. R. *Science* **2008,** *320*, 664-667.

49. Sletten, E. M.; Bertozzi, C. R. *Acc. Chem. Res.* **2011,** *44*, 666-676.

50. Yao, J. Z.; Uttamapinant, C.; Poloukhtine, A.; Baskin, J. M.; Codelli, J. A.; Sletten, E. M.; Bertozzi, C. R.; Popik, V. V.; Ting, A. Y. *J. Am. Chem. Soc.* **2012,** *134*, 3720-3728.

51. Carpenter, R. D.; Hausner, S. H.; Sutcliffe, J. L. *ACS Med. Chem. Lett.* **2011,** *2*, 885-889.

52. Carpenter, R. D.; Hausner, S. H.; Sutcliffe, J. L. *J Labelled Compd Rad* **2011,** *54*, S1-S1.

53. Chen, K.; Wang, X.; Lin, W.-Y.; Shen, C. K. F.; Yap, L.-P.; Hughes, L. D.; Conti, P. S. *ACS Med. Chem. Lett.* **2012,** *3*, 1019-1023.

54. Sekhon, B. S. *J. Pharm. Educ. Res.* **2012,** *3*, 77-85.

55. El-Sagheer, A. H.; Brown, T. *Chem. Soc. Rev.* **2010,** *39*, 1388-1405.

56. Xiong, H.; Leonard, P.; Seela, F. *Bioconjugate Chem.* **2012,** *23*, 856-870.

57. Zhou, L.; Amer, A.; Korn, M.; Burda, R.; Balzarini, J.; De Clercq, E.; Kern, E. R.; Torrence, P. F. *Antivir Chem Chemother* **2005,** *16*, 375-383.

58. Ding, H.; Yang, R.; Song, Y.; Xiao, Q.; Wu, J. *Nucleosides Nucleotides Nucleic Acids* **2008,** *27*, 368-375.

59. Byun, Y.; Vogel, S. R.; Phipps, A. J.; Carnrot, C.; Eriksson, S.; Tiwari, R.; Tjarks, W. *Nucleosides Nucleotides Nucleic Acids* **2008,** *27*, 244-260.

60. Wu, T.; Froeyen, M.; Schepers, G.; Mullens, K.; Rozenski, J.; Busson, R.; Van Aerschot, A.; Herdewijn, P. *Org. Lett.* **2003,** *6*, 51-54.

61. Andersen, C.; Sharma, P. K.; Christensen, M. S.; Pedersen, N. S.; Nielsen, P. *Nucleic Acids Symp. Ser.* **2008,** *52*, 275-276.

62. Pedersen, S. L.; Nielsen, P. *Org. Biomol. Chem.* **2005,** *3*, 3570-3575.

63. Christensen, M. S.; Madsen, C. M.; Nielsen, P. *Org. Biomol. Chem.* **2007,** *5*, 1586-1594.

64. Christensen, M. S.; Bond, A. D.; Nielsen, P. *Org. Biomol. Chem.* **2008,** *6*, 81-91.

65. Danel, K.; Larsen, L. M.; Pedersen, E. B.; Sanna, G.; La Colla, P.; Loddo, R. *Biorg. Med. Chem.* **2008,** *16*, 511-517.

66. El-Brollosy, N. R.; Jørgensen, P. T.; Dahan, B.; Boel, A. M.; Pedersen, E. B.; Nielsen, C. *J. Med. Chem.* **2002,** *45*, 5721-5726.

67. Jepsen, J. S.; Wengel, J. *Curr. Opin. Drug Discovery Dev.* **2004,** *7*, 188-194.

68. Kurreck, J. *Eur. J. Biochem.* **2003,** *270*, 1628-1644.

69. Vester, B.; Wengel, J. *Biochemistry* **2004,** *43*, 13233-13241.

70. Enderlin, G.; Nielsen, P. *J. Org. Chem.* **2008,** *73*, 6891-6894.

71. Jorgensen, A. S.; Shaikh, K. I.; Enderlin, G.; Ivarsen, E.; Kumar, S.; Nielsen, P. *Org. Biomol. Chem.* **2011,** *9*, 1381-1388.

72. Lee, L.; Chang, K.-H.; Valiyev, F.; Liu, H.-J.; Li, W.-S. *J. Chin. Chem. Soc.* **2006,** *53*, 1547-1555.

73. Somu, R. V.; Boshoff, H.; Qiao, C.; Bennett, E. M.; Barry, C. E.; Aldrich, C. C. *J. Med. Chem.* **2005,** *49*, 31-34.

74. O′Mahony, G.; Svensson, S.; Sundgren, A.; Gr⌀tli, M. *Nucleosides Nucleotides Nucl. Acids* **2008,** *27*, 449-459.

75. Lincecum Jr, T. L.; Tukalo, M.; Yaremchuk, A.; Mursinna, R. S.; Williams, A. M.; Sproat, B. S.; Van Den Eynde, W.; Link, A.; Van Calenbergh, S.; Grøtli, M.; Martinis, S. A.; Cusack, S. *Mol. Cell* **2003,** *11*, 951-963.

76. Kosiova, I.; Kovackova, S.; Kois, P. *Tetrahedron* **2007,** *63*, 312-320.

77. Anand, N.; Jaiswal, N.; Pandey, S. K.; Srivastava, A. K.; Tripathi, R. P. *Carbohydr. Res.* **2011,** *346*, 16-25.

78. Chittepu, P.; Sirivolu, V. R.; Seela, F. *Biorg. Med. Chem.* **2008,** *16*, 8427-8439.

79. Winz, M. L.; Samanta, A.; Benzinger, D.; Jaschke, A. *Nucleic Acids Res.* **2012,** *40*, e78.

80. Berndl, S.; Herzig, N.; Kele, P.; Lachmann, D.; Li, X. H.; Wolfbeis, O. S.; Wagenknecht, H. A. *Bioconjugate Chem.* **2009,** *20*, 558-564.

81. Roy, S.; Caruthers, M. *Molecules* **2013,** *18*, 14268-14284.

82. Yamada, T.; Peng, C. G.; Matsuda, S.; Addepalli, H.; Jayaprakash, K. N.; Alam, M. R.; Mills, K.; Maier, M. A.; Charisse, K.; Sekine, M.; Manoharan, M.; Rajeev, K. G. *J. Org. Chem.* **2011,** *76*, 1198-1211.

83. Kawagoe, N.; Kasori, Y.; Hasegawa, T. *Cellulose* **2011,** *18*, 83-93.

84. Dean, N. M.; Bennett, C. F. *Oncogene* **2003,** *22*, 9087-9096.

85. Tamm, I.; Wagner, M. *Mol. Biotechnol.* **2006,** *33*, 221-238.

86. Varizhuk, A.; Chizhov, A.; Florentiev, V. *Bioorg. Chem.* **2011,** *39*, 127-131.

87. Mutisya, D.; Selvam, C.; Kennedy, S. D.; Rozners, E. *Bioorg. Med. Chem. Lett.* **2011,** *21*, 3420-3422.

88. Pujari, S. S.; Xiong, H.; Seela, F. *J. Org. Chem.* **2010,** *75*, 8693-8696.

89. Pujari, S. S.; Seela, F. *J. Org. Chem.* **2012,** *77*, 4460-4465.

90. Pujari, S. S.; Seela, F. *J. Org. Chem.* **2013,** *78*, 8545-8561.

91. Egli, M.; Minasov, G.; Tereshko, V.; Pallan, P. S.; Teplova, M.; Inamati, G. B.; Lesnik, E. A.; Owens, S. R.; Ross, B. S.; Prakash, T. P.; Manoharan, M. *Biochemistry* **2005,** *44*, 9045-9057.

92. Manoharan, M.; Guinosso, C. J.; Cook, P. D. *Tetrahedron Lett.* **1991,** *32*, 7171-7174.

93. Manoharan, M.; Tivel, K. L.; Andrade, L. K.; Cook, P. D. *Tetrahedron Lett.* **1995,** *36*, 3647-3650.

94. El-Sagheer, A. H.; Brown, T. *J. Am. Chem. Soc.* **2009,** *131*, 3958-3964.

95. Jawalekar, A. M.; Malik, S.; Verkade, J. M. M.; Gibson, B.; Barta, N. S.; Hodges, J. C.; Rowan, A.; van Delft, F. L. *Molecules* **2013,** *18*, 7346-7363.

96. Sirivolu, V. R.; Vernekar, S. K. V.; Ilina, T.; Myshakina, N. S.; Parniak, M. A.; Wang, Z. *J. Med. Chem.* **2013,** *56*, 8765-8780.

97. Nuzzi, A.; Massi, A.; Dondoni, A. *QSAR & Comb. Sci.* **2007,** *26*, 1191-1199.

98. Fujino, T.; Yamazaki, N.; Isobe, H. *Tetrahedron Lett.* **2009,** *50*, 4101-4103.

99. Wu, J.; Yu, W.; Fu, L.; He, W.; Wang, Y.; Chai, B.; Song, C.; Chang, J. *Eur. J. Med. Chem.* **2013,** *63*, 739-745.

100. Brase, S.; Gil, C.; Knepper, K.; Zimmermann, V. *Angew Chem Int Edit* **2005,** *44*, 5188-5240.

101. Suchy, M.; Milne, M.; Li, A. X.; McVicar, N.; Dodd, D. W.; Bartha, R.; Hudson, R. H. E. *Eur. J. Org. Chem.* **2011**, 6532-6543.

102. Gunji, H.; Vasella, A. *Helv. Chim. Acta* **2000,** *83*, 1331-1345.

103. Gunji, H.; Vasella, A. *Helv. Chim. Acta* **2000,** *83*, 3229-3245.

104. Schaeffer, H. J.; Thomas, H. J. *J. Am. Chem. Soc.* **1958,** *80*, 3738-3742.

105. Cosyn, L.; Palaniappan, K. K.; Kim, S. K.; Duong, H. T.; Gao, Z. G.; Jacobson, K. A.; Van Calenbergh, S. *J. Med. Chem.* **2006,** *49*, 7373-7383.

106. Gupte, A.; Boshoff, H. I.; Wilson, D. J.; Neres, J.; Labello, N. P.; Somu, R. V.; Xing, C. G.; Barry, C. E.; Aldrich, C. C. *J. Med. Chem.* **2008,** *51*, 7495-7507.

107. Lakshman, M. K.; Kumar, A.; Balachandran, R.; Day, B. W.; Andrei, G.; Snoeck, R.; Balzarini, J. *J. Org. Chem.* **2012,** *77*, 5870-5883.

108. Beyer, C.; Wagenknecht, H.-A. *Chem. Commun.* **2010,** *46*, 2230-2231.

109. Kumar, P.; Hornum, M.; Nielsen, L. J.; Enderlin, G.; Andersen, N. K.; Len, C.; Herve, G.; Sartori, G.; Nielsen, P. *J. Org. Chem.* **2014,** *79*, 2854-2863.

110. Neef, A. B.; Luedtke, N. W. *ChemBioChem* **2014,** *15*, 789-793.

111. Burley, G. A.; Gierlich, J.; Mofid, M. R.; Nir, H.; Tal, S.; Eichen, Y.; Carell, T. *J. Am. Chem. Soc.* **2006,** *128*, 1398-1399.

112. Gierlich, J.; Burley, G. A.; Gramlich, P. M. E.; Hammond, D. M.; Carell, T. *Org. Lett.* **2006,** *8*, 3639-3642.

113. Gourdain, S.; Martinez, A.; Petermann, C.; Harakat, D.; Clivio, P. *J. Org. Chem.* **2009,** *74*, 6885-6887.

114. Jin, X.; Yang, R.; Jin, P.; Xiao, Q.; Ju, Y. *Synthesis* **2007,** *2007*, 2967-2972.

115. Jin, X.; Ding, H.; Yang, R.; Xiao, Q.; Ju, Y. *Synthesis* **2008,** *2008*, 865-870.

116. De Clercq, E. *Med. Res. Rev.* **2003,** *23*, 253-274.

117. Amblard, F.; Cho, J. H.; Schinazi, R. F. *Chem. Rev.* **2009,** *109*, 4207-4220.

118. Gonzalez, G. A.; Montminy, M. R. *Cell* **1989,** *59*, 675-680.

119. Hunter, T. *Cell* **2000,** *100*, 113-127.

120. Montminy, M. R.; Sevarino, K. A.; Wagner, J. A.; Mandel, G.; Goodman, R. H. *Proc. Natl. Acad. Sci. U. S. A.* **1986,** *83*, 6682-6686.

121. Nagai, Y.; Miyazaki, M.; Aoki, R.; Zama, T.; Inouye, S.; Hirose, K.; Iino, M.; Hagiwara, M. *Nat. Biotechnol.* **2000,** *18*, 313-316.

122. Zaccolo, M.; De Giorgi, F.; Cho, C. Y.; Feng, L. X.; Knapp, T.; Negulescu, P. A.; Taylor, S. S.; Tsien, R. Y.; Pozzan, T. *Nat. Cell Biol.* **2000,** *2*, 25-29.

123. Zhang, C. L.; Katoh, M.; Shibasaki, T.; Minami, K.; Sunaga, Y.; Takahashi, H.; Yokoi, N.; Iwasaki, M.; Miki, T.; Seino, S. *Science* **2009,** *325*, 607-610.

124. Ito, K.; Liu, H.; Komiyama, M.; Hayashi, T.; Xu, Y. *Molecules* **2013,** *18*, 12909-12915.

125. Agrofoglio, L. A.; Gillaizeau, I.; Saito, Y. *Chem. Rev.* **2003,** *103*, 1875-1916.

126. Dyrager, C.; Börjesson, K.; Dinér, P.; Elf, A.; Albinsson, B.; Wilhelmsson, L. M.; Grøtli, M. *Eur. J. Org. Chem.* **2009,** *2009*, 1515-1521.

127. Dierckx, A.; Diner, P.; El-Sagheer, A. H.; Kumar, J. D.; Brown, T.; Grotli, M.; Wilhelmsson, L. M. *Nucleic Acids Res.* **2011,** *39*, 4513-4524.

128. O'Mahony, G.; Ehrman, E.; Grøtli, M. *Tetrahedron* **2008,** *64*, 7151-7158.

129. Yoshimura, Y.; Takahata, H. *Molecules* **2012,** *17*, 11630-11654.

130. Kocalka, P.; Andersen, N. K.; Jensen, F.; Nielsen, P. *ChemBioChem* **2007,** *8*, 2106-2116.

131. Sun, H.; Peng, X. *Bioconjugate Chem.* **2013,** *24*, 1226-1234.

132. Paredes, E.; Zhang, X.; Ghodke, H.; Yadavalli, V. K.; Das, S. R. *ACS Nano* **2013,** *7*, 3953-3961.

133. Seela, F.; Xiong, H.; Budow, S. *Tetrahedron* **2010,** *66*, 3930-3943.

134. Sirivolu, V. R.; Chittepu, P.; Seela, F. *ChemBioChem* **2008,** *9*, 2305-2316.

135. Jao, C. Y.; Salic, A. *Proc. Natl. Acad. Sci. U. S. A.* **2008,** *105*, 15779-15784.

136. Ami, T.; Fujimoto, K. *ChemBioChem* **2008,** *9*, 2071-2074.

137. Yoshimura, Y.; Okamura, D.; Ogino, M.; Fujimoto, K. *Org. Lett.* **2006,** *8*, 5049-5051.

138. Ami, T.; Ozaki, G.; Yoshimura, Y.; Fujimoto, K. *Chem. Lett.* **2008,** *37*, 134-135.

139. Ogasawara, S.; Fujimoto, K. *Angew. Chem. Int. Ed.* **2006,** *45*, 4512-4515.

140. Timper, J.; Gutsmiedl, K.; Wirges, C.; Broda, J.; Noyong, M.; Mayer, J.; Carell, T.; Simon, U. *Angew. Chem., Int. Ed.* **2012,** *51*, 7586-7588.

141. Watson, S. M. D.; Pike, A. R.; Pate, J.; Houlton, A.; Horrocks, B. R. *Nanoscale* **2014,** *6*, 4027-4037.

142. Qu, D.; Wang, G.; Wang, Z.; Zhou, L.; Chi, W.; Cong, S.; Ren, X.; Liang, P.; Zhang, B. *Anal. Biochem.* **2011,** *417*, 112-121.

143. Diermeier-Daucher, S.; Clarke, S. T.; Hill, D.; Vollmann-Zwerenz, A.; Bradford, J. A.; Brockhoff, G. *Cytom Part A* **2009,** *75A*, 535-546.

144. Salic, A.; Mitchison, T. J. *Proc. Natl. Acad. Sci. U. S. A.* **2008,** *105*, 2415-2420.

145. Buck, S. B.; Bradford, J.; Gee, K. R.; Agnew, B. J.; Clarke, S. T.; Salic, A. *BioTechniques* **2008,** *44*, 927-929.

146. Ren, X.; Gerowska, M.; El-Sagheer, A. H.; Brown, T. *Biorg. Med. Chem.* **2014,** *22*, 4384-4390.

147. Kumar, R.; El-Sagheer, A.; Tumpane, J.; Lincoln, P.; Wilhelmsson, L. M.; Brown, T. *J. Am. Chem. Soc.* **2007,** *129*, 6859-6864.

148. Ackermann, D.; Schmidt, T. L.; Hannam, J. S.; Purohit, C. S.; Heckel, A.; Famulok, M. *Nat Nanotechnol* **2010,** *5*, 436-442.

149. Schmidt, T. L.; Heckel, A. *Nano Lett.* **2011,** *11*, 1739-1742.

150. Lohmann, F.; Ackermann, D.; Famulok, M. *J. Am. Chem. Soc.* **2012,** *134*, 11884-11887.

151. Sannohe, Y.; Sugiyama, H. *Biorg. Med. Chem.* **2012,** *20*, 2030-2034.

152. Ackermann, D.; Famulok, M. *Nucleic Acids Res.* **2013,** *41*, 4729-4739.

153. Nilsson, M.; Malmgren, H.; Samiotaki, M.; Kwiatkowski, M.; Chowdhary, B. P.; Landegren, U. *Science* **1994,** *265*, 2085-2088.

154. Escude, C.; Garestier, T.; Helene, C. *Proc. Natl. Acad. Sci. U. S. A.* **1999,** *96*, 10603-10607.

155. Roulon, T.; Helene, C.; Escude, C. *Bioconjugate Chem.* **2002,** *13*, 1134-1139.

156. Liu, Y.; Kuzuya, A.; Sha, R. J.; Guillaume, J.; Wang, R. S.; Canary, J. W.; Seeman, N. C. *J. Am. Chem. Soc.* **2008,** *130*, 10882-+.

157. Wang, S. H.; Kool, E. T. *Nucleic Acids Res.* **1994,** *22*, 2326-2333.

158. Ryan, K.; Kool, E. T. *Chem. Biol.* **1998,** *5*, 59-67.

159. Fujimoto, K.; Matsuda, S.; Yoshimura, Y.; Ami, T.; Saito, I. *Chem. Commun.* **2007**, 2968-2970.

160. Onizuka, K.; Nagatsugi, F.; Ito, Y.; Abe, H. *J. Am. Chem. Soc.* **2014,** *136*, 7201-7204.

161. Ning, X.; Guo, J.; Wolfert, M. A.; Boons, G.-J. *Angew. Chem. Int. Ed.* **2008,** *47*, 2253-2255.

162. Dommerholt, J.; Schmidt, S.; Temming, R.; Hendriks, L. J.; Rutjes, F. P.; van Hest, J. C.; Lefeber, D. J.; Friedl, P.; van Delft, F. L. *Angew. Chem. Int. Ed. Engl.* **2010,** *49*, 9422-9425.

163. Debets, M. F.; van Berkel, S. S.; Schoffelen, S.; Rutjes, F. P. J. T.; van Hest, J. C. M.; van Delft, F. L. *Chem. Commun.* **2010,** *46*, 97-99.

164. Marks, I. S.; Kang, J. S.; Jones, B. T.; Landmark, K. J.; Cleland, A. J.; Taton, T. A. *Bioconjugate Chem.* **2011,** *22*, 1259-1263.

165. van Delft, P.; Meeuwenoord, N. J.; Hoogendoorn, S.; Dinkelaar, J.; Overkleeft, H. S.; van der Marel, G. A.; Filippov, D. V. *Org. Lett.* **2010,** *12*, 5486-5489.

166. Kim, Y.; Kim, S. H.; Ferracane, D.; Katzenellenbogen, J. A.; Schroeder, C. M. *Bioconjugate Chem.* **2012,** *23*, 1891-1901.

167. Aldovini, A.; Young, R. A. *J. Virol.* **1990,** *64*, 1920-1926.

168. Haque, M. M.; Peng, X. *Sci. China: Chem.* **2014,** *57*, 215-231.

169. Manoharan, M. *Curr. Opin. Chem. Biol.* **2004,** *8*, 570-579.

170. Manoharan, M. *Antisense Nucleic Acid Drug Dev.* **2002,** *12*, 103-128.

171. Jayaprakash, K. N.; Peng, C. G.; Butler, D.; Varghese, J. P.; Maier, M. A.; Rajeev, K. G.; Manoharan, M. *Org. Lett.* **2010,** *12*, 5410-5413.

172. Singh, I.; Freeman, C.; Madder, A.; Vyle, J. S.; Heaney, F. *Org. Biomol. Chem.* **2012,** *10*, 6633-6639.

173. Holstein, J. M.; Schulz, D.; Rentmeister, A. *Chem. Commun.* **2014,** *50*, 4478-4481.

174. Shelbourne, M.; Chen, X.; Brown, T.; El-Sagheer, A. H. *Chem. Commun.* **2011,** *47*, 6257-6259.

175. Lang, K.; Chin, J. W. *Chem. Rev. (Washington, DC, U. S.)* **2014,** *114*, 4764-4806.

176. Heuer-Jungemann, A.; Kirkwood, R.; El-Sagheer, A. H.; Brown, T.; Kanaras, A. G. *Nanoscale* **2013,** *5*, 7209-7212.

177. Lee, S.; Koo, H.; Na, J. H.; Han, S. J.; Min, H. S.; Lee, S. J.; Kim, S. H.; Yun, S. H.; Jeong, S. Y.; Kwon, I. C.; Choi, K.; Kim, K. *ACS Nano* **2014,** *8*, 2048-2063.

178. Wang, S.; Yang, X.; Zhu, W.; Zou, L.; Zhang, K.; Chen, Y.; Xi, F. *Polymer* **2014,** *55*, 4812-4819.

179. Qiu, J.; El-Sagheer, A. H.; Brown, T. *Chem. Commun.* **2013,** *49*, 6959-6961.

180. Zimmet, J.; Järlebark, L.; Hammarberg, T.; Van Galen, P. J. M.; Jacobson, K. A.; Heilbronn, E. *Nucleosides Nucleotides* **1993,** *12*, 1-20.

181. Sinkeldam, R. W.; Greco, N. J.; Tor, Y. *Chem. Rev.* **2010,** *110*, 2579-2619.

182. Ranasinghe, R. T.; Brown, T. *Chem. Commun.* **2005**, 5487-5502.

183. Tanpure, A. A.; Pawar, M. G.; Srivatsan, S. G. *Isr. J. Chem.* **2013,** *53*, 366-378.

184. Millar, D. P. *Curr. Opin. Struct. Biol.* **1996,** *6*, 322-326.

185. Wojczewski, C.; Stolze, K.; Engels, J. W. *Synlett* **1999**, 1667-1678.

186. Hawkins, M. E. *Cell Biochem. Biophys.* **2001,** *34*, 257-281.

187. Bokacheva, L. P.; Semenov, S. G.; Rapoport, V. L. *Opt. Spektrosk.* **1992,** *72*, 326-334.

188. Bokacheva, L. P.; Semenov, S. G. *Vestn. Leningr. Univ., Ser. 4: Fiz., Khim.* **1986**, 131-132.

189. Bokacheva, L. P.; Semenov, S. G. *Vestn. Leningr. Univ., Ser. 4: Fiz., Khim.* **1988**, 73-77.

190. Pope, A. J.; Haupts, U. M.; Moore, K. J. *Drug Discovery Today* **1999,** *4*, 350-362.

191. Hurley, D. J.; Tor, Y. *J. Am. Chem. Soc.* **1998,** *120*, 2194-2195.

192. Kool, E. T. *Acc. Chem. Res.* **2002,** *35*, 936-943.

193. Strassler, C.; Davis, N. E.; Kool, E. T. *Helv. Chim. Acta* **1999,** *82*, 2160-2171.

194. Ren, R. X. F.; Chaudhuri, N. C.; Paris, P. L.; Rumney, S. I. V.; Kool, E. T. *J. Am. Chem. Soc.* **1996,** *118*, 7671-7678.

195. Coleman, R. S.; Madaras, M. L. *J. Org. Chem.* **1998,** *63*, 5700-5703.

196. Stoop, M.; Zahn, A.; Leumann, C. J. *Tetrahedron* **2007,** *63*, 3440-3449.

197. Tor, Y.; Del Valle, S.; Jaramillo, D.; Srivatsan, S. G.; Rios, A.; Weizman, H. *Tetrahedron* **2007,** *63*, 3608-3614.

198. Ward, D. C.; Reich, E.; Stryer, L. *J. Biol. Chem.* **1969,** *244*, 1228-1237.

199. Rachofsky, E. L.; Osman, R.; Ross, J. B. A. *Biochemistry* **2001,** *40*, 946-956.

200. Kirk, S. R.; Luedtke, N. W.; Tor, Y. *Bioorg. Med. Chem.* **2001,** *9*, 2295-2301.

201. Seela, F.; Sirivolu, V. R. *Org. Biomol. Chem.* **2008,** *6*, 1674-1687.

202. Singleton, S. F.; Shan, F.; Kanan, M. W.; McIntosh, C. M.; Stearman, C. J.; Helm, J. S.; Webb, K. J. *Org. Lett.* **2001,** *3*, 3919-3922.

203. Hawkins, M. E. *Methods Enzymol.* **2008,** *450*, 201-231.

204. Hawkins, M. E.; Pfleiderer, W.; Jungmann, O.; Balis, F. M. *Anal. Biochem.* **2001,** *298*, 231-240.

205. Hawkins, M. E.; Pfleiderer, W.; Balis, F. M.; Porter, D.; Knutson, J. R. *Anal. Biochem.* **1997,** *244*, 86-95.

206. Secrist, J. A., III; Barrio, J. R.; Leonard, N. J. *Science* **1972,** *175*, 646-647.

207. Secrist, J. A., III; Barrio, J. R.; Leonard, N. J.; Weber, G. *Biochemistry* **1972,** *11*, 3499-3506.

208. Leonard, N. J. *Acc. Chem. Res.* **1982,** *15*, 128-135.

209. Krueger, A. T.; Lu, H.; Lee, A. H. F.; Kool, E. T. *Acc. Chem. Res.* **2007,** *40*, 141-150.

210. Seela, F.; Schweinberger, E.; Xu, K.; Sirivolu, V. R.; Rosemeyer, H.; Becker, E.-M. *Tetrahedron* **2007,** *63*, 3471-3482.

211. Arzumanov, A.; Godde, F.; Moreau, S.; Toulmé, J.-J.; Weeds, A.; Gait, M. J. *Helv. Chim. Acta* **2000,** *83*, 1424-1436.

212. Netzel, T. L.; Zhao, M.; Nafisi, K.; Headrick, J.; Sigman, M. S.; Eaton, B. E. *J. Am. Chem. Soc.* **1995,** *117*, 9119-9128.

213. Manoharan, M.; Tivel, K. L.; Zhao, M.; Nafisi, K.; Netzel, T. L. *J. Phys. Chem.* **1995,** *99*, 17461-17472.

214. Hurley, D. J.; Seaman, S. E.; Mazura, J. C.; Tor, Y. *Org. Lett.* **2002,** *4*, 2305-2308.

215. Xiao, Q.; Ranasinghe, R. T.; Tang, A. M. P.; Brown, T. *Tetrahedron* **2007,** *63*, 3483-3490.

216. Blount, K. F.; Tor, Y. *Nucleic Acids Res.* **2003,** *31*, 5490-5500.

217. Greco, N. J.; Tor, Y. *J. Am. Chem. Soc.* **2005,** *127*, 10784-10785.

218. Petrin, D.; Delgaty, K.; Bhatt, R.; Garber, G. *Clin. Microbiol. Rev.* **1998,** *11*, 300-317.

219. Rodriguez-Cerdeira, C.; Sanchez-Blanco, E.; Alba, A. *ISRN Obstet. Gynecol.* **2012,** *2012*, 240190.

220. Fouts, A. C.; Kraus, S. J. *J. Infect. Dis.* **1980,** *141*, 137-143.

221. Swygard, H.; Sena, A. C.; Hobbs, M. M.; Cohen, M. S. *Sex. Trans. Inf.* **2004,** *80*, 91-95.

222. Faro, S. *Infect. Dis. Obstetr. Gynecol.* **1994,** *1*, 257-258.

223. Heine, P.; McGregor, J. A. *Clin. Obstet. Gynecol.* **1993,** *36*, 137-144.

224. Muller, M. *Biochem. Pharmacol.* **1986,** *35*, 37-41.

225. Nielsen, M. H. *Acta Pathol. Microbiol. Scand. B* **1976,** *84*, 93-100.

226. Schwebke, J. R.; Burgess, D. *Clin. Microbiol. Rev.* **2004,** *17*, 794-803.

227. Dunne, R. L.; Dunn, L. A.; Upcroft, P.; O'Donoghue, P. J.; Upcroft, J. A. *Cell research* **2003,** *13*, 239-249.

228. Lumsden, W. H.; Robertson, D. H.; Heyworth, R.; Harrison, C. *Genitourin. Med.* **1988,** *64*, 217-218.

229. Narcisi, E. M.; Secor, W. E. *Antimicrob. Agents Chemother.* **1996,** *40*, 1121-1125.

230. Dornbush, P. J.; Cho, C.; Chang, E. S.; Xu, L.; Russu, W. A.; Wrischnik, L. A.; Land, K. M. *Bioorg. Med. Chem. Lett.* **2010,** *20*, 5299-5301.

231. Rapp, M.; Haubrich, T. A.; Perrault, J.; Mackey, Z. B.; McKerrow, J. H.; Chiang, P. K.; Wnuk, S. F. *J. Med. Chem.* **2006,** *49*, 2096-2102.

232. Dornbush, P. J.; Vazquez-Anaya, G.; Shokar, A.; Benson, S.; Rapp, M.; Wnuk, S. F.; Wrischnik, L. A.; Land, K. M. *Bioorg. Med. Chem. Lett.* **2010,** *20*, 7466-7468.

233. Korba, B. E.; Montero, A. B.; Farrar, K.; Gaye, K.; Mukerjee, S.; Ayers, M. S.; Rossignol, J.-F. *Antiviral Res.* **2008,** *77*, 56-63.

234. Navarrete-Vazquez, G.; Chávez-Silva, F.; Argotte-Ramos, R.; Rodríguez-Gutiérrez, M. d. C.; Chan-Bacab, M. J.; Cedillo-Rivera, R.; Moo-Puc, R.; Hernández-Nuñez, E. *Bioorg. Med. Chem. Lett.* **2011,** *21*, 3168-3171.

235. Torres-Gómez, H.; Hernández-Núñez, E.; León-Rivera, I.; Guerrero-Alvarez, J.; Cedillo-Rivera, R.; Moo-Puc, R.; Argotte-Ramos, R.; Carmen Rodríguez-Gutiérrez, M. d.; Chan-Bacab, M. J.; Navarrete-Vázquez, G. *Bioorg. Med. Chem. Lett.* **2008,** *18*, 3147-3151.

236. Adams, M.; Li, Y.; Khot, H.; De Kock, C.; Smith, P. J.; Land, K.; Chibale, K.; Smith, G. S. *Dalton Transactions* **2013,** *42*, 4677-4685.

237. Singh, B. N.; Lucas, J. J.; Beach, D. H.; Shin, S. T.; Gilbert, R. O. *Infect. Immun.* **1999,** *67*, 3847-3854.

238. Čerkasovová, A.; Čerkasov, J.; Kulda, J. *Mol. Biochem. Parasitology* **1984,** *11*, 105-118.

239. Meingassner, J. G.; Mieth, H.; Czok, R.; Lindmark, D. G.; Müller, M. *Antimicrob. Agents Chemother.* **1978,** *13*, 1-3.

240. Cobo, E. R.; Reed, S. L.; Corbeil, L. B. *Int. J. Antimicrob. Agents* **2012,** *39*, 259-262.

241. Harada, M.; Kondo, E.; Hayashi, H.; Suezawa, C.; Suguri, S.; Arai, M. *Parasitol. Res.* **2012,** *110*, 1565-1567.

242. Carvalho, K. P.; Gadelha, A. P. *FEMS Microbiol. Lett.* **2007,** *275*, 292-300.

243. Aronov, A. M.; Munagala, N. R.; Ortiz De Montellano, P. R.; Kuntz, I. D.; Wang, C. C. *Biochemistry* **2000,** *39*, 4684-4691.

244. Xenoulis, P. G.; Lopinski, D. J.; Read, S. A.; Suchodolski, J. S.; Steiner, J. M. *J. Feline Med. Surg.* **2013,** *15*, 1098-1103.

245. Kather, E. J.; Marks, S. L.; Kass, P. H. *J. Vet. Intern. Med.* **2007,** *21*, 966-970.

246. Nisha; Kumar, K.; Bhargava, G.; Land, K. M.; Chang, K.-H.; Arora, R.; Sen, S.; Kumar, V. *Eur. J. Med. Chem.* **2014,** *74*, 657-663.

247. Yang, P. Y.; Wang, M.; He, C. Y.; Yao, S. Q. *Chem. Commun.* **2012,** *48*, 835-837.

248. Lydon, J. *Biochem. Educ.* **1995,** *23*, 226-226.

249. Holmes, R. E.; Robins, R. K. *J. Am. Chem. Soc.* **1965,** *87*, 1772-1776.

250. Rayala, R.; Wnuk, S. F. *Tetrahedron Lett.* **2012,** *53*, 3333-3336.

251. Kuzmin, A.; Poloukhtine, A.; Wolfert, M. A.; Popik, V. V. *Bioconjugate Chem.* **2010,** *21*, 2076-2085.

252. Chenoweth, K.; Chenoweth, D.; Goddard, W. A. *Org. Biomol. Chem.* **2009,** *7*, 5255-5258.

253. Kovalovs, A.; Novosjolova, I.; Bizdena, E.; Bizane, I.; Skardziute, L.; Kazlauskas, K.; Jursenas, S.; Turks, M. *Tetrahedron Lett.* **2013,** *54*, 850-853.

254. Lioux, T.; Gosselin, G.; Mathé, C. *Eur. J. Org. Chem.* **2003,** *2003*, 3997-4002.

255. Gourdain, S.; Petermann, C.; Harakat, D.; Clivio, P. *Nucleosides, Nucleotides Nucleic Acids* **2010,** *29*, 542-546.

256. Zhang, B.; Wang, W.; Qu, D. Kit and method for modifying in vitro synthesized RNA by using click reaction. CN101550175A, 2009.

257. Sun, K. M.; McLaughlin, C. K.; Lantero, D. R.; Manderville, R. A. *J. Am. Chem. Soc.* **2007,** *129*, 1894-1895.

258. Andréasson, J.; Holmén, A.; Albinsson, B. *J. Phys. Chem. B* **1999,** *103*, 9782-9789.

259. Daniels, M.; Hauswirth, W. *Science* **1971,** *171*, 675-677.

260. Nir, E.; Kleinermanns, K.; Grace, L.; de Vries, M. S. *J. Phys. Chem. A* **2001,** *105*, 5106-5110.

261. Noé, M. S.; Ríos, A. C.; Tor, Y. *Org. Lett.* **2012,** *14*, 3150-3153.

262. Manderville, R. A.; Omumi, A.; Rankin, K. M.; Wilson, K. A.; Millen, A. L.; Wetmore, S. D. *Chem. Res. Toxicol.* **2012,** *25*, 1271-1280.

263. Rankin, K. M.; Sproviero, M.; Rankin, K.; Sharma, P.; Wetmore, S. D.; Manderville, R. A. *J. Org. Chem.* **2012,** *77*, 10498-10508.

264. Striker, G.; Subramaniam, V.; Seidel, C. A. M.; Volkmer, A. *J. Phys. Chem. B* **1999,** *103*, 8612-8617.

265. Molina-Arcas, M.; Casado, F. J.; Pastor-Anglada, M. *Curr. Vasc. Pharmacol.* **2009,** *7*, 426-434.

266. Lee, J.; Twomey, M.; Machado, C.; Gomez, G.; Doshi, M.; Gesquiere, A. J.; Moon, J. H. *Macromol. Biosci.* **2013,** *13*, 913-920.

267. Berezin, M. Y.; Achilefu, S. *Chem. Rev.* **2010,** *110*, 2641-2684.

268. Ikehara, M.; Uesugi, S.; Yoshida, K. *Biochemistry* **1972,** *11*, 830-836.

269. Sarma, R. H.; Lee, C.-H.; Evans, F. E.; Yathindra, N.; Sundaralingam, M. *J. Am. Chem. Soc.* **1974,** *96*, 7337-7348.

270. Seksek, O.; Bolard, J. *J. Cell Sci.* **1996,** *109 (Pt 1)*, 257-262.

271. Yoo, H.; Yang, J.; Yousef, A.; Wasielewski, M. R.; Kim, D. *J. Am. Chem. Soc.* **2010,** *132*, 3939-3944.

272. Islam, M. S.; Honma, M.; Nakabayashi, T.; Kinjo, M.; Ohta, N. *Int. J. Mol. Sci.* **2013,** *14*, 1952-1963.

273. Kore, A. R.; Srinivasan, B. *Curr. Org. Synth.* **2013,** *10*, 903-934.

274. Ukita, C.; Imura, N.; Nagasawa, K.; Aimi, N. *Chem. Pharm. Bull.* **1962,** *10*, 1113-1118.

275. Eckstein, F.; Scheit, K. H. *Angew. Chem., Int. Ed. Engl.* **1967,** *6*, 362.

276. Yoshikawa, M.; Kato, T.; Takenishi, T. *Tetrahedron Lett.* **1967**, 5065-5068.

277. Dixit, V. M.; Poulter, C. D. *Tetrahedron Lett.* **1984,** *25*, 4055-4058.

278. Davisson, V. J.; Davis, D. R.; Dixit, V. M.; Poulter, C. D. *J. Org. Chem.* **1987,** *52*, 1794-1801.

279. Ludwig, J.; Eckstein, F. *J. Org. Chem.* **1989,** *54*, 631-635.

280. Meffert, R.; Dose, K.; Rathgeber, G.; Schêfer, H.-J. 2008; Vol. 543, pp 389-402.

281. Reutsch, G. *Angew. Chem.* **1956,** *68*, 439-440.

282. Pravdin, N. S.; Shakhnovskaya, S. B. *Farmakol. Toksikol. (Moscow)* **1945,** *8*, 50-54.

283. Lewis, D. F. V.; Ioannides, C.; Parke, D. V. *Mutagenesis* **1990,** *5*, 433-435.

284. Staudinger, H.; Meyer, J. *Helv. Chim. Acta* **1919,** *2*, 635-646.

285. Staudinger, H.; Hauser, E. *Helv. Chim. Acta* **1921,** *4*, 861-886.

286. Artin, E.; Wang, J.; Lohman, G. J. S.; Yokoyama, K.; Yu, G.; Griffin, R. G.; Bar, G.; Stubbe, J. *Biochemistry* **2009,** *48*, 11622-11629.

287. Hazra, S.; Ort, S.; Konrad, M.; Lavie, A. *Biochemistry* **2010,** *49*, 6784-6790.

288. Komodzinski, K.; Gdaniec, Z.; Skalski, B. *Nucleosides Nucleotides Nucleic Acids* **2015,** *34*, 235-245.

289. Sabini, E.; Hazra, S.; Ort, S.; Konrad, M.; Lavie, A. *J. Mol. Biol.* **2008,** *378*, 607-621.

290. Van Rompay, A. R.; Johansson, M.; Karlsson, A. *Mol. Pharmacol.* **1999,** *56*, 562-569.

291. Symons, R. H. *Nucleic Acids Res.* **1977,** *4*, 4347-4355.

292. Brevet, A.; Roustan, C.; Pradel, L.-A.; Van Thoai, N. *Eur. J. Biochem.* **1975,** *52*, 345-350.

293. Baron, S. 4th ed.; University of Texas Medical Branch at Galveston: Galveston, Tex., 1996; p xvii, 1273 p.

294. Lang, A. B.; Horn, M. P.; Imboden, M. A.; Zuercher, A. W. *Vaccine* **2004,** *22, Supplement 1*, S44-S48.

295. Lister, P. D.; Wolter, D. J.; Hanson, N. D. *Clin. Microbiol. Rev.* **2009,** *22*, 582-610.

296. Lundgren, B. R.; Villegas-Peñaranda, L. R.; Harris, J. R.; Mottern, A. M.; Dunn, D. M.; Boddy, C. N.; Nomura, C. T. *J. Bacteriol.* **2014,** *196*, 2543-2551.

297. Campbell, J. J. R.; Stokes, F. N. *J. Biol. Chem.* **1951,** *190*, 853-858.

298. Laurent, S.; Chen, H.; Bedu, S.; Ziarelli, F.; Peng, L.; Zhang, C. C. *Proc. Natl. Acad. Sci. U. S. A.* **2005,** *102*, 9907-9912.

299. Lundquist, J. T.; Pelletier, J. C. *Org. Lett.* **2001,** *3*, 781-783.

300. Alper, P. B.; Hung, S. C.; Wong, C. H. *Tetrahedron Lett.* **1996,** *37*, 6029-6032.

301. Ahn, H. J.; Kim, H.-W.; Yoon, H.-J.; Lee, B. I.; Suh, S. W.; Yang, J. K. *EMBO J.* **2003,** *22*, 2593-2603.

302. Bjork, G. R.; Wikstrom, P. M.; Bystrom, A. S. *Science* **1989,** *244*, 986-989.

303. Elkins, P. A.; Watts, J. M.; Zalacain, M.; van Thiel, A.; Vitazka, P. R.; Redlak, M.; Andraos-Selim, C.; Rastinejad, F.; Holmes, W. M. *J. Mol. Biol.* **2003,** *333*, 931-949.

304. Martin, J. L.; McMillan, F. M. *Curr. Opin. Struct. Biol.* **2002,** *12*, 783-793.

305. Motorin, Y.; Burhenne, J.; Teimer, R.; Koynov, K.; Willnow, S.; Weinhold, E.; Helm, M. *Nucleic Acids Res.* **2011,** *39*, 1943-1952.

306. Klimašauskas, S.; Weinhold, E. *Trends Biotechnol.* **2007,** *25*, 99-104.

307. Peters, W.; Willnow, S.; Duisken, M.; Kleine, H.; Macherey, T.; Duncan, K. E.; Litchfield, D. W.; Luescher, B.; Weinhold, E. *Angew. Chem., Int. Ed.* **2010,** *49*, 5170-5173, S5170/5171-S5170/5179.

308. Morales-Serna, J. A.; Sanchez, E.; Velazquez, R.; Bernal, J.; Garcia-Rios, E.; Gavino, R.; Negron-Silva, G.; Cardenas, J. *Org. Biomol. Chem.* **2010,** *8*, 4940-4948.

309. Robins, M. J.; Hawrelak, S. D.; Hernandez, A. E.; Wnuk, S. F. *Nucleosides Nucleotides* **1992,** *11*, 821-834.

310. Kim, B. T. *Bull. Korean Chem. Soc.* **2005,** *26*, 171-174.

311. Krishnakumar, K. S.; Goudedranche, S.; Bouchu, D.; Strazewski, P. *J. Org. Chem.* **2011,** *76*, 2253-2256.

312. Shendage, D. M.; Frohlich, R.; Haufe, G. *Org. Lett.* **2004,** *6*, 3675-3678.

313. Muranaka, K.; Ichikawa, S.; Matsuda, A. *Tetrahedron Lett.* **2009,** *50*, 5102-5106.

314. Prakash, T. P.; Kawasaki, A. M.; Fraser, A. S.; Vasquez, G.; Manoharan, M. *J. Org. Chem.* **2001,** *67*, 357-369.

315. Wagner, D.; Verheyden, J. P. H.; Moffatt, J. G. *J. Org. Chem.* **1974,** *39*, 24-30.

316. Wagner, D.; Verheyden, J. P. H.; Moffatt, J. G. *J. Org. Chem.* **1974,** *39*, 24-30.

317. Schmidt, B. *Eur. J. Org. Chem.* **2004**, 1865-1880.

318. Chattopadhyaya, J. B.; Reese, C. B. *Synthesis* **1977**, 725-726.

319. Buenger, G. S.; Nair, V. *Synthesis* **1990**, 962-966.

320. Pankiewicz, K. W.; Krzeminski, J.; Ciszewski, L. A.; Ren, W. Y.; Watanabe, K. A. *J. Org. Chem.* **1992,** *57*, 553-559.

321. Oliveira, J. M.; Zeni, G.; Malvestiti, I.; Menezes, P. H. *Tetrahedron Lett.* **2006,** *47*, 8183-8185.

322. Robins, M. J.; Hansske, F.; Wnuk, S. F.; Kanai, T. *Can. J. Chem.* **1991,** *69*, 1468-1474.

323. Borchardt, R. T.; Wu, Y. S. *J. Med. Chem.* **1974,** *17*, 862-868.

324. Robins, M. J.; Hawrelak, S. D.; Hernandez, A. E.; Wnuk, S. F. *Nucleosides Nucleotides* **1992,** *11*, 821-834.

325. Wohnsland, F.; Faller, B. *J. Med. Chem.* **2001,** *44*, 923-930.

326. Eaton, D. F. *Pure Appl. Chem.* **1988,** *60*, 1107-1114.

327. Lukavenko, O. N.; Eltsov, S. V.; Grigorovich, A. V.; McHedlov-Petrossyan, N. O. *J. Mol. Liq.* **2009,** *145*, 167-172.

328. Haga, Y.; Ishii, K.; Hibino, K.; Sako, Y.; Ito, Y.; Taniguchi, N.; Suzuki, T. *Nat Commun* **2012,** *3*, 907-913.

329. Belardi, B.; de la Zerda, A.; Spiciarich, D. R.; Maund, S. L.; Peehl, D. M.; Bertozzi, C. R. *Angew Chem Int Edit* **2013,** *52*, 14045-14049.

VITA

JESSICA ZAYAS

Born, Hialeah, Florida

2005-2007	A.A., Chemistry Miami Dade College Miami, Florida
2007-2010	MBRS RISE Undergraduate Fellowship Florida International University Miami, Florida
2007-2010	B.A., Chemistry Florida International University Miami, Florida
2014	SoFLACS Graduate Travel Award
2010-2015	MBRS RISE Graduate Fellowship Florida International University Miami, Florida
2010-2015	Doctoral Candidate Florida International University Miami, Florida

PUBLICATIONS AND PRESENTATIONS

Liu, N.; Zayas, J.; Nguyen, M.; Tran, R.; Fong, G.; Thompson, J. D.; Haberkern, N. T.; Hopper, M.; Chang, K.; Patel, N.; Marks, S. L.,; Zhao, W.; Wnuk, S.F.; Wrischnik, L; Land, K.M.; (2015) *Antiprotozoal activity of adenosine analogs on parasitic trichomonads.* Bioorganic and Medicinal Chemistry Letters (submitted)

Zayas, J.; Annoual, M.; Das, J. D.; Felty, Q.; Gonzalez, W. G.; Miksovska, J.; Sharifai, N.; Chiba, A.; Wnuk, S. F.; (2015). *Strain Promoted Click Chemistry of 2- or 8-*

Azidopurine and 5-Azidopyrimidine Nucleosides and 8-Azidoadenosine Triphosphate with Cyclooctynes. Application to Living Cell Fluorescent Imaging. Bioconjugate Chemistry, DOI: 10.1021/acs.bioconjchem.5b00300 (accepted).

Zayas, J.; Wnuk, S.F.; Wrischnik, L; Land, K.M.; (2015) *Drug discovery against the protozoal pathogen Trichomonas vaginalis.* Journal of Medicinal Chemistry, (accepted, pending revisions)

Zayas, J.; Annoual, M.; Wnuk, S.F. *Strain promoted click chemistry (SPAAC) of 8-azido purine and 5-azido pyrimidine nucleosides with cyclooctynes.* (March, 2014). Poster presented at the 247th ACS National Meeting & Exposition, Dallas, Texas.

Zayas, J.; Chang, K.; Patel, N.; Wnuk, S.F.; Land, K.M. *In vitro activity of nucleoside analogs on the veterinary protozoan parasite Tritrichomonas foetus.* (April, 2013). Poster presented at the 245th ACS National Meeting & Exposition, New Orleans, Louisiana.

Shokar, A.; Au, A.; An, S.H.; Tong, E.; Garza, G.; Zayas, J.; Wnuk, S.F.; Land, K.M. (2012). *S-Adenosylhomocysteine hydrolase of the protozoan parasite Trichomonas vaginalis: Potent inhibitory activity of 9-(2-deoxy-2-fluoro-β,d-arabinofuranosyl) adenine.* Bioorganic & Medicinal Chemistry Letters, 22 (12), 4203-4205.

Zayas, J.; Au, A.; Shokar, A.; An, S.; Land, K.M.; Wnuk, S.F. *Inhibition of adenosylhomocysteine hydrolase of Trichomonas vaginalis with 9-(2-deoxy-2-fluoro-β,D-arabinofuranosyl)adenine.* (March, 2012). Poster presented at the 243rd ACS National Meeting & Exposition, San Diego, California.

Sacasa, P.R.; Zayas, J.; Wnuk, S.F. (2009) *Radical-mediated thiodesulfonylation of the vinyl sulfones: access to (α-fluoro)vinyl sulfide.* Tetrahedron Letters, 50 (38), 5424-5427.

Zayas, J.; Sacasa, P.R.; Wnuk, S.F. *Radical desulfonylation reactions in aqueous medium using tris(trimethylsilyl)silane and thiols.* (March 2009). Poster presented at the 237th ACS National Meeting & Exposition, Salt Lake City, Utah.